2017

Frontal Crash Analysis of a Conformable CNG tank using Finite Element Analysis

Datta Sandesh Manjunath
Michigan Technological University, dmanjuna@mtu.edu

FRONTAL CRASH ANALYSIS OF A CONFORMABLE CNG TANK USING FINITE ELEMENT ANALYSIS

By

Datta Sandesh Manjunath

A REPORT

Submitted in partial fulfillment of the requirements for the degree of

MASTER OF SCIENCE

In Mechanical Engineering

MICHIGAN TECHNOLOGICAL UNIVERSITY

2017

This report has been approved in partial fulfillment of the requirements for the Degree of MASTER OF SCIENCE in Mechanical Engineering.

Department of Mechanical Engineering-Engineering Mechanics

Report Advisor: *Dr. Gregory M. Odegard*

Committee Member: *Dr. Adam Loukus*

Committee Member: *Mr. Jeremy Worm*

Department Chair: *Dr. William W. Predebon*

Table of Contents

List of Figures v

List of Tables ix

Acknowledgements x

Abstract xi

1. Introduction 1

    1.1 Project Background 3

    1.2 Scope of the project 5

2. Geometry 7

    2.1 Chassis Geometry 7

    2.2 Bracket Geometry 9

    2.3 Tank Geometry 11

    2.4 Tank-Bracket Assembly 13

    2.5 Integration of the Tanks 14

3. Mesh Generation 16

    3.1 Mesh Generation of the Chassis 16

    3.2 Mesh Validation of Chassis 19

    3.3 Mesh Generation of the Brackets 22

    3.4 Mesh Validation of Brackets 24

    3.5 Mesh Generation of Tank 27

    3.6 Mesh Validation of the Tank 28

    3.6 Mesh Generation of the Rubber Pad 29

    3.7 Element Quality and Checks 29

4. Material Properties 30
4.1 Material Properties of Chassis 30
4.2 Material Properties of the Bracket 32
4.3 Material Properties of Tank 32
4.4 Effective Material Properties 33
4.5 Material Properties of Rubber Pad 36
5. Contact Modeling 37
5.1 Self Contact among all parts 38
5.2 Contact in the Tank-Bracket assembly 40
6. Loading and Boundary Conditions 41
7. Results and Discussion 43
7.1 von Mises stress in the Tanks 43
7.2 Plastic Strain in the Brackets 52
7.3 Positioning of the Tanks 55
8. Conclusion and Recommendations for future work 61
9. References 63
10. Appendix 65

List of Figures

Figure 1-Conventional CNG tank fitted to an automobile [4] 2
Figure 2- Conformable CNG tank advantages [5] 3
Figure 3- Conformable tank used in a truck [5] 4
Figure 4 – CAD model of the truck having 7 tanks [6] 5
Figure 5- The Truck having seven tanks [6] 5
Figure 6- CAD model of 2015 Chevrolet Silverado [4] 7
Figure 7- Bottom view of 2015 Chevrolet Silverado [4] 8
Figure 8-Few of the Deleted parts 8
Figure 9-1986 Chevy C10 Fuel tank brackets [7] 9
Figure 10-CAD Model of the Bracket 10
Figure 11-Conformable CNG Tank Geometry 11
Figure 12- Quarter portion of the Conformable CNG Tank 12
Figure 13-Equivalent CNG Tank 12
Figure 14- Rubber pad on the Bracket 13
Figure 15- Rubber pad fitted in the tank-bracket assembly 13
Figure 16- Tanks integrated to the chassis 14
Figure 17- Tanks installed in the truck chassis [6] 15
Figure 18- front view of the tanks attached to the chassis 15
Figure 19-Part and its mid surface 17
Figure 20-2D meshed part 18
Figure 21-Detailed view of the 1D weld elements used to connect the components 19
Figure 22-Model for mesh validation of Chassis 20
Figure 23-Mesh Validation for the chassis 21
Figure 24-Simulation time vs element sizes for Mesh Validation of the Chassis 22
Figure 25-Solid Model of the Bracket imported in HyperMesh 23
Figure 26-Mid Surface of the Bracket extracted in HyperMesh 23
Figure 27-Meshed Bracket in HyperMesh 24
Figure 28-Model for Mesh Validation of Brackets 25
Figure 29-Detailed view showing the Brackets 25

Figure 30-Mesh validation of the bracket 26
Figure 31-Simulation time vs Element Size for Mesh Validation of the Bracket 27
Figure 32-Conformable CNG tank meshed with 3D elements..... 28
Figure 33-Mesh Validation of the CNG tank..... 28
Figure 34-Stress Strain Curve for SAE980X 31
Figure 35-Perfectly Plastic Curve used for simulation..... 32
Figure 36-Symmetric Boundary Conditions applied to the CNG tank..... 34
Figure 37-Symmetric Boundary Conditions applied to the Approximated Tank 34
Figure 38-Uniaxial Pressure Load applied to the CNG tank..... 35
Figure 39-Uniaxial Pressure Load applied to the Approximated Tank 35
Figure 40-Most common type of Contacts [9]..... 37
Figure 41-Penalty method in RADIOSS [9] 38
Figure 42- Master-Slave set in Type 7 Interface [15]..... 39
Figure 43-Example of Auto impact surface [15] 39
Figure 44- Tied Contact (Type2) [15] 40
Figure 45-Rigid Wall with slave nodes [9] 41
Figure 46-Final Model with the Rigid Barrier 42
Figure 47-Nomenclature of Tanks..... 43
Figure 48- Screenshot of Results for 35mph..... 44
Figure 49-Screenshot of Results for 35mph (Top View)..... 44
Figure 50- Von Mises stress on the tanks- 35mph..... 45
Figure 51-Von Mises stress on the tanks – 35mph (Top View)..... 45
Figure 52- Von Mises stress on the tanks- 35mph (Bottom View)..... 46
Figure 53-Von Mises stress on the tank – 35mph (Left View)..... 46
Figure 54- Von Mises stress on the tank- 35mph (Right View) 47
Figure 55- Screenshot of Results for 55mph (Isometric View) 48
Figure 56- Screenshot of Results for 55mph (Top View)..... 48
Figure 57-Von Mises stress on the tanks- 55mph..... 49
Figure 58-Von Mises stress on the tanks- 55 mph (Top View)..... 49
Figure 59- Von Mises stress on the tanks- 55mph (Bottom View)..... 50

Figure 60-Von Mises stress on the tanks- 55mph (Left View) 50
Figure 61- Von Mises stress on the tanks- 55mph (Right View) 51
Figure 62-Nomenclature of brackets 52
Figure 63- Plastic Strain in the Brackets (35 mph) 53
Figure 64-Plastic Strain in the Brackets (55 mph) 53
Figure 65- Full Model view 55
Figure 66- Detailed View for rotation of bracket 56
Figure 67- Initial Measurement of rotation of bracket relative to chassis 56
Figure 68- Rotation of bracket relative to chassis 57
Figure 69- Movement of Frontal Bracket 1 [35 mph] 57
Figure 70- Movement of Tank 59
Figure 71- Movement of Frontal Tank 59
Figure 72- Energy Curves for 35mph 65
Figure 73- Energy curves for 55 mph 65
Figure 74- Movement of Frontal Tank1- Mag [35mph] 66
Figure 75-Movement of Frontal Tank1- X direction [35mph] 66
Figure 76-Movement of Frontal Tank1- Y direction [35mph] 67
Figure 77-Movement of Frontal Tank1- Z direction [35mph] 67
Figure 78-Movement of Frontal Tank 2- Mag [35mph] 68
Figure 79-Movement of Frontal Tank 2- X direction [35mph] 68
Figure 80-Movement of Frontal Tank 2- Y direction [35mph] 69
Figure 81-Movement of Frontal Tank 2- Z direction [35mph] 69
Figure 82-Movement of Rear Tank 1- Mag [35mph] 70
Figure 83-Movement of Rear Tank 1- X direction [35mph] 70
Figure 84-Movement of Rear Tank 1- Y direction [35mph] 71
Figure 85-Movement of Rear Tank 1- Z direction [35mph] 71
Figure 86-Movement of Rear Tank 2- Mag [35mph] 72
Figure 87-Movement of Rear Tank 2- X direction [35mph] 72
Figure 88-Movement of Rear Tank 2- Y direction [35mph] 73
Figure 89-Movement of Rear Tank 2- Z direction [35mph] 73

Figure 90-Movement of Frontal Bracket 1A [35mph] 74
Figure 91-Movement of Frontal Bracket 2A [35mph] 74
Figure 92-Movement of Rear Bracket 1A [35mph] 75
Figure 93-Movement of Rear Bracket 2A [35mph] 75
Figure 94-Movement of Frontal Tank 1- Mag [55mph] 76
Figure 95- Movement of Frontal Tank 1- X direction [55mph] 76
Figure 96-Movement of Frontal Tank 1- Y direction [55mph] 77
Figure 97-Movement of Frontal Tank 1- Z direction [55mph] 77
Figure 98-Movement of Frontal Tank 2- Mag [55mph] 78
Figure 99-Movement of Frontal Tank 2- X direction [55mph] 78
Figure 100-Movement of Frontal Tank 2- Y direction [55mph] 79
Figure 101-Movement of Frontal Tank 2- Z direction [55mph] 79
Figure 102-Movement of Rear Tank 1- Mag [55mph] 80
Figure 103-Movement of Rear Tank 1- X direction [55mph] 80
Figure 104-Movement of Rear Tank 1- Y direction [55mph] 81
Figure 105-Movement of Rear Tank 1- Z direction [55mph] 81
Figure 106-Movement of Rear Tank 2- Mag [55mph] 82
Figure 107-Movement of Rear Tank 2- X direction [55mph] 82
Figure 108-Movement of Rear Tank 2- Y direction [55mph] 83
Figure 109-Movement of Rear Tank 2- Z direction [55mph] 83
Figure 110-Movement of Frontal Bracket 1A [55mph] 84
Figure 111-Movement of Frontal Bracket 2A [55mph] 84
Figure 112-Movement of Rear Bracket 1A [55mph] 85
Figure 113-Movement of Rear Bracket 2A [55mph] 85

List of Tables

Table 1-Mesh Validation of Chassis 20
Table 2-Simulation Time for various element sizes for Mesh Validation of the Chassis 21
Table 3-Mesh validation of the Bracket 26
Table 4-Simulation time for Mesh Validation of the Bracket 27
Table 5-2D element quality criteria 29
Table 6-3D element quality criteria 29
Table 7-Material Properties of SAE 980X HSLA steel 30
Table 8-Material Properties of Aluminum alloy Al206.0-T7 33
Table 9-Material Properties of the Effective Tank 36
Table 10-Strain Energy of the tanks for various loads 36
Table 11-Material Properties of Rubber Pad 36
Table 12-Max von Mises stress on the tanks for Speed of 35 mph 47
Table 13-Max von Mises stress on the tanks for Speed of 55 mph 51
Table 14-Rotation of Brackets – 35mph 58
Table 15-Rotation of Brackets – 55mph 58
Table 16-Movement of the Tanks- 35mph 60
Table 17-Movement of the Tanks- 55mph 60

Acknowledgements

I would like to thank my advisor Dr. Gregory M. Odegard, Associate Chair and Director of Undergraduate Studies, Department of Mechanical Engineering- Engineering Mechanics, for accepting me in his FEA modeling group and giving me this project. His valuable support, expert subject knowledge and motivation has helped me in this project. I shall remain ever grateful for all his patience while dealing with my constantly recurring doubts.

I want to take this opportunity to thank my committee members Mr. Jeremy Worm and Dr. Adam Loukus who have agreed to serve as my advisory committee members and guided me in my research, and for providing feedback on my report.

I would also like to thank my colleagues Paul Roehm, Sumit Bongir, Sandesh Gandhi for their valuable comments and for giving me crucial tips in the project during our team meetings.

Finally yet importantly, I would like to thank my parents, Malathy and Manjunath for always being there for me and for supporting me throughout my Master's degree.

Abstract

The purpose of this study is to computationally model and analyze a Conformable Compressed Natural Gas (CNG) fuel tank for frontal crashes using Finite Element Analysis. Researchers have developed a CNG fuel tank, which is conformable, non-conventional and non-cylindrical. This tank increases cost efficiency, volumetric efficiency and cargo efficiency in CNG vehicle applications. A lightweight pickup truck (2015 Chevrolet Silverado) has been used to integrate the CNG tanks and field-testing has been conducted to demonstrate the application.

The report mainly focuses on the effective finite element modeling of the chassis, brackets and tanks using HYPERMESH and RADIOSS. The frontal crash analysis is simulated according to FMVSS 208 standard for two impact velocities of 35 mph and 55 mph. CAD models of the brackets have been developed for this study. Material models of the truck chassis and bracket are developed using the available data.

An important aspect of this study is to determine an appropriate way to model the CNG tank. The conformable tank's complex geometry, limitations in the software capabilities and the high computational expenses posed a challenge in this study. An equivalent tank model, having a simpler geometry has been developed and used for this study. The effective modulus of the equivalent tank was determined by equating the strain energy of the conformable tank to the strain energy of the equivalent tank, both subjected to same loading.

The results obtained from the crash analysis conclude that the tanks do not fail in frontal crash and rear crash, and the positioning of the tanks are validated. Recommendation for future work is also provided at the end of this report.

1. Introduction

Most of the automobile engines in the world are currently being powered by either gasoline (petrol) or diesel. Gasoline is being widely used as it has many advantages, a few being its availability in the liquid form, easy transportation and high density. One of the disadvantages of gasoline is the environmental pollution due to the hazardous substances produced by the emissions.

Due to these reasons, efforts are being made to use alternate fuels like CNG, bio diesel, electricity (batteries) and fuel cells to power vehicles. One such alternate fuel is Compressed Natural Gas (CNG).

Compressed Natural Gas (CNG) is mainly composed of methane. It is made by compressing natural gas to less than 1 percent of the volume. CNG is odorless, colorless and tasteless [1]. Some of the advantages of CNG are as follows-

- It is domestically produced in USA and is an abundant fuel.
- It is environment friendly. CNG powered vehicles produce less emissions than traditional vehicles. An experimental study has shown that there is almost 80% drop in the carbon monoxide content in the emissions of CNG powered vehicles compared to gasoline-powered vehicles [2].
- The maintenance cost of CNG powered engines is comparatively less than gasoline-powered engines.
- The performance of these engines is superior compared to gasoline engines as CNG has an octane rating close to 130. CNG engines have less knock and there is no vapor locking. [3]

Despite having so many advantages CNG is not being widely used in the United States. According to a report by GE, there are 12 million CNG powered vehicles in the world but

only 250,000 are being used in the US. The growth rate shows a 3.7% per year increase in the US whereas the growth rate around the world is about 30.6%. [1]

Two of the main reasons for CNG not being used widely in USA are-

- Lack of CNG fueling stations. Even tough there is abundant CNG available, they are a very few fuel stations where CNG is available. There are about 12000 CNG fueling stations in the world but only 500 are present in the US.
- The packaging of the current cylindrical CNG tanks in automotive is not efficient enough as it consumes a lot of cargo space.

The current CNG tanks used in automotive is a cylindrical tank. These tanks are robust and they are efficient in holding the pressures of the CNG. However, due to the shape of these tanks, they take a lot of cargo space. These cylindrical tanks are always kept in the rear and they cannot be kept under the vehicle due to safety issues.

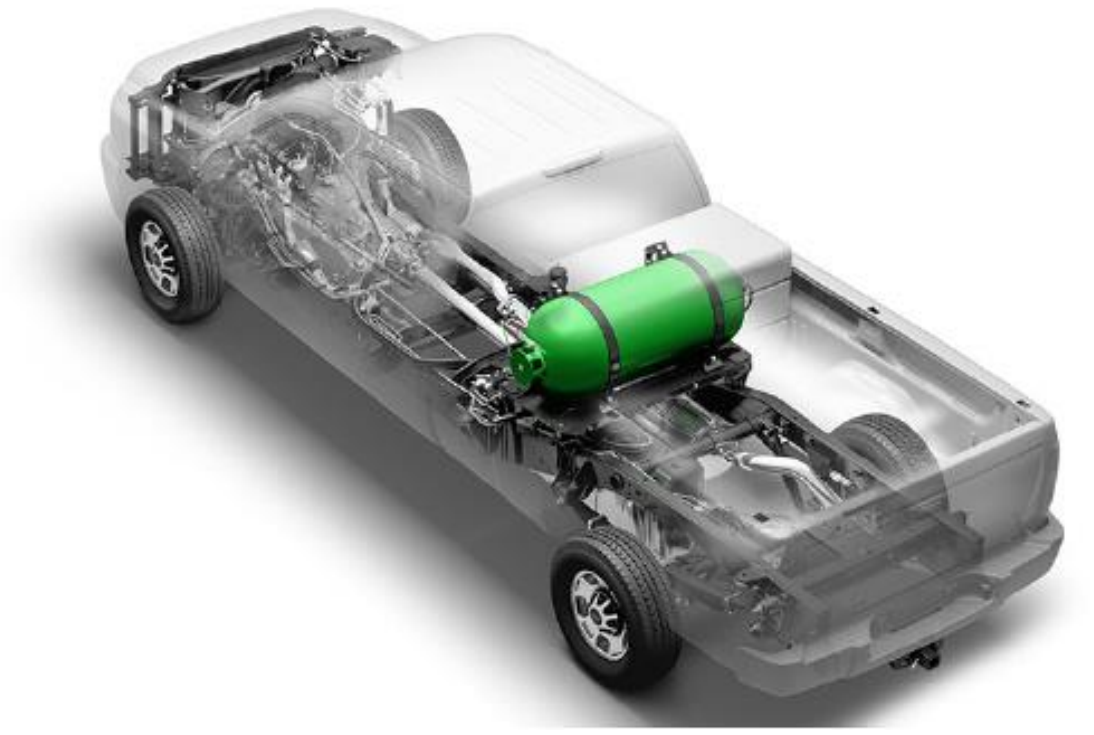

Figure 1-Conventional CNG tank fitted to an automobile [4]

1.1 Project Background

To address the packaging problem of the cylindrical tanks, Southwestern Energy Company (an oil and gas company) has partnered with REL Inc. and Michigan Tech to come up with a new design of a CNG tank which solves this issue.

Researchers from MTU and REL have come up with an innovative design of a CNG tank. The new design of the CNG tank is a conformable tank, which is not cylindrical in shape but has the same fuel handling capacity and performance of the conventional tank. These tanks are made up of Schwarz P-surface, which eliminates sharp corners and a unit cell that can be replicated to form a rectangular array. They are better than the conventional tanks as they are cost, cargo and structurally efficient.

Figure 2- Conformable CNG tank advantages [5]

The primary use of this conformable CNG tank is in automobiles. They also have potential applications in forklifts, airport shuttles, fueling stations etc.

The conventional cylindrical tank can be replaced by this tank in automobiles. Figure 3 shows the usage of the conformable matrix tank in a pickup truck. We can see that the conformable tank can be placed underneath the body inside the chassis, thus increasing the cargo space.

Figure 3- Conformable tank used in a truck [5]

They are being manufactured by a special casting technique by REL. Michigan Tech is primarily involved in computational analysis (FEA) and vehicle integration of this tank. Some of the work the FEA team at MTU is involved in are structural optimization of the tank, drop test simulations and crash simulations of the tank.

1.2 Scope of the project

As mentioned in the previous section, one of the main applications of the tank is in automobiles. To demonstrate this, a light duty pickup truck (2015 Chevrolet Silverado) has been purchased and several tanks are integrated. The integration team has integrated the tanks by carrying out the required modifications i.e. altering the exhaust system, fuel intake system etc. Seven tanks were installed in the truck. Prathmesh (PhD. Student at Michigan Tech) performed FEA of the initial brackets used in Phase 1.

Figure 4 – CAD model of the truck having 7 tanks [6]

Figure 5- The Truck having seven tanks [6]

The rear two tanks are removed after an initial iteration and only four tanks are used. The main motive of this project is to analyze the stresses induced on the four tanks during frontal crash and to validate the positioning of the tanks by Finite Element Analysis (FEA). Altair's HyperMesh is used as the pre-processor for the FEA. RADIOSS, which is an explicit-implicit dynamic software, will be used as the solver. HyperView will be used as the post processor.

The project mainly focuses on the following-

1) Generating the CAD models of the new brackets installed by visual inspection.

2) Generating effective finite element models of the chassis, brackets and tank.

3) Developing the material properties of an alternate tank, which is much simpler in geometry and can be used for the crash simulation.

4) Integrating the tank assembly to the chassis as it is done on the truck.

5) Establish a general procedure for crash simulations using RADIOSS which can be used in the future for further projects.

Each part is explained in detail in this report.

2. Geometry

2.1 Chassis Geometry

A 3D Computer Aided Design (CAD) model of the pickup truck- 2015 Chevrolet Silverado was received. This CAD file was opened in NX. It was a huge assembly, which had many sub-assemblies like powertrain assembly, chassis assembly, etc. For the project only the chassis CAD was required, so all other assemblies were deleted.

Figure 6- CAD model of 2015 Chevrolet Silverado [4]

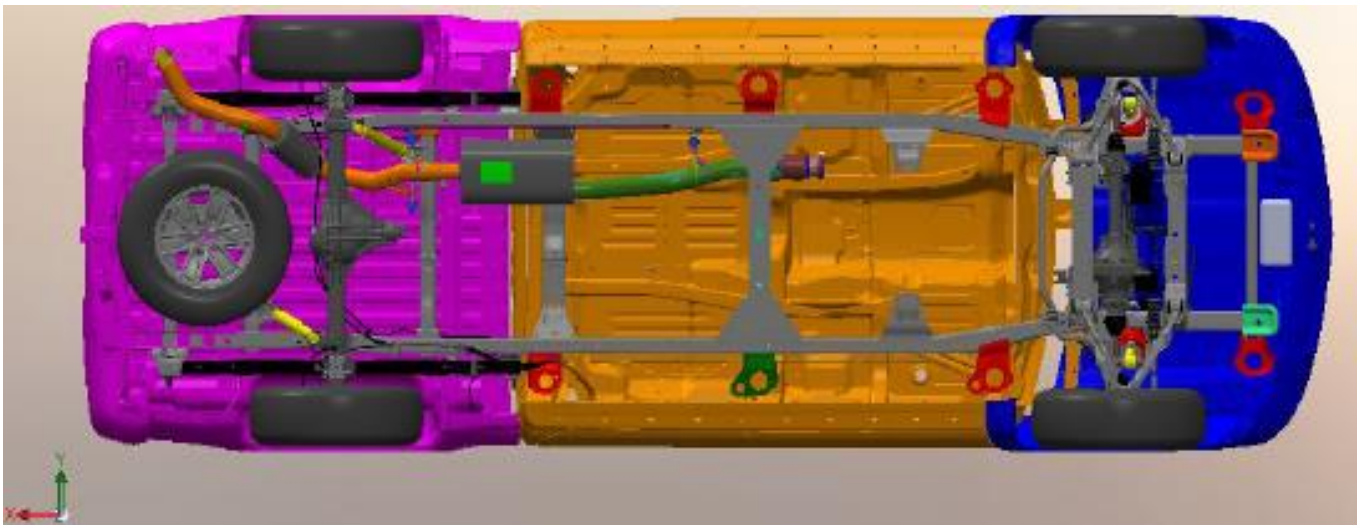

Figure 7- Bottom view of 2015 Chevrolet Silverado [4]

The chassis sub assembly consisted of 171 parts. Many parts in the chassis like nuts, bolts, name plate, etc were deleted as these parts do not add any significance to the study here. These parts do not contain any loads or any constraints. The deletion of these parts reduces the complexity in the chassis structure and also decreases the total simulation time. Some of the deleted parts are shown below.

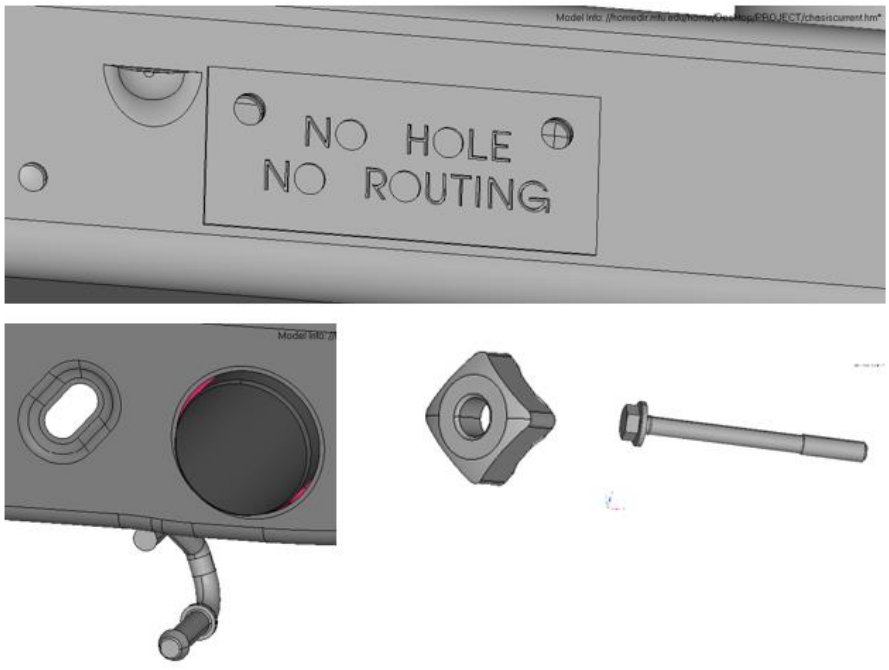

Figure 8-Few of the Deleted parts

After deleting the redundant parts, the thickness of all the remaining parts was measured and noted. The assembly was saved as a .step file format to be imported in HyperMesh. These parts were all thin structures, i.e. the third dimension was very small compared to the other two dimensions.

2.2 Bracket Geometry

After thorough investigation of the pickup truck, the brackets used to integrate the tanks were found to be a 1986 Chevy C10 Truck Rear Side Mounted Fuel Tank mounting bracket. It is a mounting bracket available in the market, which is commonly used to assemble fuel tanks to the chassis in pickup trucks.

Figure 9-1986 Chevy C10 Fuel tank brackets [7]

A CAD model of the Chevy Mounting bracket was not available. A CAD model had to be developed for the analysis by taking the visually available dimensions. The bracket is an assembly of many parts like bended plate, screws, etc. These parts were so small that it was not possible to measure each one of them to prepare them individually and assemble them.

A simplified similar CAD model of the bracket was built by using all the significantly measurable dimensions. The simplified CAD model was developed in such a way that it exactly replicates the functionality of the main bracket. The CAD model was prepared in NX 10.

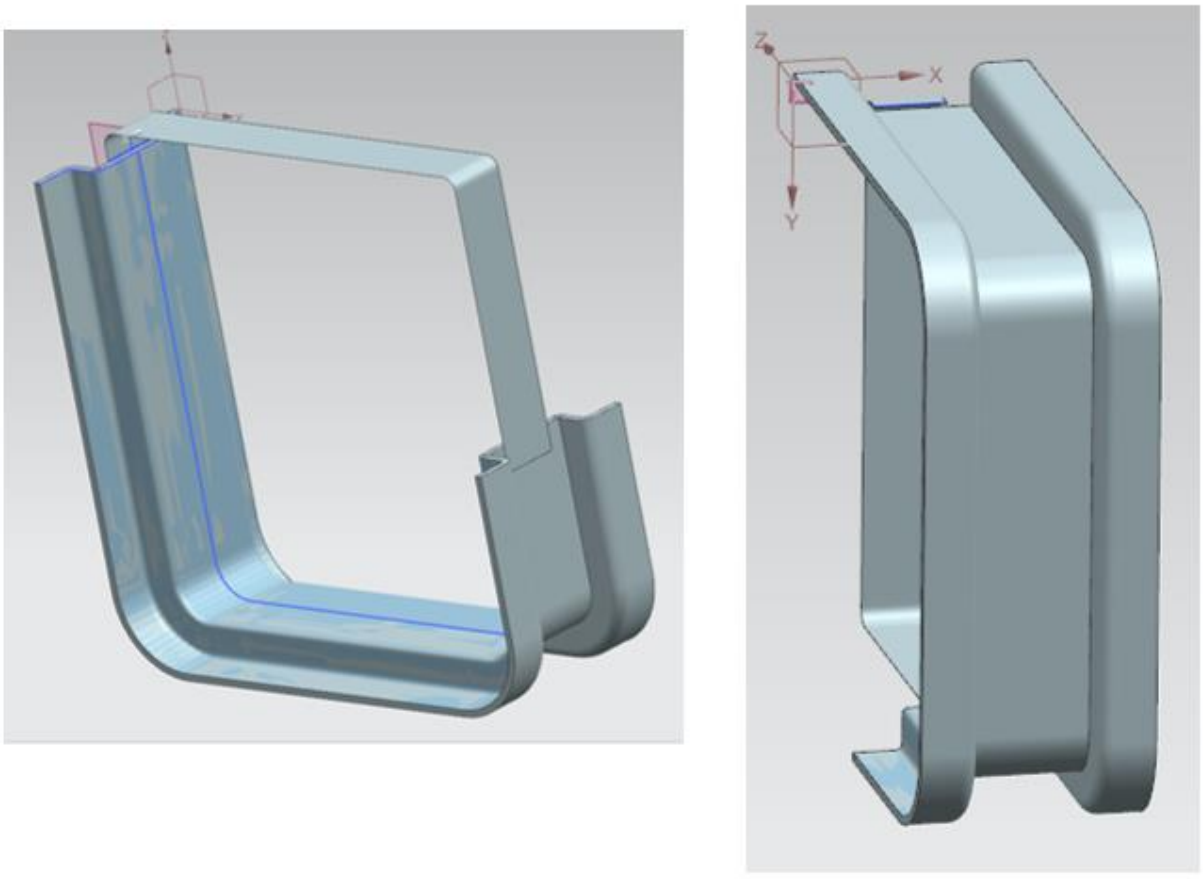

Figure 10-CAD Model of the Bracket

2.3 Tank Geometry

The tank, designed and developed by REL Inc., has a non-cylindrical tank geometry. The tank is a matrix structure. It has a unique inner structure known as the Schwarz P-surface. They are spherical cells which are packed in an array to eliminate sharp corners. The dimensions of the tank are 22.25 inches × 11.6 inches × 12.24 inches.

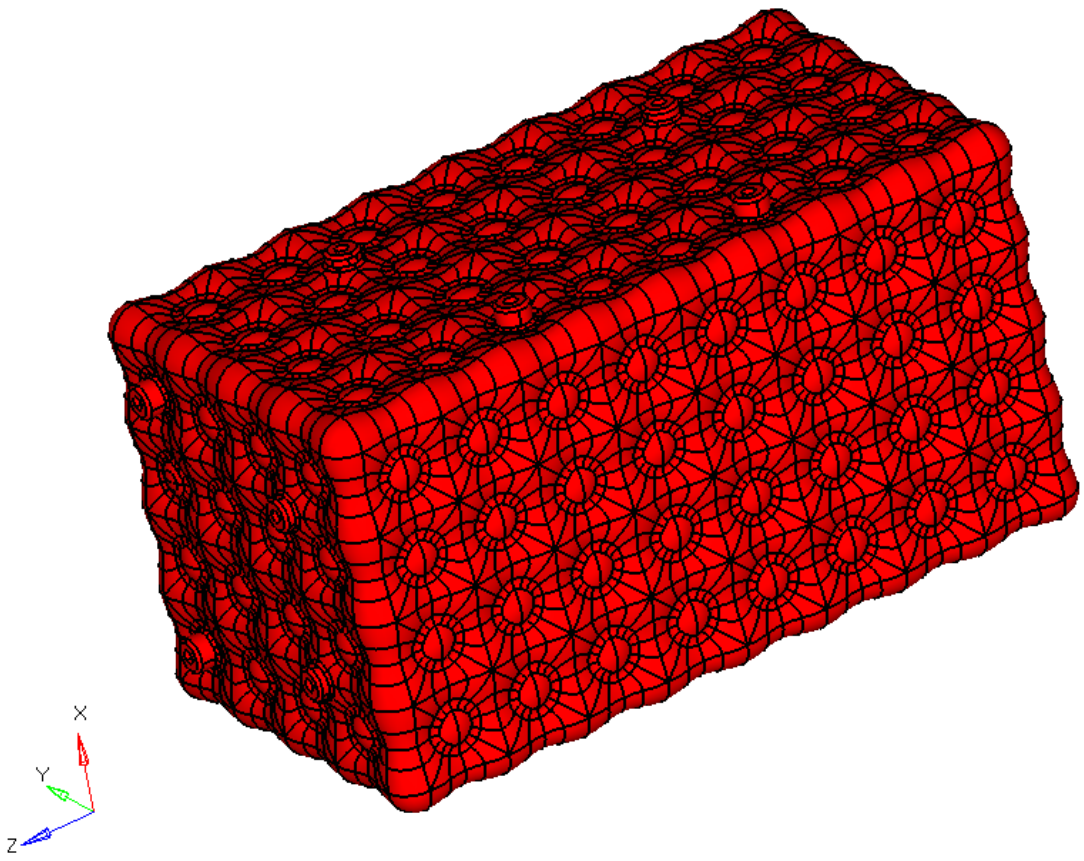

Figure 11-Conformable CNG Tank Geometry

This tank is symmetrical about all the three axes. As we can see, the tank geometry is quite complicated. The thickness of the tank is quite small and meshing this tank would create a lot of 3D elements with very less element size. In dynamic analysis the simulation time is directly proportional to the time step, which, in turn, is inversely proportional to element size. So if the element size is small, the simulation time drastically increases. The tank also brings in a lot of geometric non-linearity in the

analysis. To overcome this, an approximated tank is considered for the analysis. The approximated tank is a solid block having the same dimensions and mass of the Conformable CNG tank.

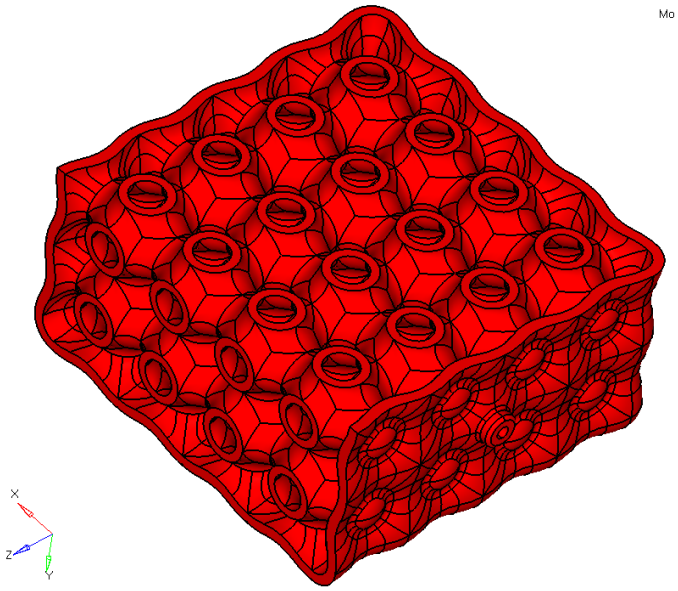

Figure 12- Quarter portion of the Conformable CNG Tank

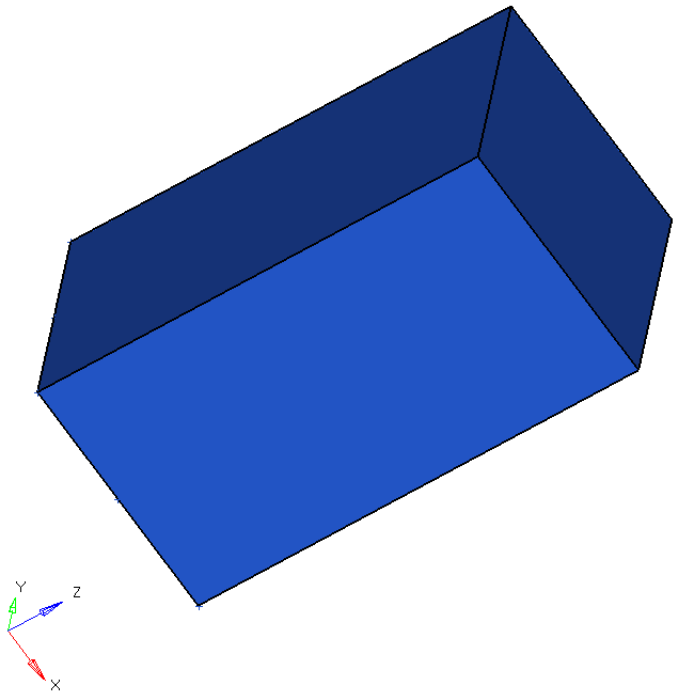

Figure 13-Equivalent CNG Tank

2.4 Tank-Bracket Assembly

After creating the tanks and bracket they had to be assembled. In the actual truck, two brackets support each tank. The tank is kept on the bracket, which has rubber padding and is wrapped around and bolted.

Figure 14- Rubber pad on the Bracket

A similar thing has been done here. A rubber pad is created and is placed on the bracket, such that there is a perfect fit between the tank and bracket.

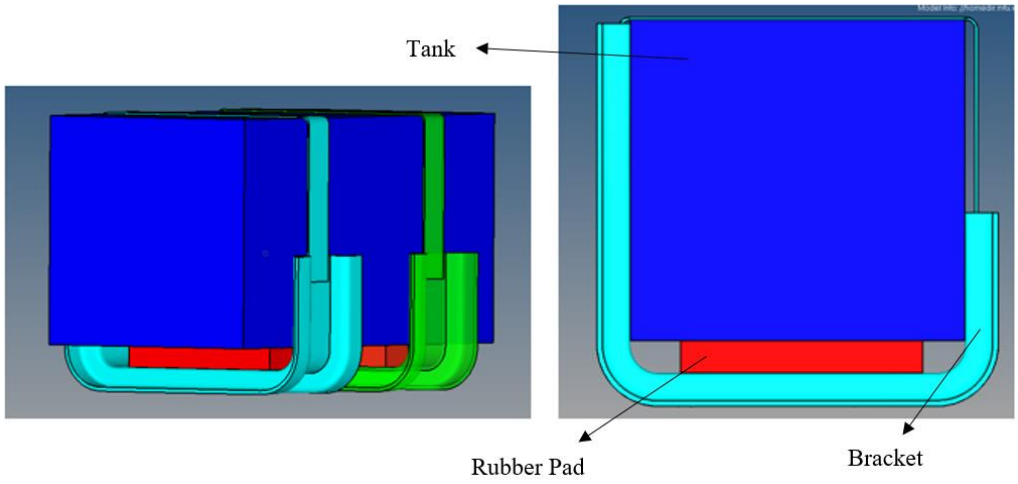

Figure 15- Rubber pad fitted in the tank-bracket assembly

2.5 Integration of the Tanks

After the tank-bracket assembly was created, they were integrated to the chassis. Totally, there are four tanks to be placed on the chassis - two are placed on the left side and two on the right side. The tanks are positioned exactly the same way they are placed in the truck.

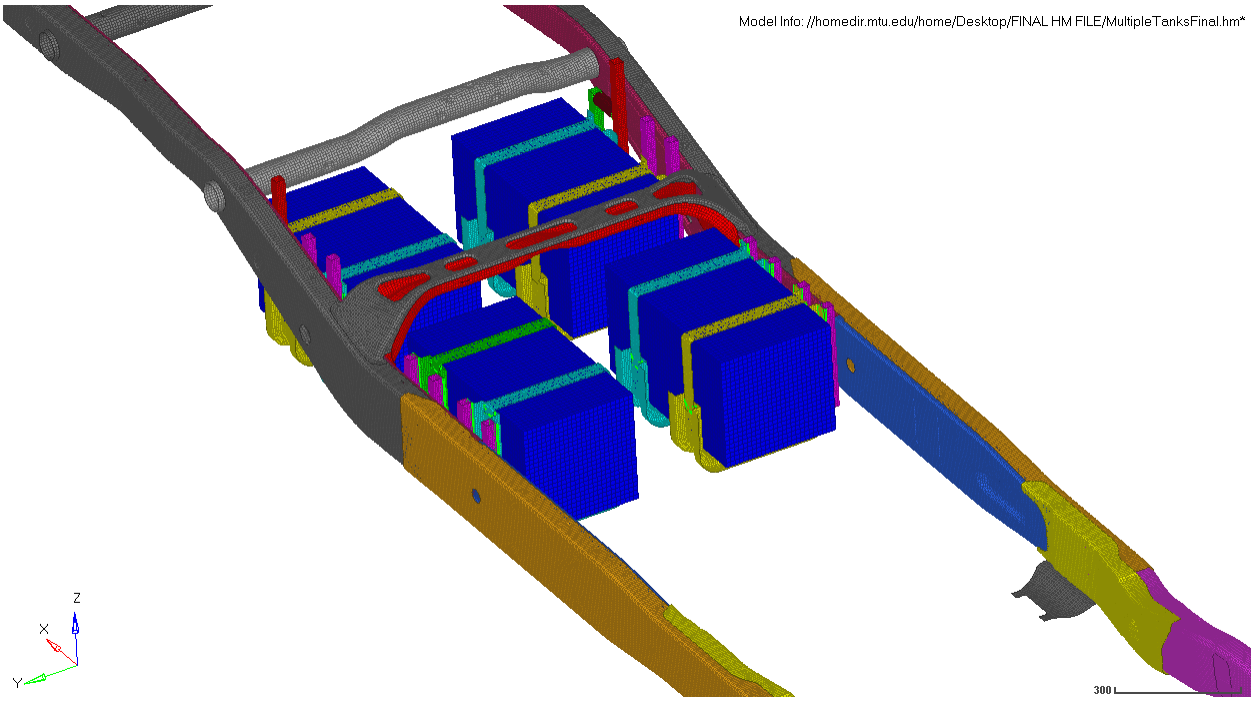

Figure 16- Tanks integrated to the chassis

Figure 17- Tanks installed in the truck chassis [6]

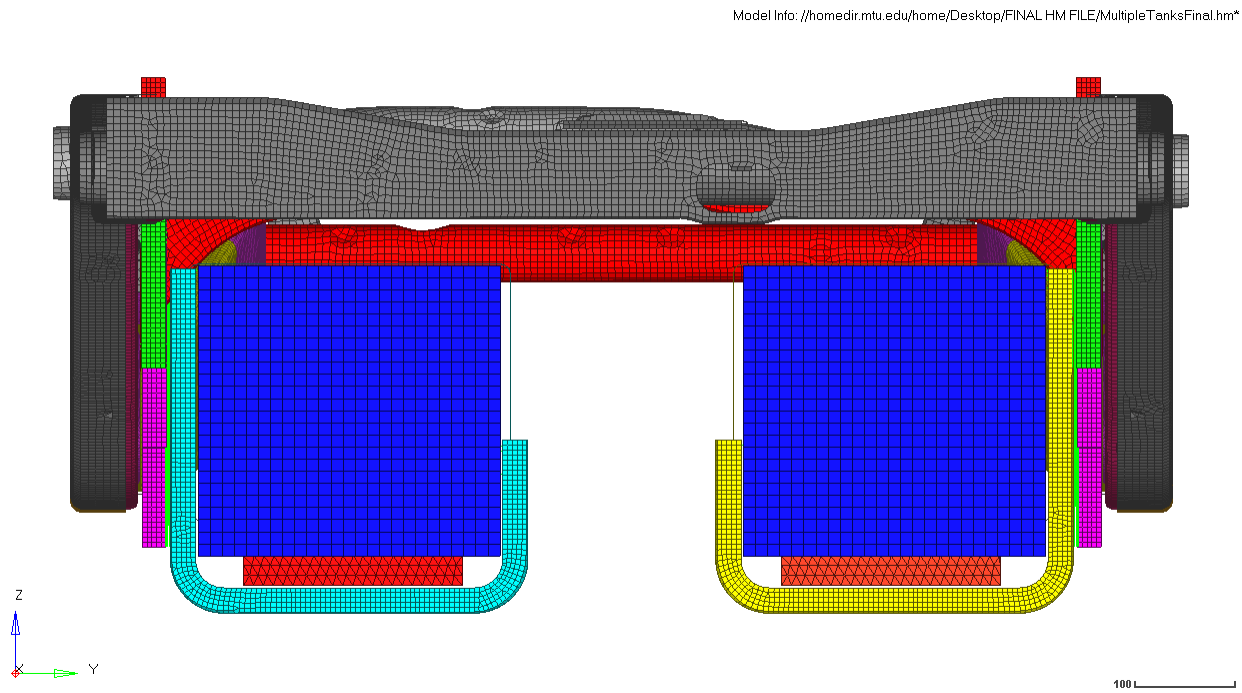

Figure 18- front view of the tanks attached to the chassis

3. Mesh Generation

3.1 Mesh Generation of the Chassis

After deleting the unnecessary parts, the CAD file was imported to HyperMesh in .step format. HyperMesh automatically places each part in a collector called component. The component in HyperMesh is an entity which contains the geometry and the mesh for a particular part. Every component is linked to a material and a property.

As mentioned earlier in section 1.1 all the parts in the chassis assembly were thin structures. It is not advisable to mesh these parts with 3D elements because if we do so, we would need at least 3 to 4 elements across the thickness. This will increase the total number of elements, which in turn increases the simulation time drastically. For this reason, the decision to perform the 2D meshing for the chassis was taken.

Whenever 2D mesh is done, HyperMesh creates shell elements on the surface. Shell elements have no visual thickness representation. The user assigns a thickness to the shell elements. The software assigns this thickness symmetrically to the mesh, assuming that the mesh is at the mid plane of the component. For this reason, the first step in 2D meshing was to extract the mid-surface of all the components. The method of extracting mid surfaces has been discussed in Altair [8]. There is an auto- mid surface extraction option in HyperMesh which extracts the mid surface. The mid surface of each part has been extracted and is saved in a separate component.

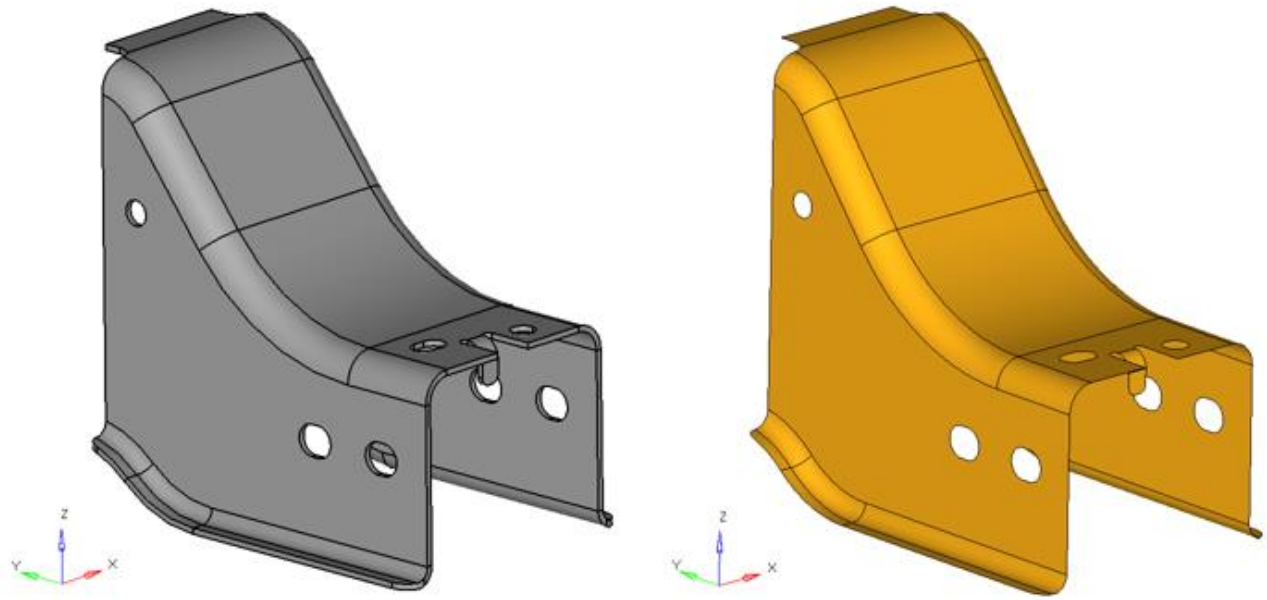

Figure 19-Part and its mid surface

After creating the mid-surfaces, a geometry cleanup was performed where any discrepancies in the CAD was corrected. Once the surfaces were checked, the 2D mesh was generated. HyperMesh 2D Automesh option was used. In Automesh the user can select the surfaces to mesh and provide a target element size & type and the software meshes the part. There are two types of 2D shell elements in HyperMesh, trias (3 node triangle element) and quads (4 node quadrilateral elements). All the surfaces are meshed with both types of elements. All the elements were first order elements.

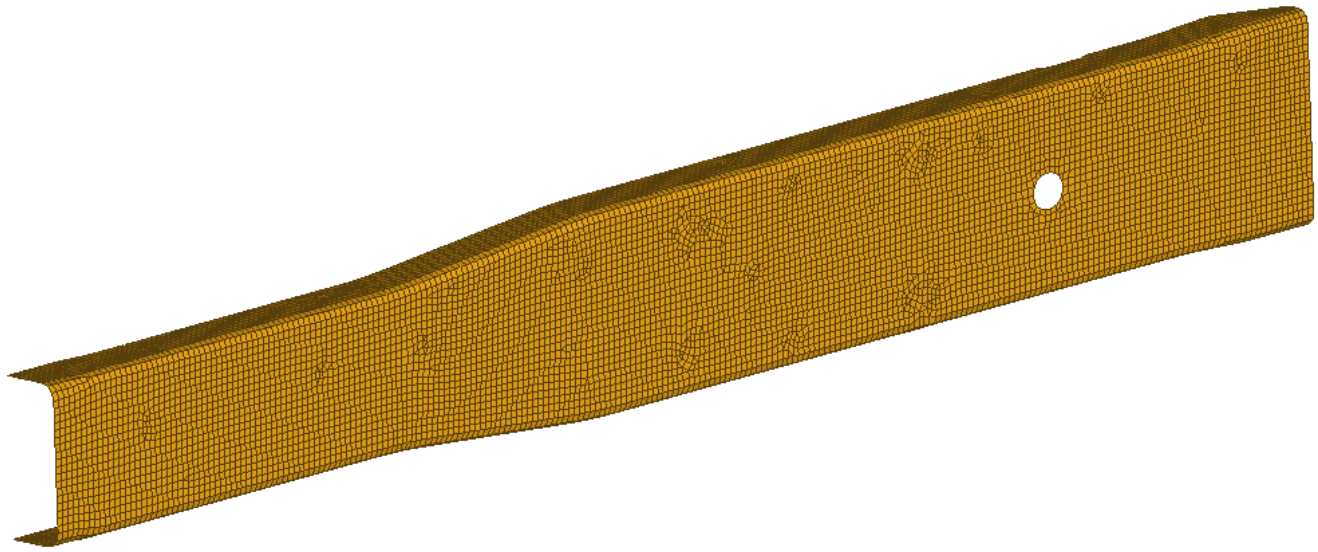

Figure 20-2D meshed part

After meshing, all the components had to be connected. In reality all the parts in the chassis are welded. A similar thing was performed in FEA where all the components are connected together by weld connections. HyperMesh has a connector option, where the user can connect parts by weld. The nodes of the edge of a part are selected, and the parts to be welded are selected. A 1D element is created connecting the two nodes.

There are many types of 1D elements which can be used for this function. As there was no data about the welds actually used, a Rigid element was used. The rigid element type used here in RADIOSS is RBE2. A picture showing the rigid element weld connections is shown below.

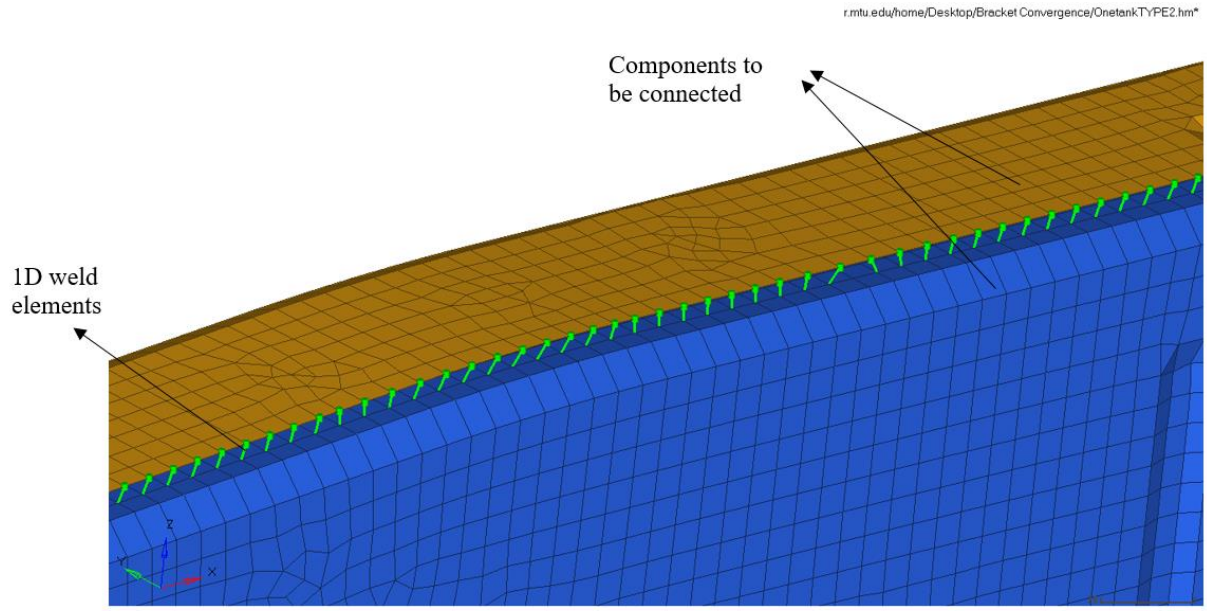

Figure 21-Detailed view of the 1D weld elements used to connect the components

3.2 Mesh Validation of Chassis

The right element size must be used for meshing, so that the results are not affected by the mesh. This is found out by Mesh Validation study. It is also called Mesh Convergence study. It is important as the mesh convergence study tells us the number of elements required to capture the geometric detail of the part to get the accurate results. Mesh convergence is done by meshing the part by a coarse mesh, and then refining the mesh to a suitable element size. After this the error between the consecutive meshes is checked and a small error indicates that the results are converged. Mesh convergence study is always performed for same type of elements, same boundary and loading conditions. To perform mesh validation many factors can be considered. Some of the factors generally considered are displacement, von Mises stress, strain energy etc. Most people consider Max von Mises stress as a factor for the mesh convergence. Considering max von Mises stress is incorrect as, for every mesh the location of the maximum von Mises stress varies. If the von-Mises stress or

displacement is considered, a geometric point must be selected and the results must be checked at that point.

As the chassis model is very huge the strain energy criteria is considered for the mesh convergence. Strain energy is a better criterion as it takes all the elements into consideration.

Frontal Impact to a Rigid barrier (RWALL) with an initial velocity of 35miles per hour were the conditions considered for the chassis mesh convergence. Only the weight of the chassis is considered here, no other loads are considered.

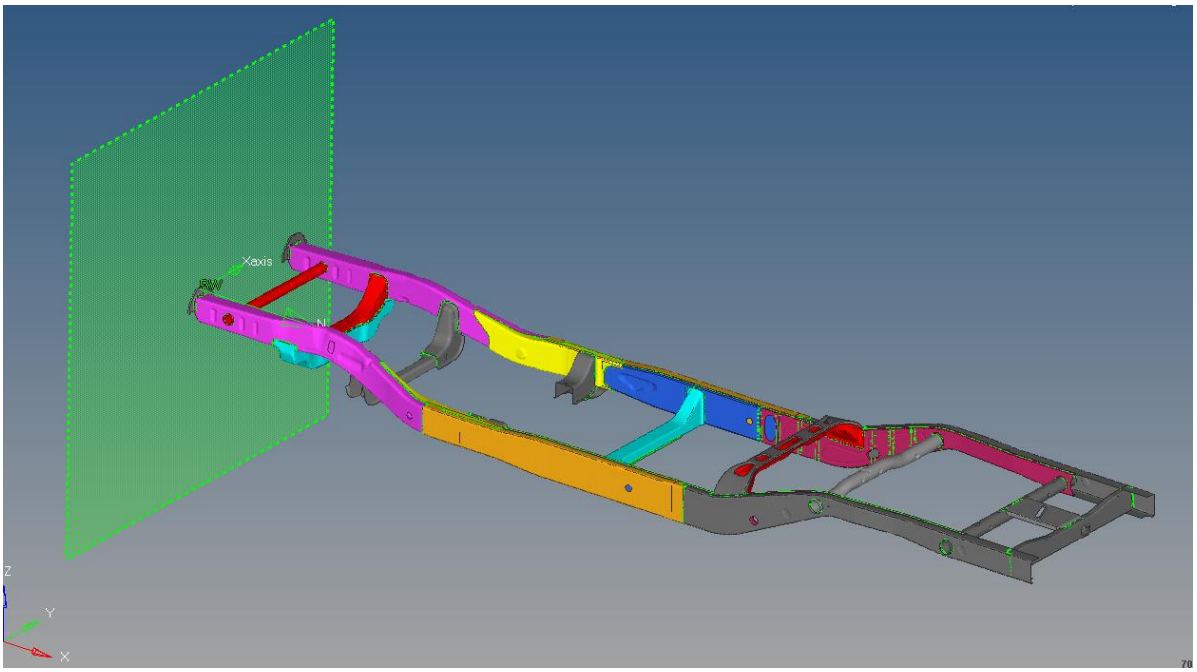

Figure 22-Model for mesh validation of Chassis

Table 1-Mesh Validation of Chassis

Element Size (mm)	Strain Energy (J)	Error (%)
5	20490	
6	20471	-0.09
7	20469	-0.01
8	20373	-0.47
9	20327	-0.23
10	19806	-2.56
12	19371	-2.20

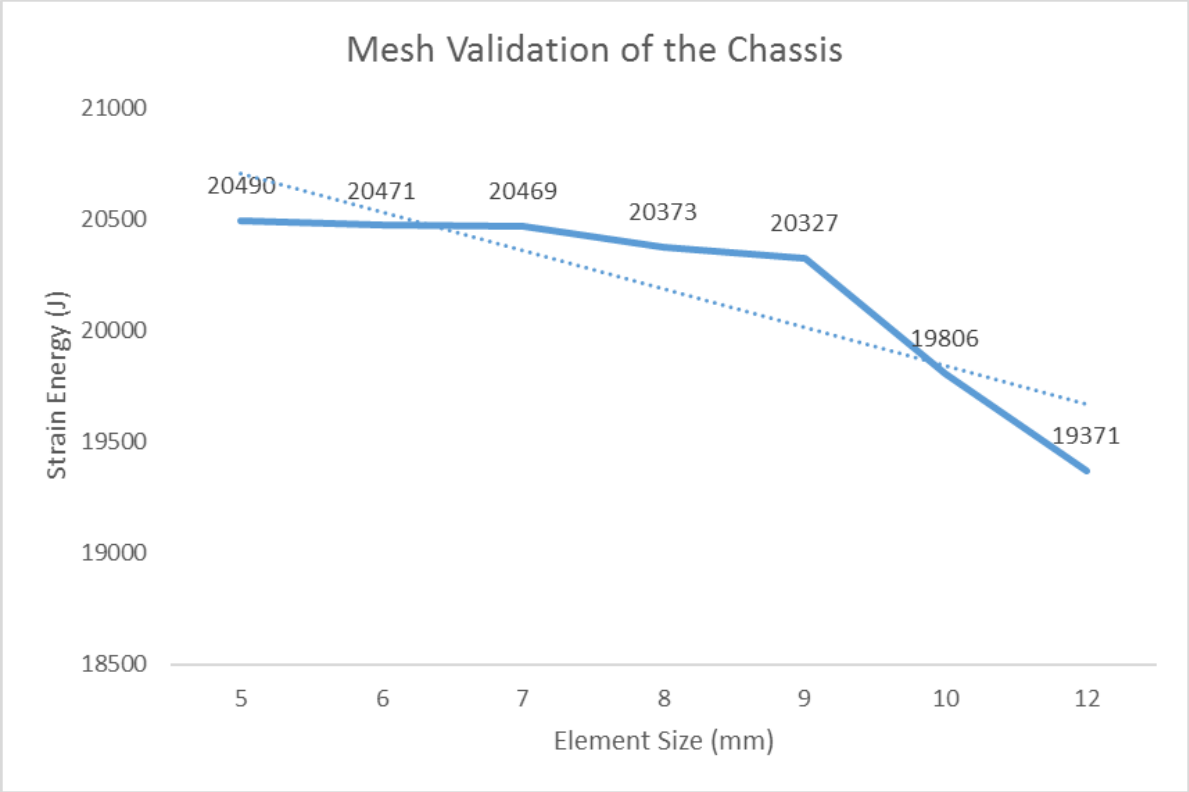

Figure 23-Mesh Validation for the chassis

From the graph, we can see that as we increase the element size the Strain Energy (J) of the model keeps decreasing. We can see from the table that for the element size of 7mm, the variation in the strain energy is very negligible. Thus 7mm was choosen as the element size to mesh the chassis. Altair's free guide 'Crash Analysis with RADIOSS' also recommends the element size to be within 5 to 10mm for crash application. [9]

Table 2-Simulation Time for various element sizes for Mesh Validation of the Chassis

Element Size (mm)	Computation Time (sec)
5	27103
6	11757
7	9551
8	7006
9	6852
10	1417
12	1769

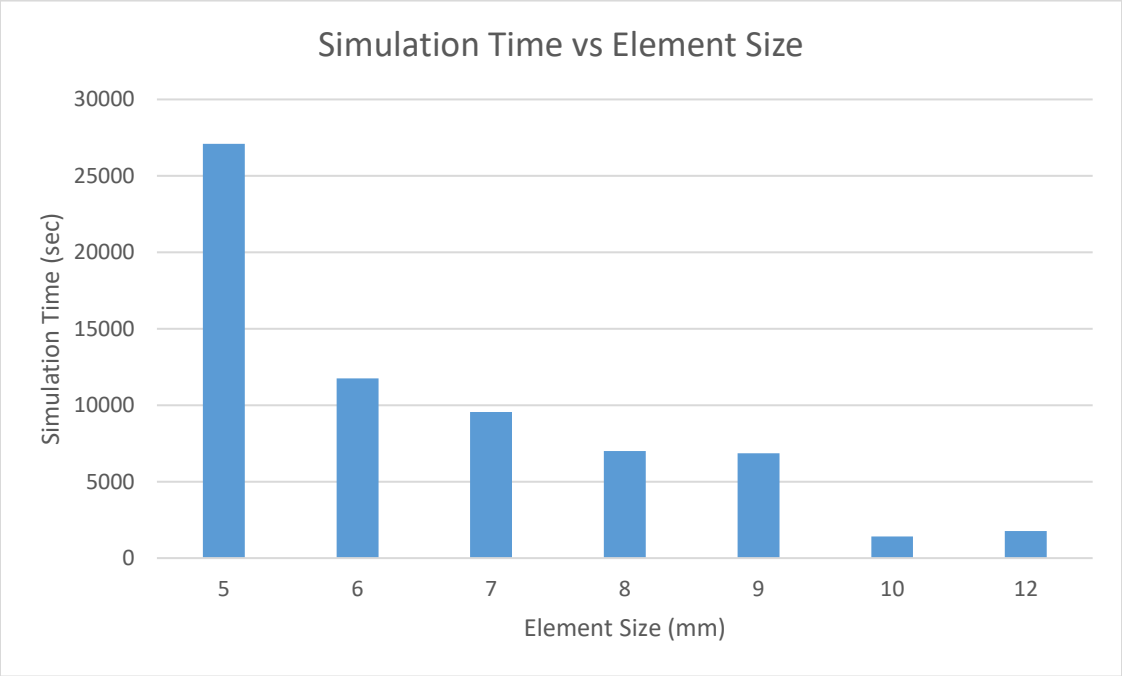

Figure 24-Simulation time vs element sizes for Mesh Validation of the Chassis

The Table and Figure above give a brief estimate on the simulation time for chassis mesh convergence. We can see that there is no clear linear relationship in the trend.

3.3 Mesh Generation of the Brackets

After creating the CAD models of the brackets, they were imported to HyperMesh in .STEP format. An initial geometry cleanup was performed to see if there are any discrepancies in the CAD, like uneven thickness, free edges, missing surfaces etc. As the thickness of the bracket was less compared to the other two dimensions, 2D elements were used to mesh the bracket. The mid surface command in HyperMesh automatically extracts the middle surface of a given geometry. The mid surface is the surface which is selected to be meshed. The surface here is meshed with first order shell elements, which include both tria and quad elements. The types of elements used for RADIOSS solver were SHELL3N and SHEL4N.

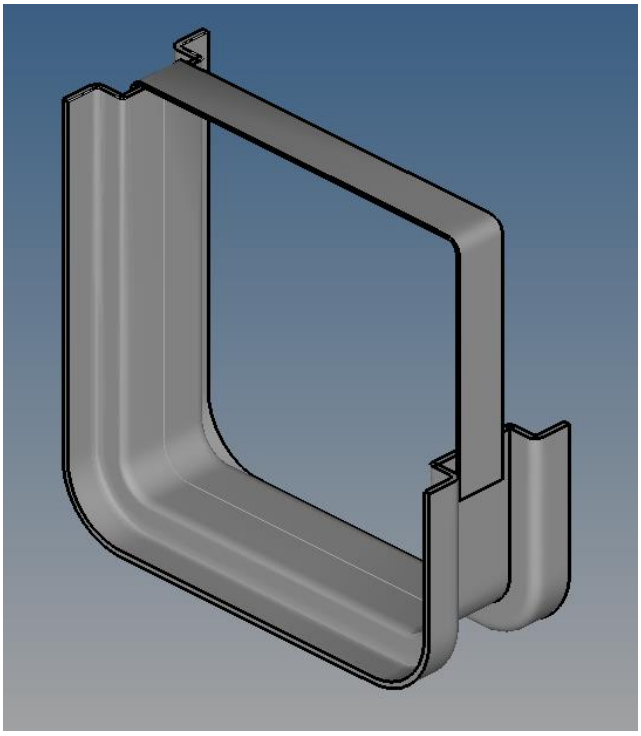

Figure 25-Solid Model of the Bracket imported in HyperMesh

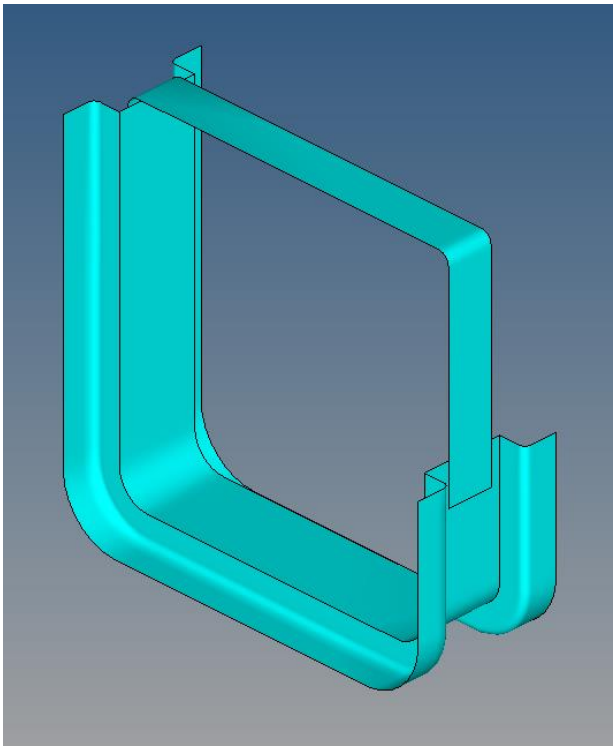

Figure 26-Mid Surface of the Bracket extracted in HyperMesh

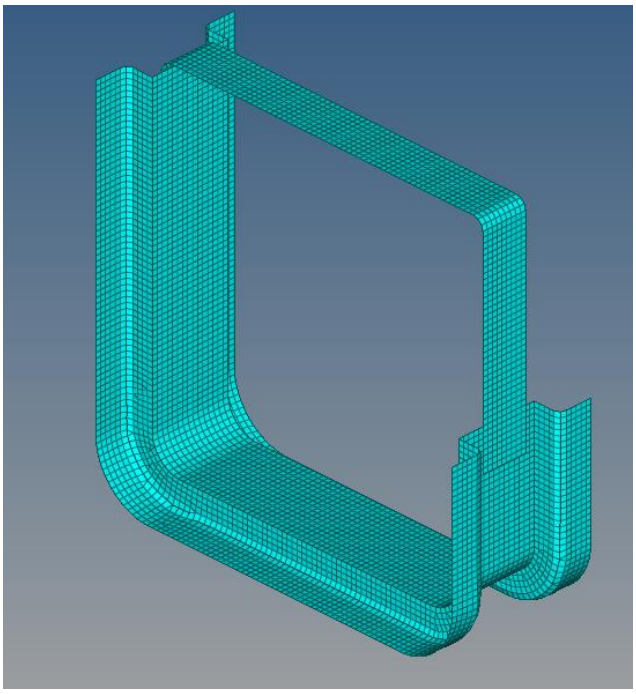

Figure 27-Meshed Bracket in HyperMesh

3.4 Mesh Validation of Brackets

Mesh convergence study is very important as it tells us the appropriate element size to be used for meshing in the model so that the results don't vary significantly. To perform mesh convergence, the loads and the boundary conditions for all models have to be the same. Here the convergence study was performed for 5 element sizes starting from 4mm to 10mm.

A dynamic analysis was carried out for the mesh convergence. Two brackets were used to perform mesh convergence. The brackets were connected to the chassis in the same position where it has been placed in the truck. The conditions for the analysis was a Frontal Impact to a Rigid barrier (RWALL) with an initial velocity of 35miles per hour. Only the weight of the chassis is considered here, no other loads are considered. Strain Energy was chosen to be the parameter for mesh convergence.

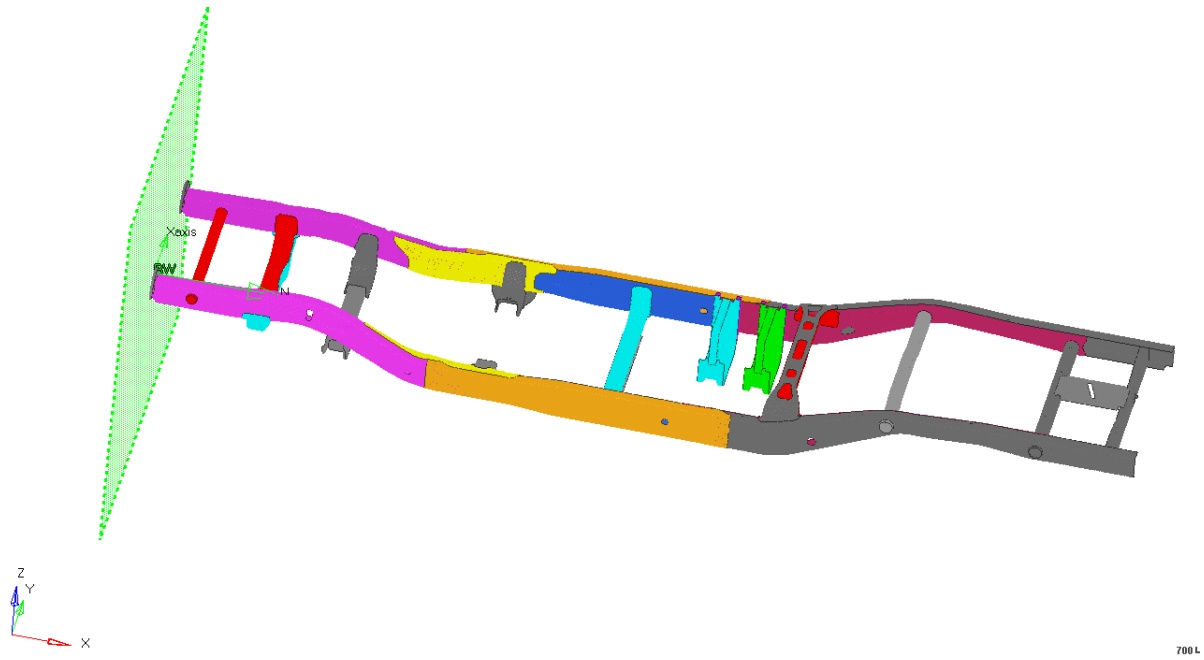

Figure 28-Model for Mesh Validation of Brackets

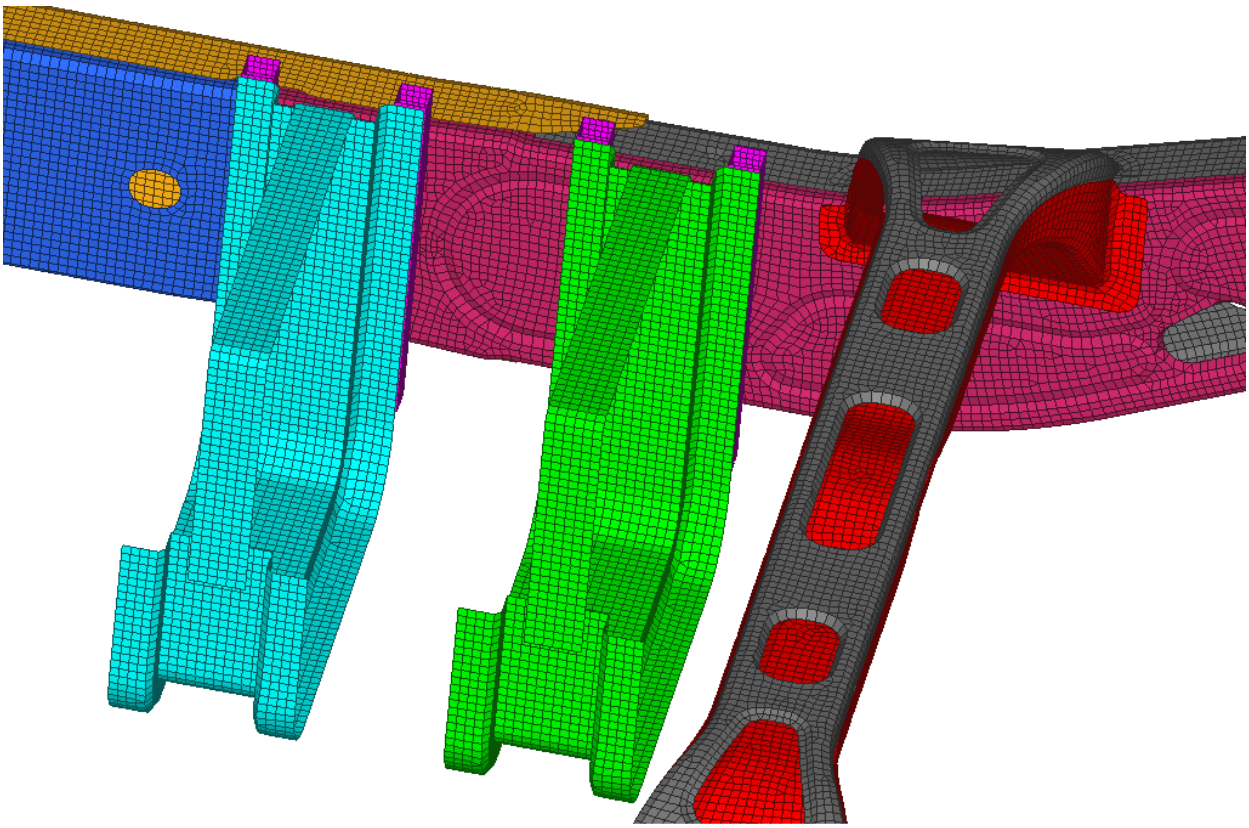

Figure 29-Detailed view showing the Brackets

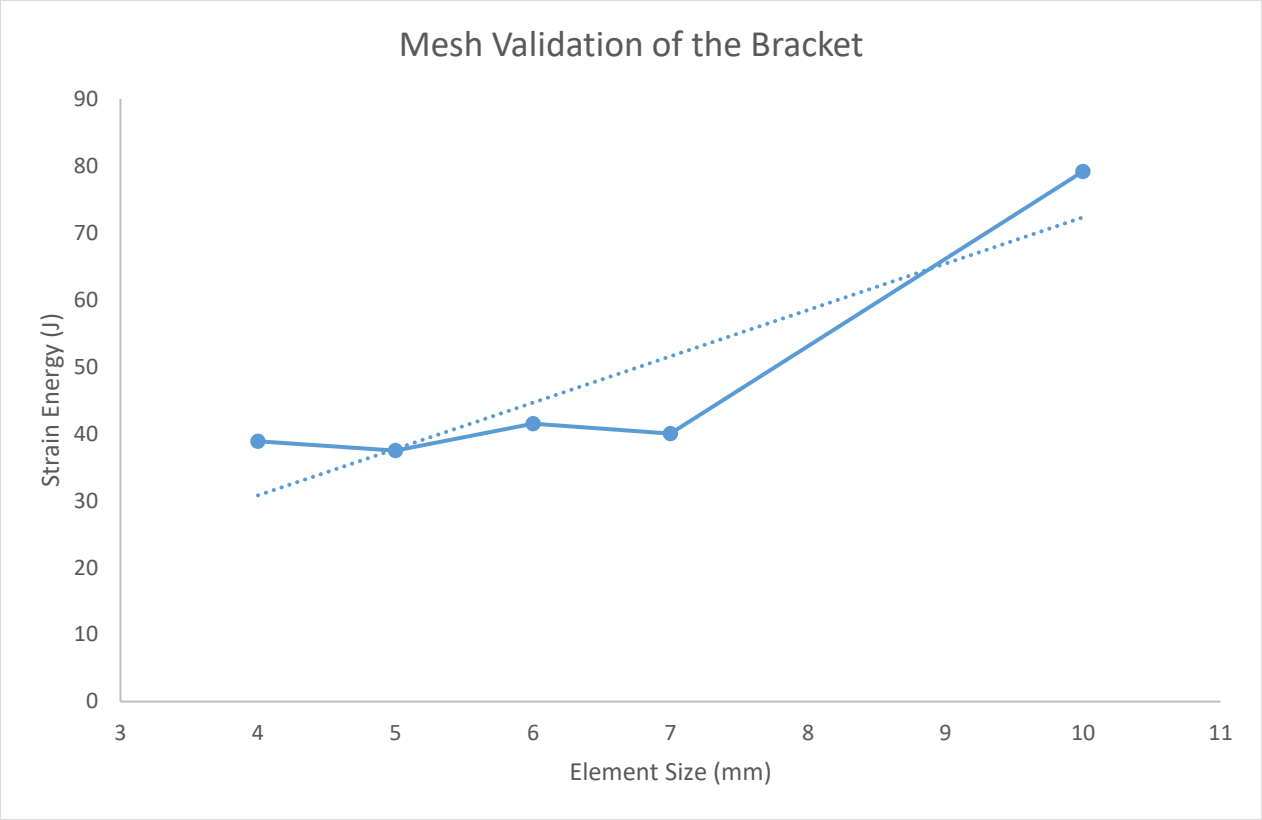

Figure 30-Mesh validation of the bracket

Table 3-Mesh validation of the Bracket

Element Size (mm)	Strain Energy (J)	Error (%)
4	38.86	
5	37.48	-3.55
6	41.48	10.67
7	40.04	-3.47
10	79.17	97.73

From the given table we can see that for element size of 5 mm the strain energy of the bracket was 37.48 and the error was not huge. So, 5 mm was chosen as the element size to mesh the bracket.

Table 4 and Figure 26 give an estimate of the simulation time for the mesh validation of the bracket. We can see that there is no clear linear relationship in the trend of the simulation time.

Table 4-Simulation time for Mesh Validation of the Bracket

Element Size (mm)	Simulation Time (sec)
4	5607
5	5478
6	5319
7	5521
10	5180

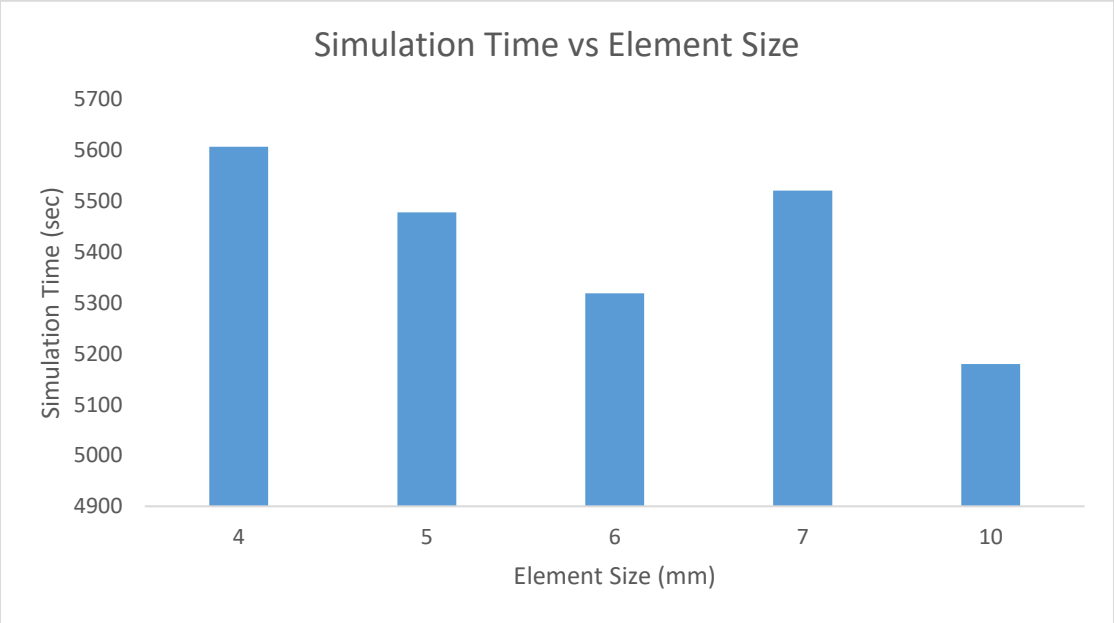

Figure 31-Simulation time vs Element Size for Mesh Validation of the Bracket

3.5 Mesh Generation of Tank

The CNG tank was meshed using 3D tetrahedral elements using HyperMesh Solid map mesh command. In the solid map mesh, the user can select a solid, the element length and other quality properties. HyperMesh automatically meshes the part.

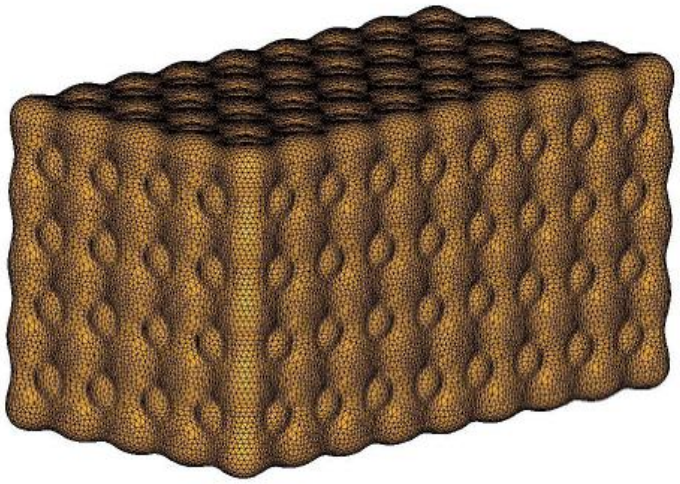

Figure 32-Conformable CNG tank meshed with 3D elements

3.6 Mesh Validation of the Tank

The mesh validation of the tank was done by Amruta Kulkarni, who defended her report titles 'FINITE ELEMENT ANALYSIS OF CONFORMABLE CNG TANK – TOPOLOGY OPTIMIZATION AND DROP TEST SIMULATION' [10]. From her report she found that for element size 0.2 inch the solution converged. The same element size was used here.

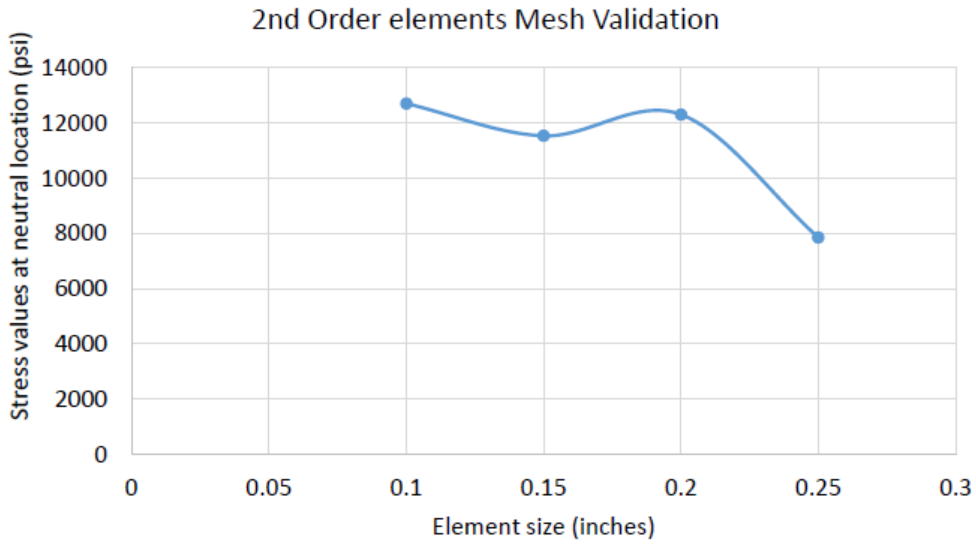

Figure 33-Mesh Validation of the CNG tank

3.6 Mesh Generation of the Rubber Pad

The rubber pad is also meshed with 3D tetrahedral elements using the solid map mesh command in HyperMesh.

3.7 Element Quality and Checks

After meshing the chassis, brackets and tanks the models were checked for their element quality. In the book “Practical Aspects of Finite Element Simulation” (Altair University, 2015) [8] the general element qualities are mentioned. The same were used as the quality for all the meshes.

Table 5-2D element quality criteria

Parameter	Criteria	Percentage of Failed Elements	
		Chassis model	Bracket model
Aspect Ratio	< 5	0	0
Jacobian	>0.6	0	0
Skew	< 45 deg	0	0
Min angle for tria	> 20 deg	0	0
Max Angle for tria	< 120 deg	0	0
Min angle for quad	> 45 deg	0	0
Max angle for quad	< 135 deg	0	0

Table 6-3D element quality criteria

Parameter	Criteria	Percentage of Failed Elements
Tetra Collapse	>0.1	0
Jacobian	>0.5	0
Volumetric Skew	< 0.7	1

4. Material Properties

4.1 Material Properties of Chassis

In automotive applications, High strength Low Alloy (HSLA) steels are used as they can handle high loads and are also light in weight i.e. they have high strength to weight ratio. Rashid (General Motors) [11] has published a paper in SAE International, titled "GM 980X- Potential Applications and Review" in 1977 International Automotive Engineering Congress and Exposition. The paper discusses the High strength low alloy steels available for automotive market. Various alloys of steels are reviewed and their micro structures are studied.

No material data was available for the chassis material. Based on the paper the material for the chassis was assumed to be SAE980X steel. The properties of SAE 980X are taken from MATWEB material database [12].

Table 7-Material Properties of SAE 980X HSLA steel

SAE 980X Mechanical Properties	
Density	7.75 g/cc
Modulus of Elasticity	206 GPa
Poissons Rato	0.29
Yield Stress	550 MPa
Ultimate Tensile Stress	655 MPa
Yield Strain	0.20%
Elongation at Break	10%

As we are simulating a crash scenario, we cannot use a perfectly elastic material model. The nonlinear properties of the material also have to be considered. In RADIOSS there are a variety of material models. The most common material models used for Elasto-Plastic deformation are Johnson Cook Law (LAW 2) and Tabulate Piecewise Linear (LAW36). The Johnson-Cook material model is an elasto-plastic material model which includes strain rate and temperature effects. For simplification, and due to lack of material data, the Johnson-Cook material model is not chosen. Instead, the Piecewise Linear model (law 36) is chosen.

In RADIOSS, the LAW 36 models an isotropic material using a user defined function. The user inputs the Elastic properties of the material and also the work-hardening portion of the stress - strain curve which is nothing but plastic strain vs stress. Here the elongation at break is considered as the ultimate tensile strain. In LAW 36, the material follows the input stress strain curve and if the strains go beyond the last point in the curve they would get deleted. To avoid this, the material model is considered perfectly plastic after the ultimate strength. The stress after the ultimate stress is considered constant up to a strain of 0.3.

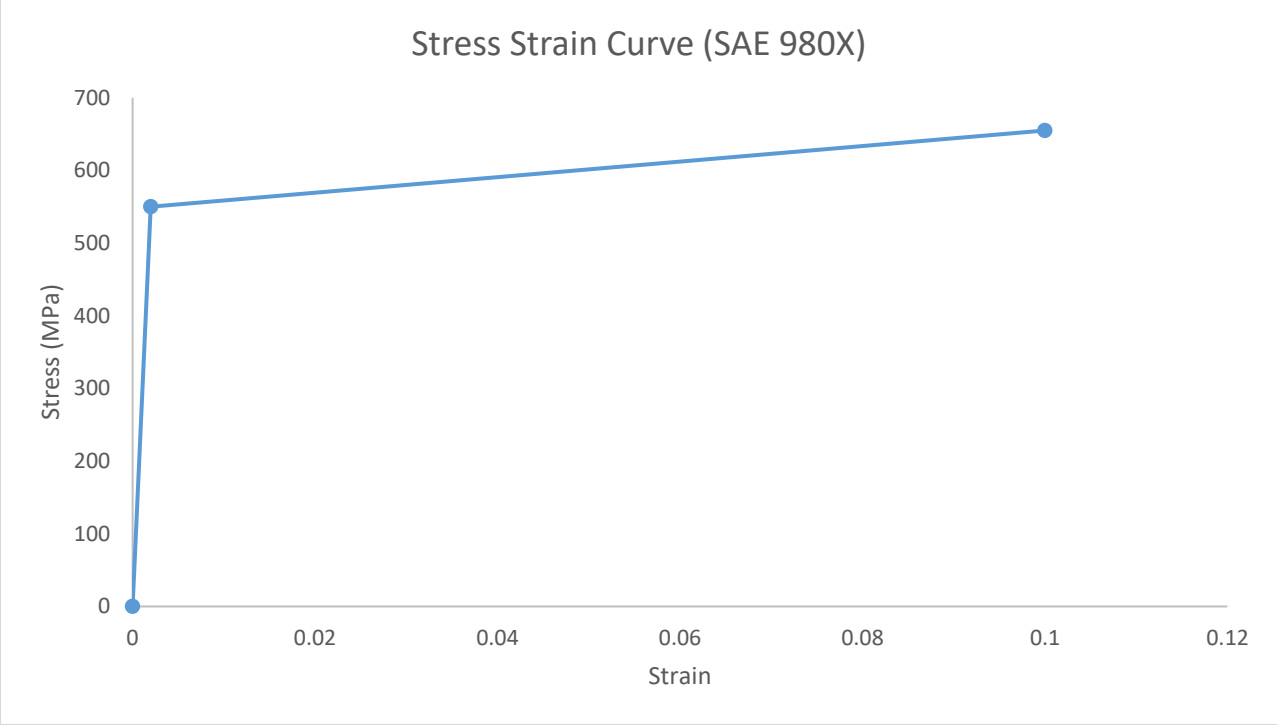

Figure 34-Stress Strain Curve for SAE980X

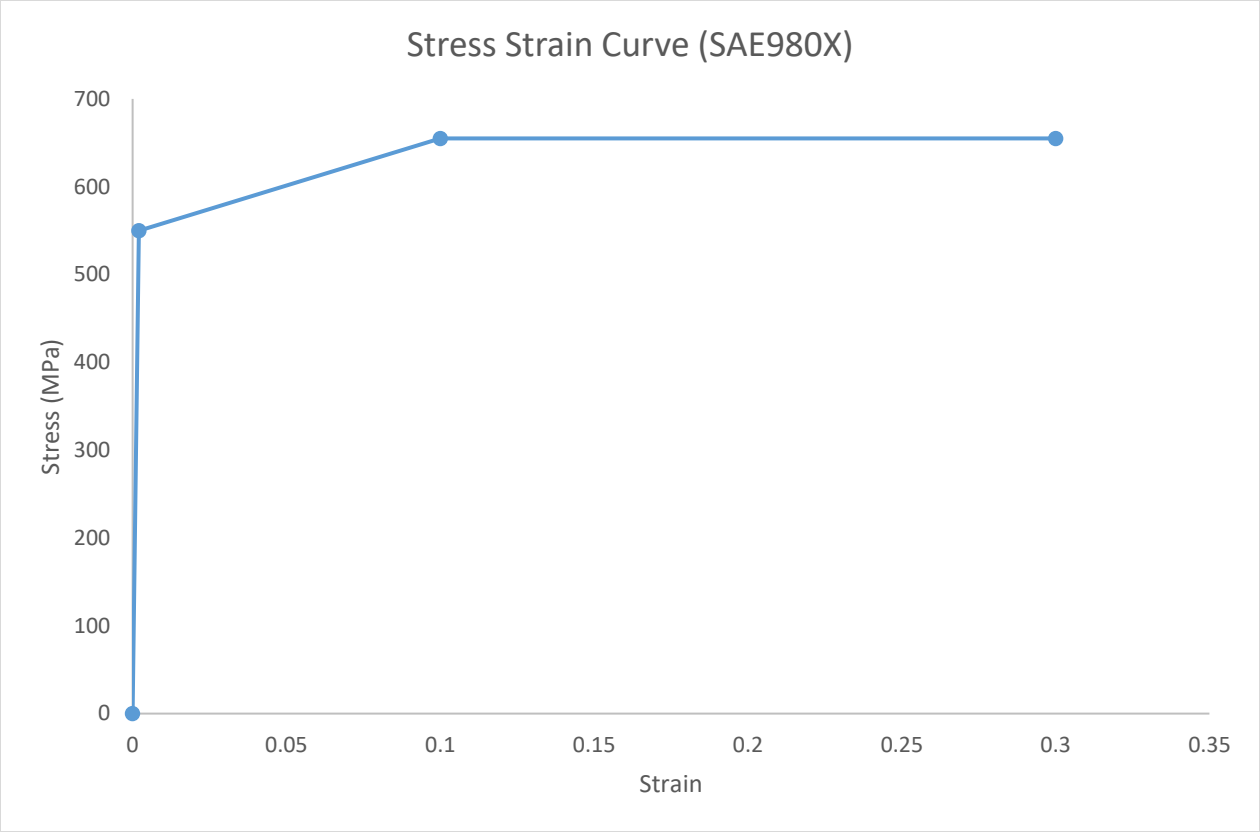

Figure 35-Perfectly Plastic Curve used for simulation

4.2 Material Properties of the Bracket

The material of the Bracket was found to be made of steel. The material of the bracket was also considered to be SAE980X steel. The same material properties listed in Table 7 were used. The same material card used for the chassis (LAW 36) was used.

4.3 Material Properties of Tank

The material used for the conformable CNG tank was Aluminum A 206-T7 casting alloy. The material properties of this alloy were taken from MATWEB material database [13]. Table 8 shows the material properties of Al206 alloy.

Table 8-Material Properties of Aluminum alloy Al206.0-T7

Al206.0-T7 Mechanical Properties	
Density	2.8 g/cc
Modulus of Elasticity	70 GPa
Poisson's Ratio	0.33
Yield Stress	350 MPa
Ultimate Tensile Stress	436 MPa

.

4.4 Effective Material Properties

As discussed in section 2.3, to simplify the analysis an equivalent tank having a simple geometry is being considered. As the geometry of the proposed equivalent tank and the conformable CNG tank are different, the material properties of AL206 alloy cannot be used. Researches from NASA have proposed a method to develop structure- property relationship of nano- structured materials using equivalent continuum modeling [20]. A similar approach is being followed here to compute the material properties of the tank.

The equivalent tank and the conformable CNG tank are assumed to be equivalent when the elastic strain energy stored in the two models is equal under identical loading conditions.

The equivalent tank is assumed to be a perfectly elastic Isotropic material. The Poisson's Ratio of the equivalent tank is assumed 0.33, which is same as the conformable CNG tank. The value of the Elastic Modulus that results in equal strain energies is the effective stiffness of the equivalent tank.

In OPTISTRUCT, (a linear- non-linear Structural Finite Element Solver) both the tanks are subjected to a uniaxial tension test. As the tanks are symmetric about all three planes, one quarter of each of the tank is chosen for the analysis. The symmetric boundary conditions are applied to both the tanks. As solid elements do not have any rotational degrees of freedom [8] the nodes are constrained in their respective

translational degrees of freedom. A pressure load of 20MPa is applied in the Z direction to simulate tension test.

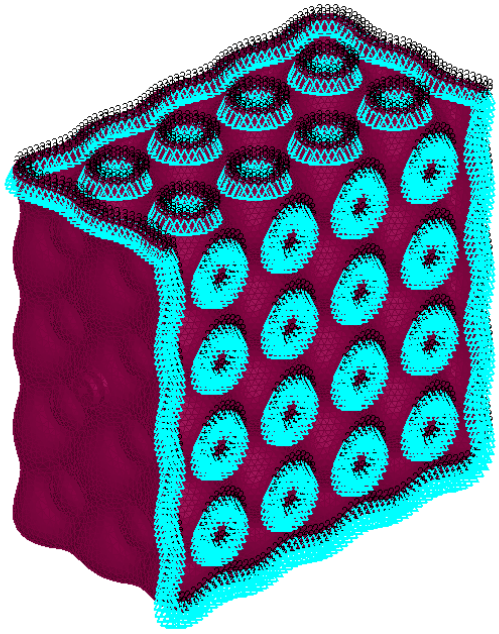

Figure 36-Symmetric Boundary Conditions applied to the CNG tank

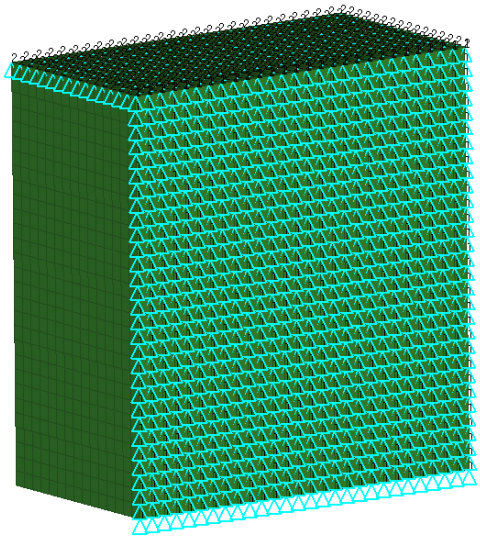

Figure 37-Symmetric Boundary Conditions applied to the Approximated Tank

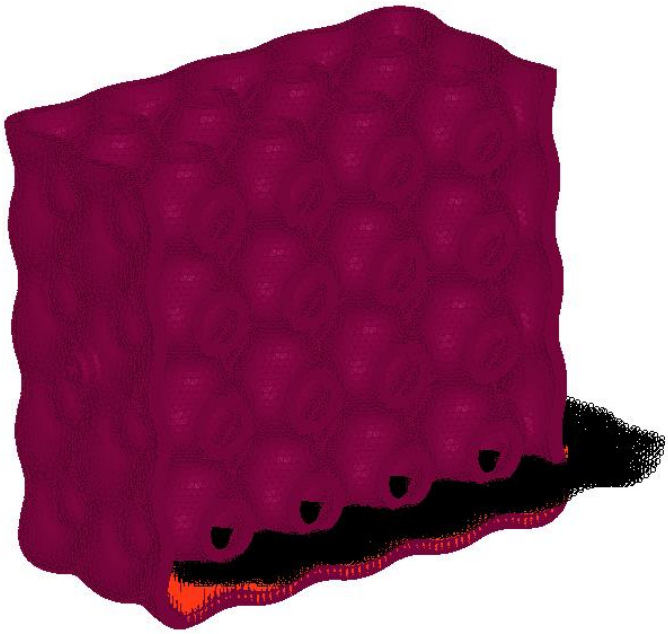

Figure 38-Uniaxial Pressure Load applied to the CNG tank

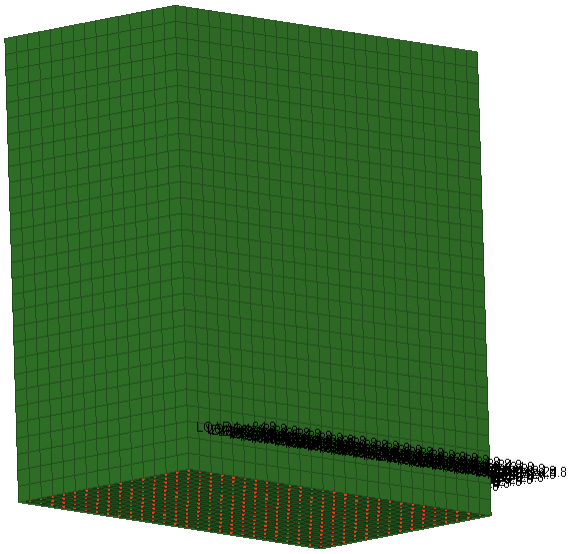

Figure 39-Uniaxial Pressure Load applied to the Approximated Tank

After conducting the uniaxial test on the conformable CNG tank, the strain energy was found out to be 5.725 J. The effective stiffness for the equivalent tank is found to be

49.925 GPa for which the strain energy is 5.725 J. The effective yield stress of the equivalent tank is computed using the strain energy and the effective stiffness.

Table 9-Material Properties of the Effective Tank

Material Properties of Effective Tank	
Density	0.8648 g/cc
Modulus of Elasticity	49.925 GPa
Poisson's Ratio	0.33
Yield Stress	164.25 MPa

The Effective stiffness was validated by applying different pressures on both the tanks to check that they had the same strain energy.

Table 10-Strain Energy of the tanks for various loads

	Strain Energy (J)	
Load (MPa)	CNG tank	Approximated Tank
10	1.431	1.431
20	5.725	5.724
24.82	8.816	8.816

4.5 Material Properties of Rubber Pad

The material properties of the rubber pad were unknown. The material was assumed to be hard rubber and the properties were taken from the Internet [17][18][19]. The Rubber was assumed Isotropic and the Material Card MAT1 in RADIOSS was used.

Table 11-Material Properties of Rubber Pad

Density	1200 kg/m3
Modulus of Elasticity	10 MPa
Poisson's Ratio	0.48

5. Contact Modeling

Contact modeling or interface modeling is the most crucial part in Dynamic Finite Element Analysis. Contact is the most common source of non-linearity in Dynamic FEA. We know that in FEA the Stiffness matrix (K) is always a function of nodal displacements. In non-linear problems where there is contact the stiffness matrix (K) changes with time. Contact/interface modeling in FEA is where the user defines how parts interact with each other when they come into contact.

RADIOSS contains several ways to model contacts. All the contacts in RADIOSS come under the section Interfaces. The user has to activate an Interface card (/INTER/) to define contacts. In the Interface definition the user has to mainly define a master set and a slave set. They can be surfaces, elements or nodes. There are more than 15 cards to define contact in RADIOSS. [9] The most common contacts are always between a set of slave nodes and a surface, a surface and a surface or self-contact.

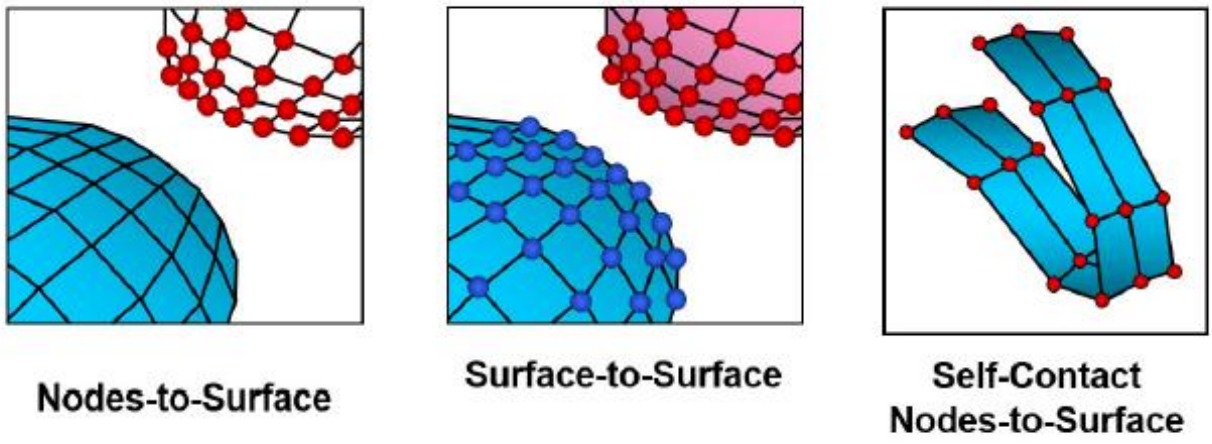

Figure 40-Most common type of Contacts [9]

In Finite Element Analysis, there are two main techniques to treat the contact problems, namely the Lagrange multiplier method and the Penalty method. Penalty method is used in most of the contacts in RADIOSS. A gap is always defined between the slave set and the master set. This gap determines if the slave node is in contact with the

master segment. As the contact occurs and if any node penetrates into the gap, an elastic spring is generated between the master and slave set and this generates a resistive force between them. This is discussed in detail in the RADIOSS User Guide under the Interfaces section. [14] This section further discusses how contacts are modelled between various components for the analysis.

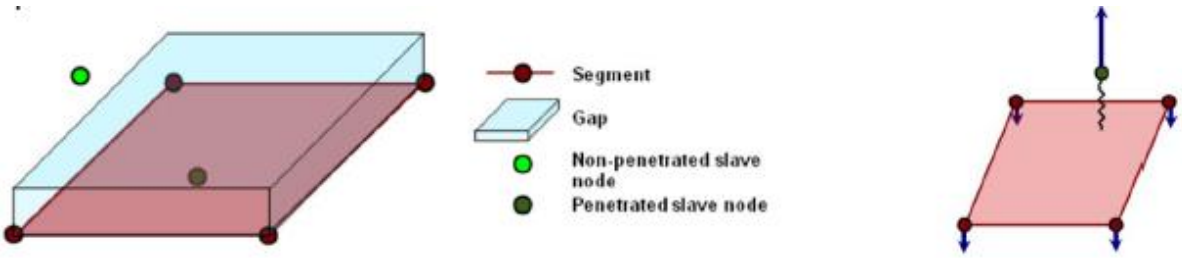

Figure 41-Penalty method in RADIOSS [9]

5.1 Self Contact among all parts

The most common type of interface used in RADIOSS for crash structure applications is the Type 7 Interface. Type 7 Interface in RADIOSS is a general purpose contact which can simulate impact between a master surface and a set of slave nodes. Interface Type 7 in RADIOSS is unique compared to other interfaces as it is non-oriented, i.e. the slave nodes can also lie on the master surface. Due to this reason, this type of contact can be used to simulate auto-impact among all the parts during the crash scenario.

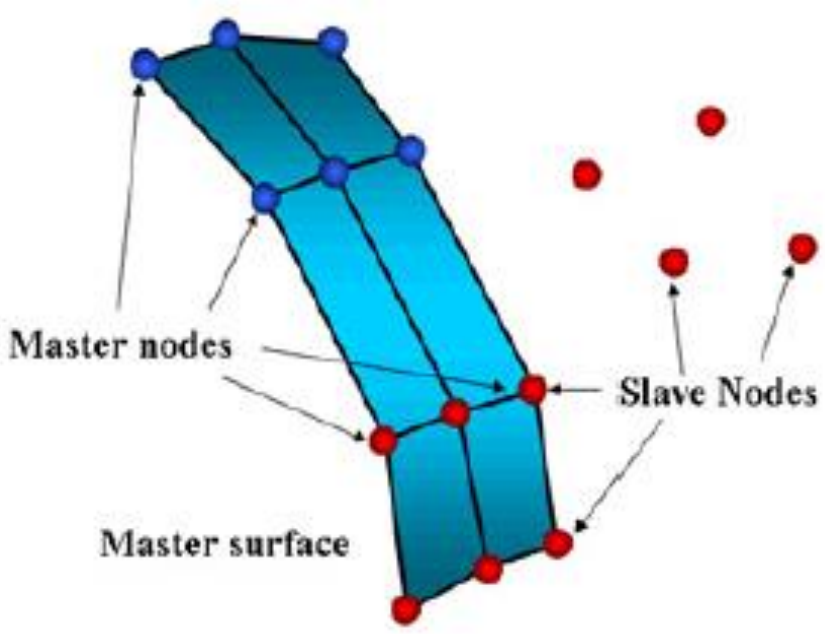

Figure 42- Master-Slave set in Type 7 Interface [15]

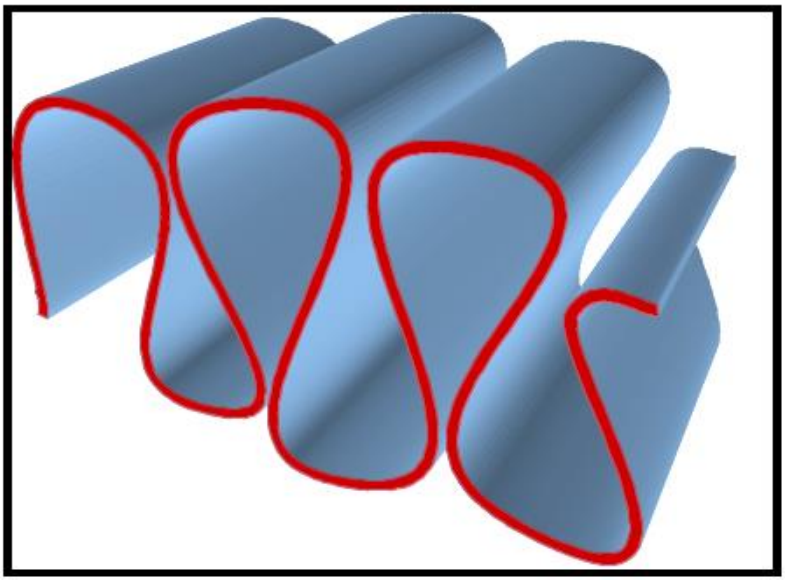

Figure 43-Example of Auto impact surface [15]

This Type 7 Interface card is used to define contacts for all the surfaces so that there is no self contact or auto impact among them. For the master segment all the components are selected. For the slave segment all the nodes are selected.

5.2 Contact in the Tank-Bracket assembly

After defining the self contact, it is important to define the contact among the tank and the bracket assembly. In reality the bracket holds the tank tightly in place such that there is no relative movement between the tank and the bracket. This can be simulated by Type 2 Interface in RADIOSS which is tied interface. In this, the user has to define a master segment and a set of slave nodes. The slave nodes are projected to the master surface with a gap and they are tied to the master surface. It is recommended that the master surface has a coarser mesh.

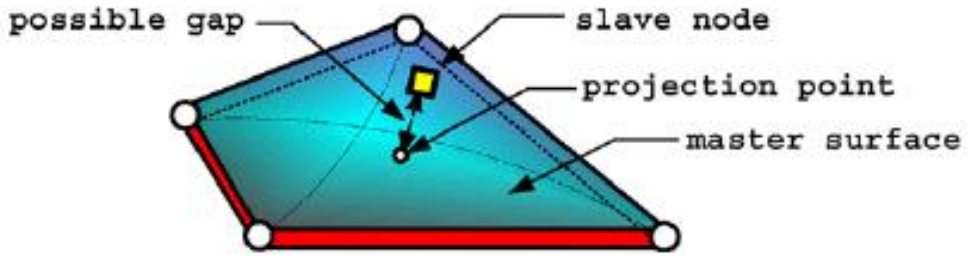

Figure 44- Tied Contact (Type2) [15]

This Type 2 contact is set up in the Tank-bracket assembly. It is defined between the bracket and the tank, bracket and the rubber pad and, the tank and rubber pad.

6. Loading and Boundary Conditions

As mentioned in chapter 1, the main objective is to analyze the stresses on the tank for frontal crash. In the automotive industry most of the crash testing is done as per FMVSS (Federal Motor Vehicle Safety Standards). One of the most important and common FMVSS standard used is the FMVSS 208. This is a frontal crash test where the automobile is crashed to a rigid barrier with a fixed speed to check for crashworthiness. For this project a similar scenario is considered, where the chassis is impacted to a rigid barrier (Rigid Wall). The boundary condition here was a rigid barrier.

In RADIOSS, there is an option of creating a rigid barrier. Rigid Wall in RADIOSS is found as a card named /RWALL. This card creates a rigid wall and a slave node set must be defined. There are four types of rigid walls available in RADIOSS. They are Infinite wall, Infinite Cylindrical wall, Spherical wall and finite planar wall. For this project an infinite Wall is considered. Rigid wall is purely rigid i.e. there is no deformation in the wall. The wall does not absorb any energy after impact and it has infinite stiffness. The slave node set defined in the card makes sure that the nodes defined do not penetrate into the wall. All nodes in the model are selected to be the slave nodes of the rigid wall. The rigid wall can be fixed or moving. Here the rigid wall is fixed.

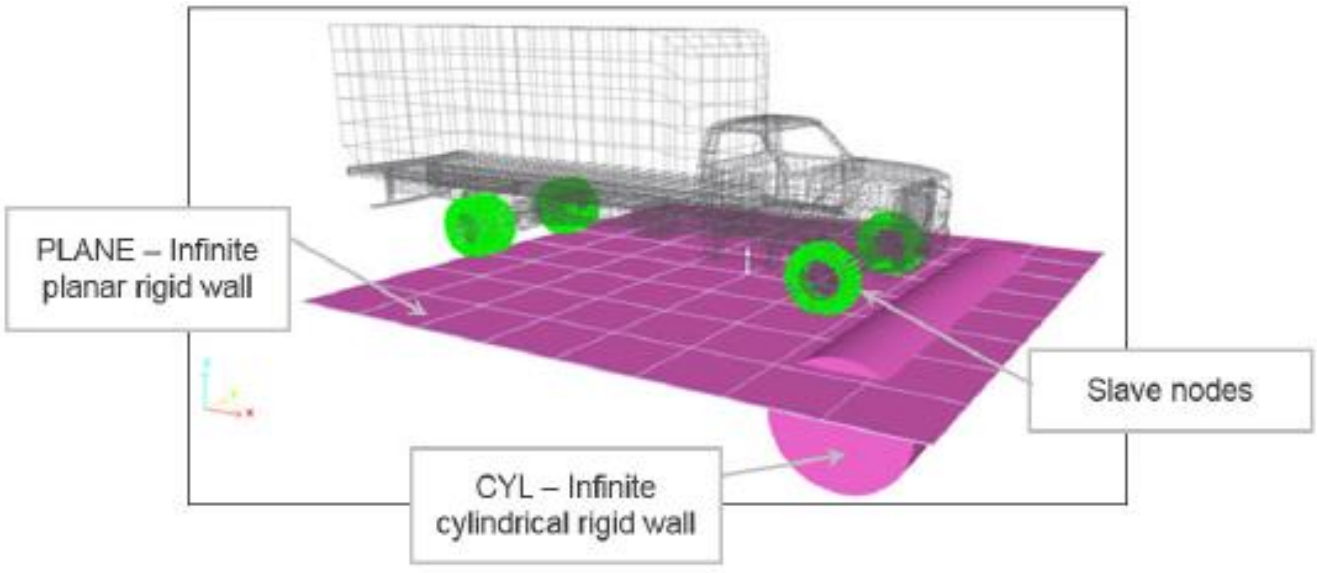

Figure 45-Rigid Wall with slave nodes [9]

Two loading conditions are considered here. They are 35 mph (miles per hour) and 55 mph. The velocity was given as an Initial velocity in the X direction to all the components in the model. For simplification, the weight of the chassis and tank-bracket assembly are only considered here. The weight of the body, engine, transmission, passengers and cargo are not considered here. The tanks are not pressurized here i.e. they are empty.

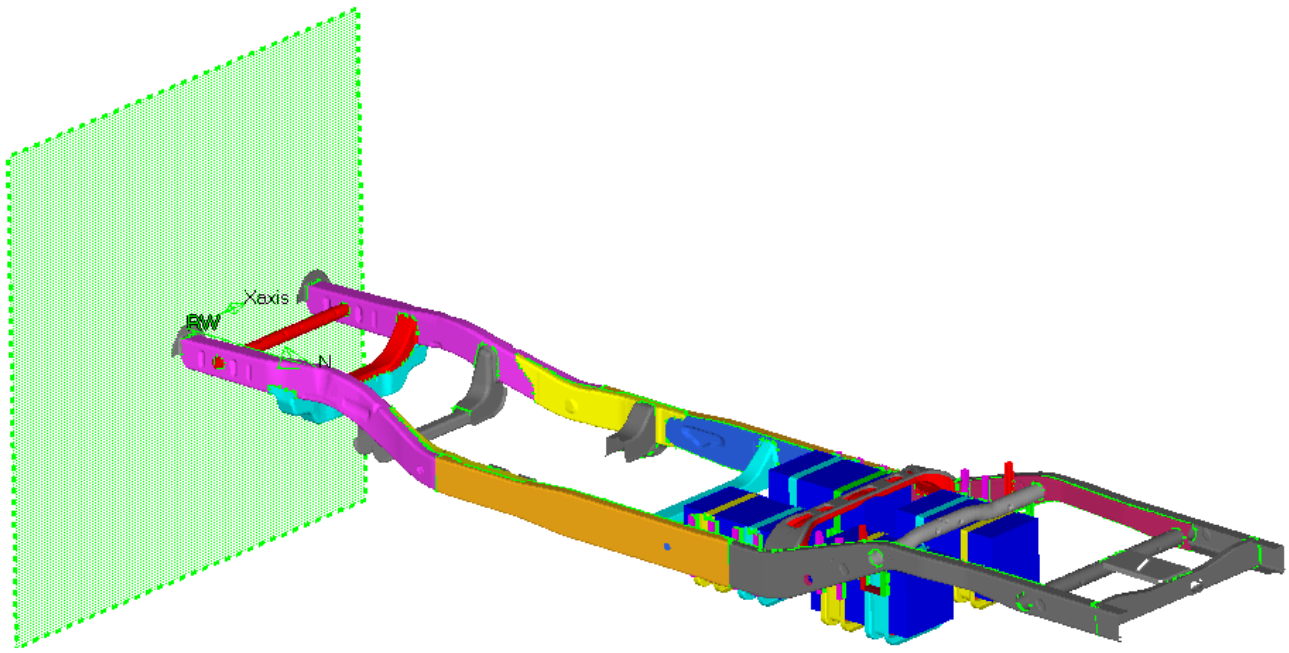

Figure 46-Final Model with the Rigid Barrier

7. Results and Discussion

7.1 von Mises stress in the Tanks

As mentioned in section 1.1 one of the main objective of the project was to check for the failure of the tanks. For ductile materials, the most common failure theories are the Maximum Shear Stress theory and the Maximum Octahedral Shear stress theory. Experiments on ductile materials show that the Maximum Octahedral Shear Stress theory gives better results than the maximum shear stress theory. [16]

The Maximum Octahedral Shear stress theory is called as the von Mises yield criterion. It states that the material fails if the von Mises stress is greater or equal to the yield stress of the material. Most of the FE software directly give out the von Mises stress. Here the von Mises stress of the tanks are compared to the yield stress of the effective tank to check for failure.

The four tanks attached to the chassis are named as Frontal 1, Frontal 2, Rear 1 and Rear 2 for better understanding of the results.

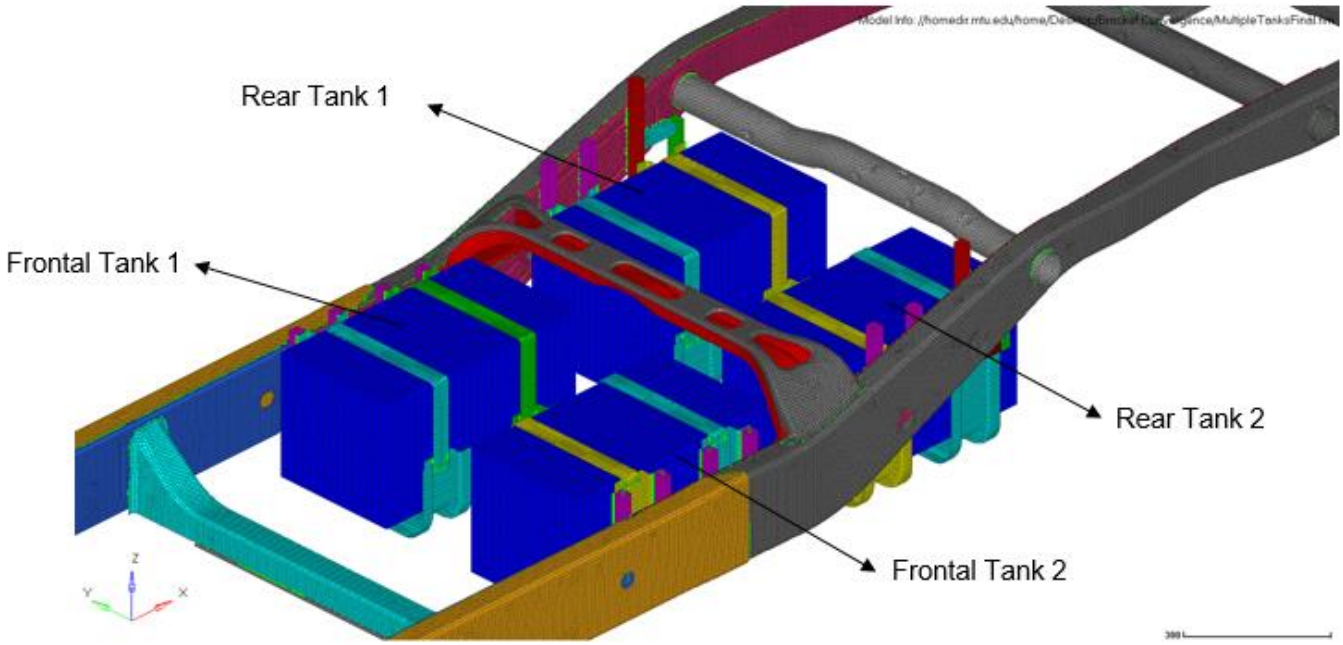

Figure 47-Nomenclature of Tanks

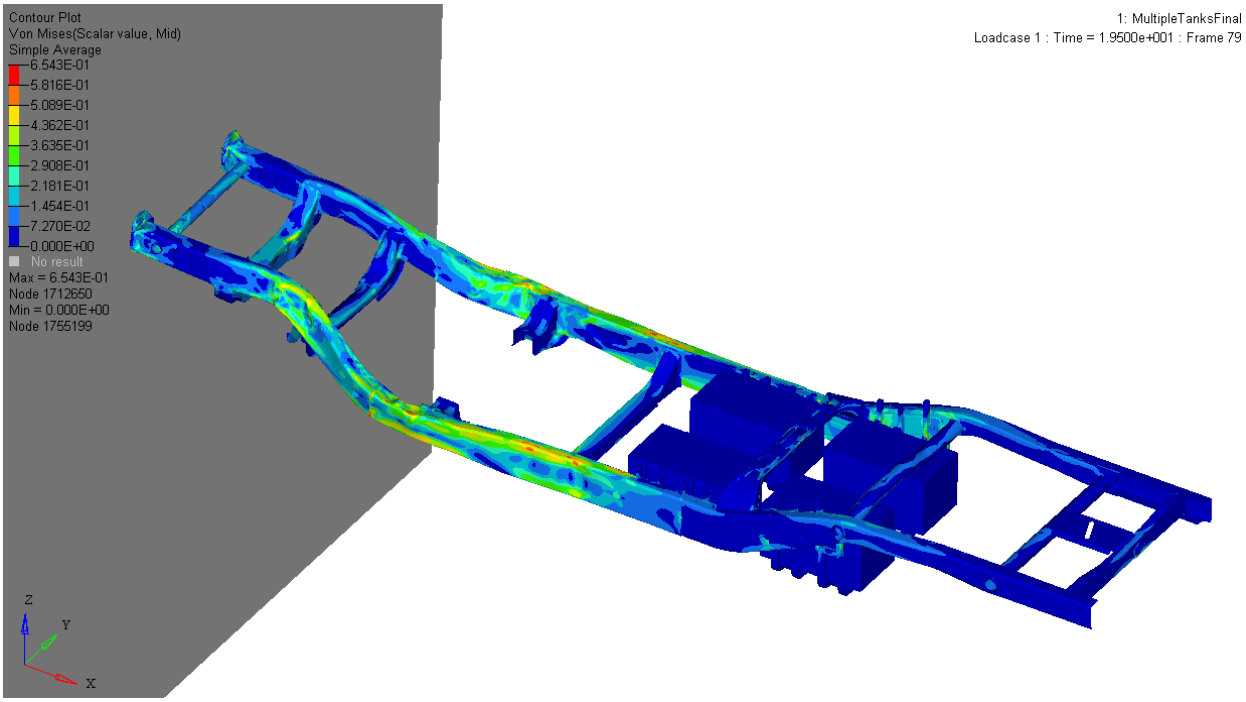

Figure 48- Screenshot of Results for 35mph

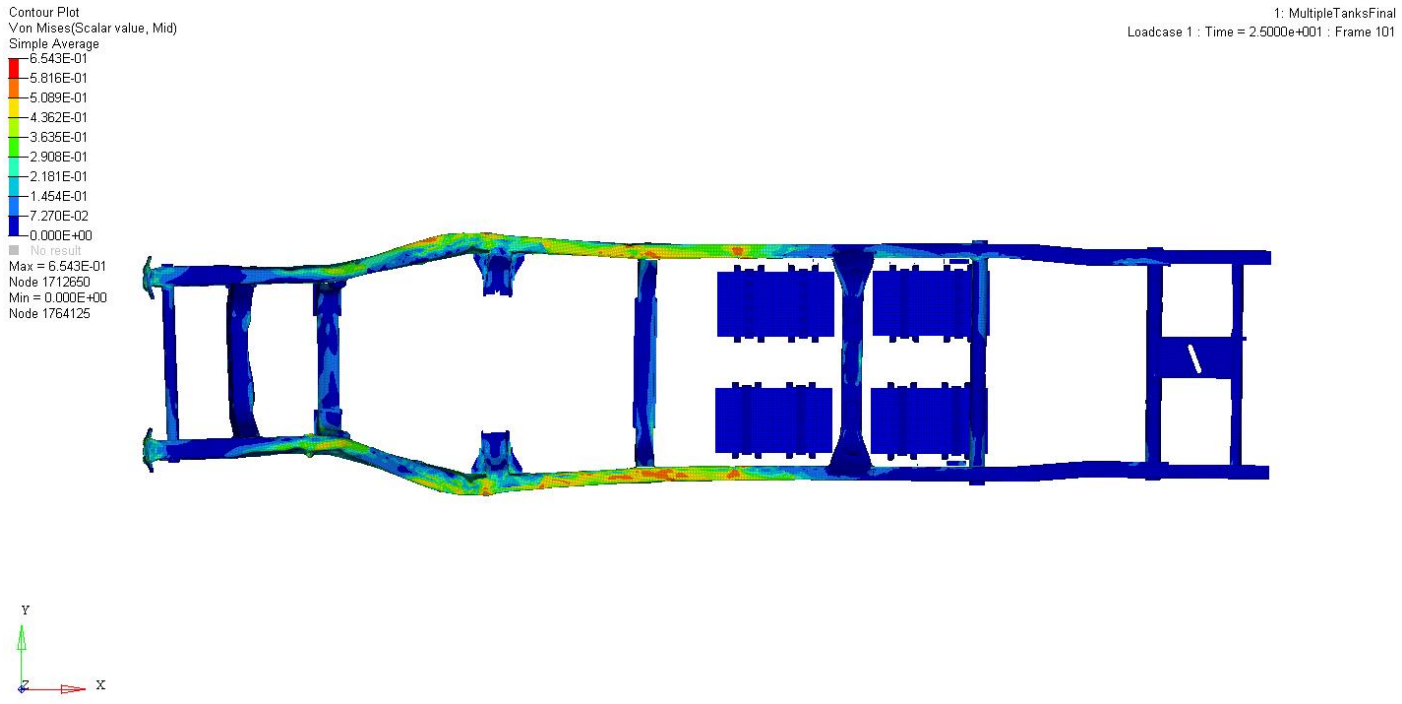

Figure 49-Screenshot of Results for 35mph (Top View)

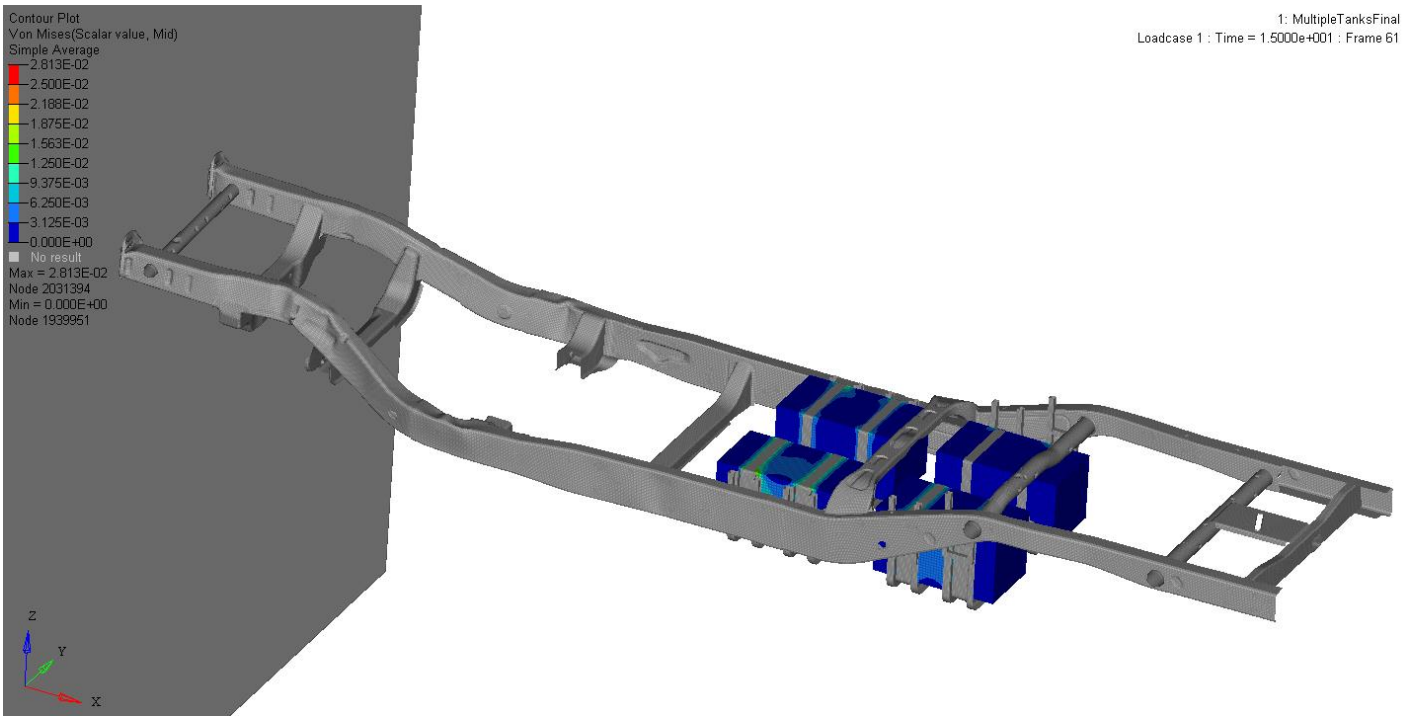

Figure 50- Von Mises stress on the tanks- 35mph

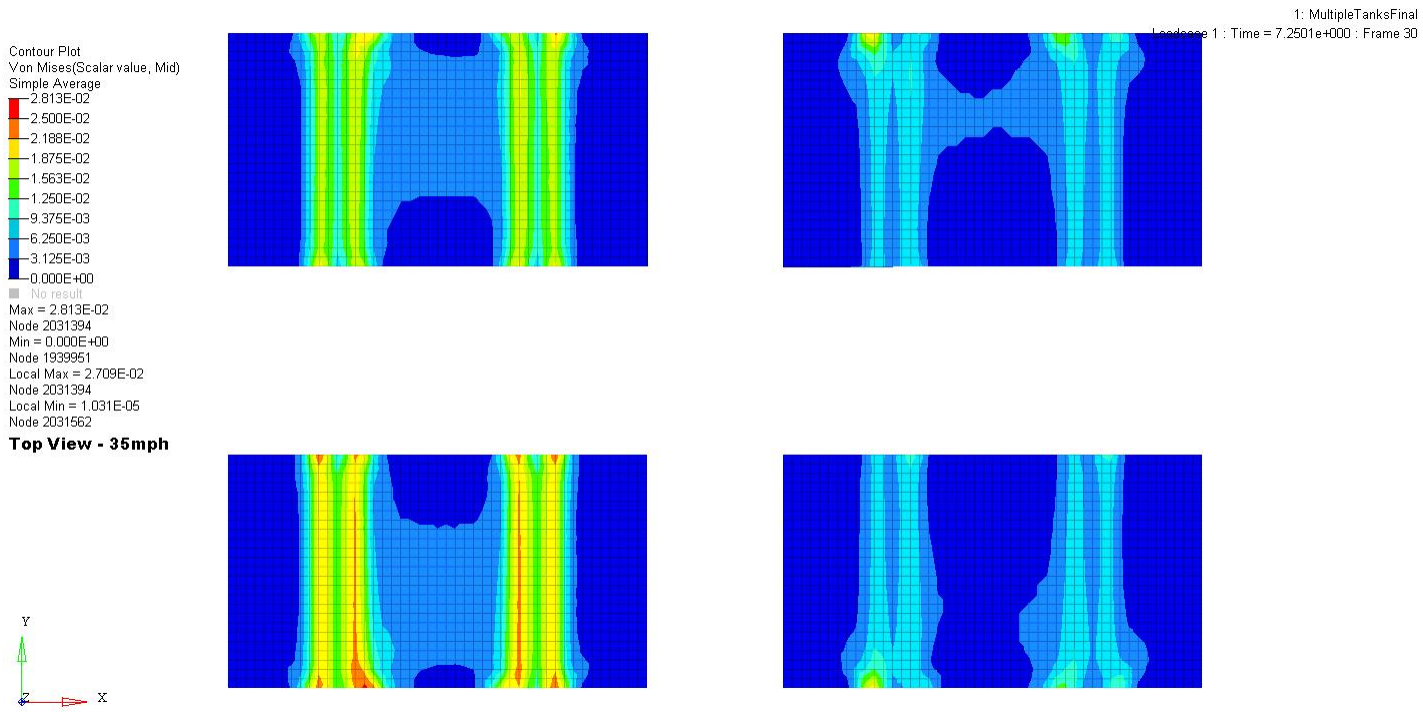

Figure 51-Von Mises stress on the tanks – 35mph (Top View)

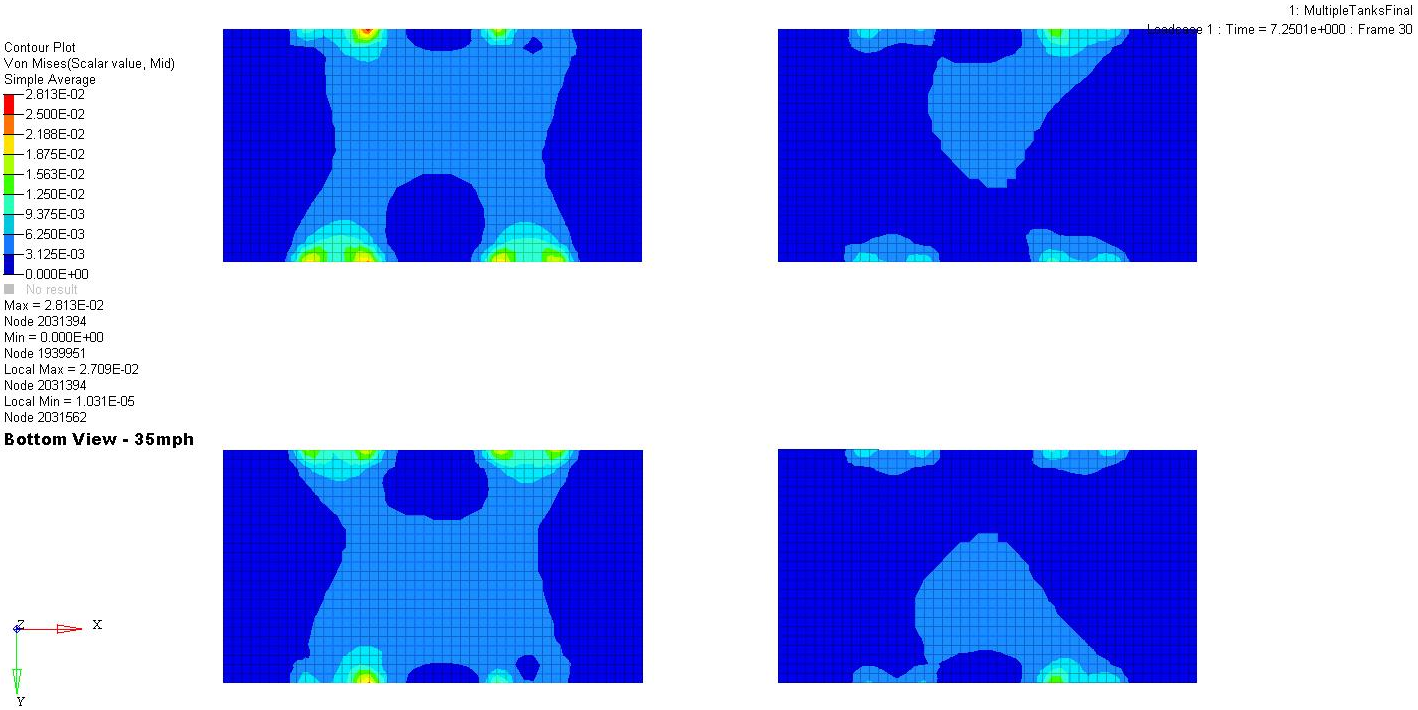

Figure 52- Von Mises stress on the tanks- 35mph (Bottom View)

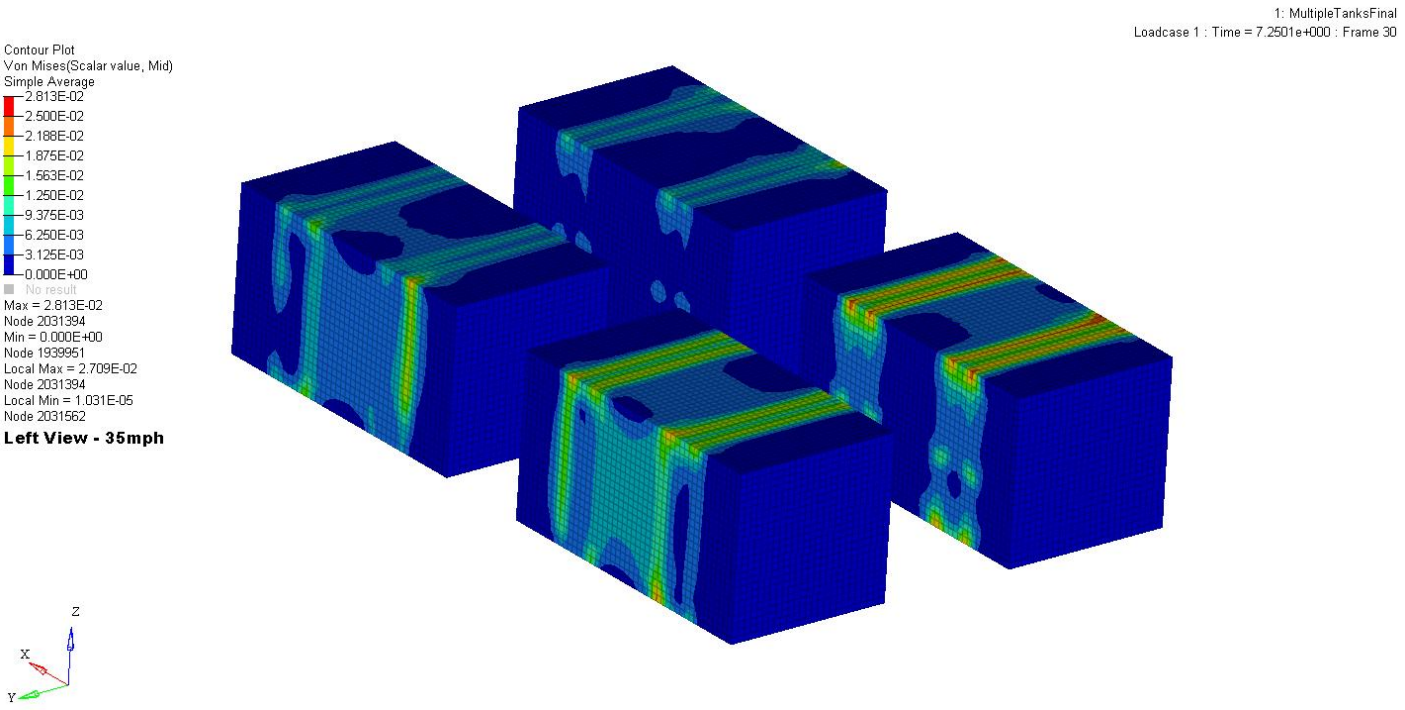

Figure 53-Von Mises stress on the tank – 35mph (Left View)

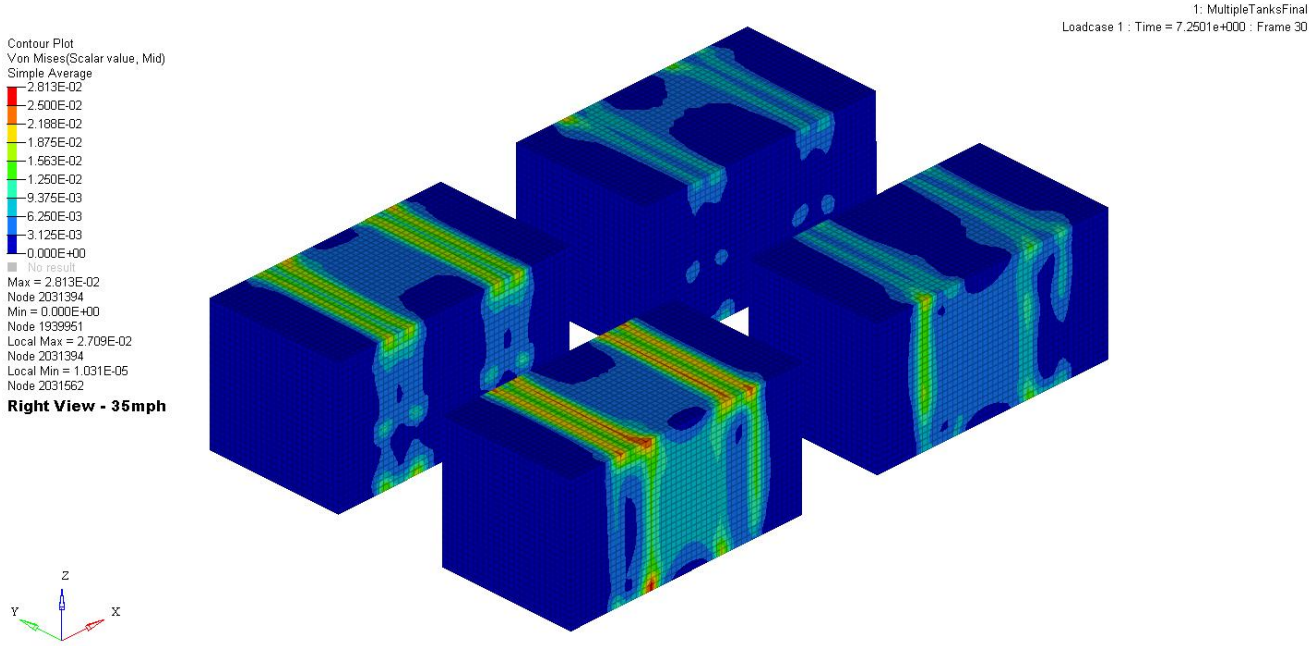

Figure 54- Von Mises stress on the tank- 35mph (Right View)

Table 12-Max von Mises stress on the tanks for Speed of 35 mph

Speed-35 mph		
	Max von-Mises Stress (MPa)	Yield Stress (MPa)
Frontal Tank 1	28.26	164.25
Frontal Tank 2	28.13	164.25
Rear Tank 1	24.49	164.25
Rear Tank 2	23.47	164.25

Figure 50 to 54 show the von Mises stress distribution of the tanks in different views at a particular instance. From the table 12 we can see that for the frontal crash (35 mph) the maximum von Mises stress in the four tanks are in the range of 23-28 MPa. The maximum von Mises stresses in the tanks are far less than the yield stress. This is because most of stresses are absorbed in the chassis before it reaches the tank. The location of the maximum von Mises stress is on the region of the tank where the brackets are in contact.

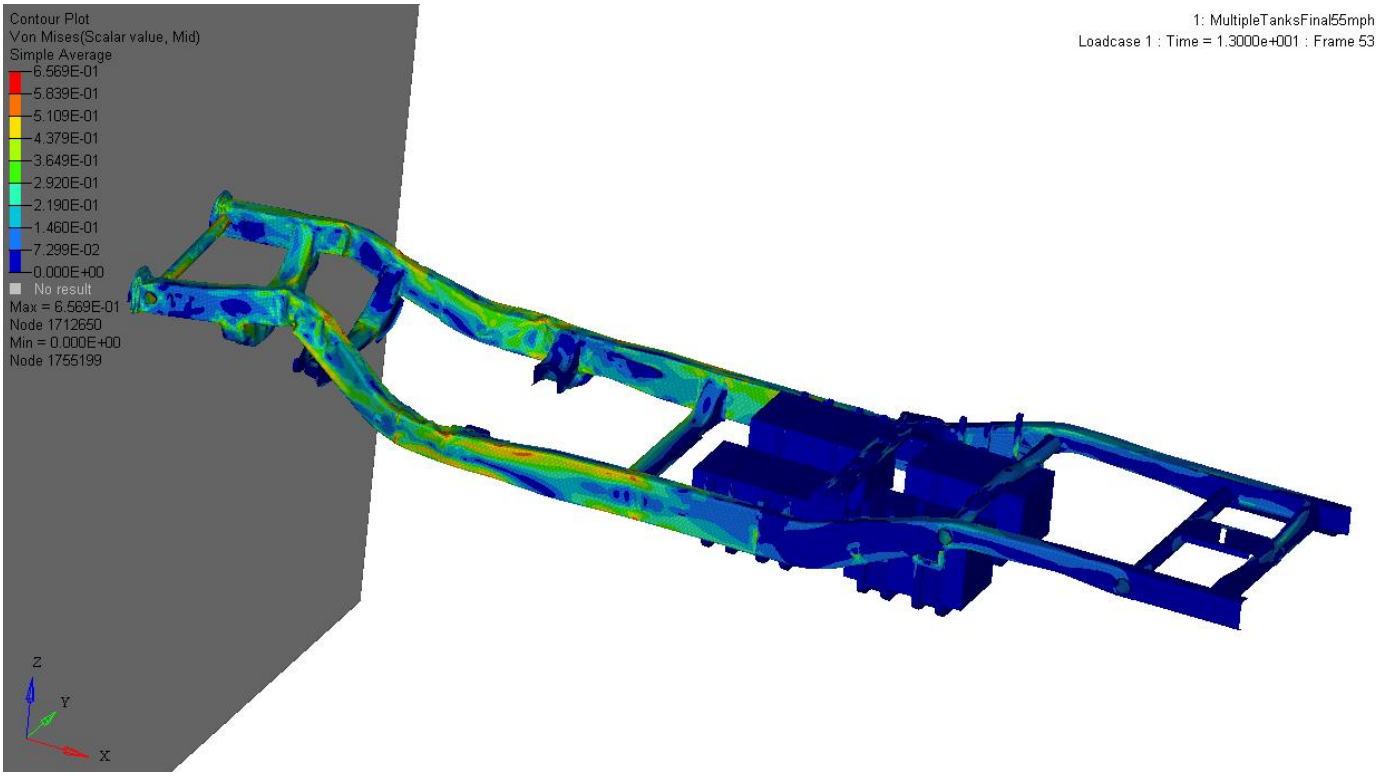

Figure 55- Screenshot of Results for 55mph (Isometric View)

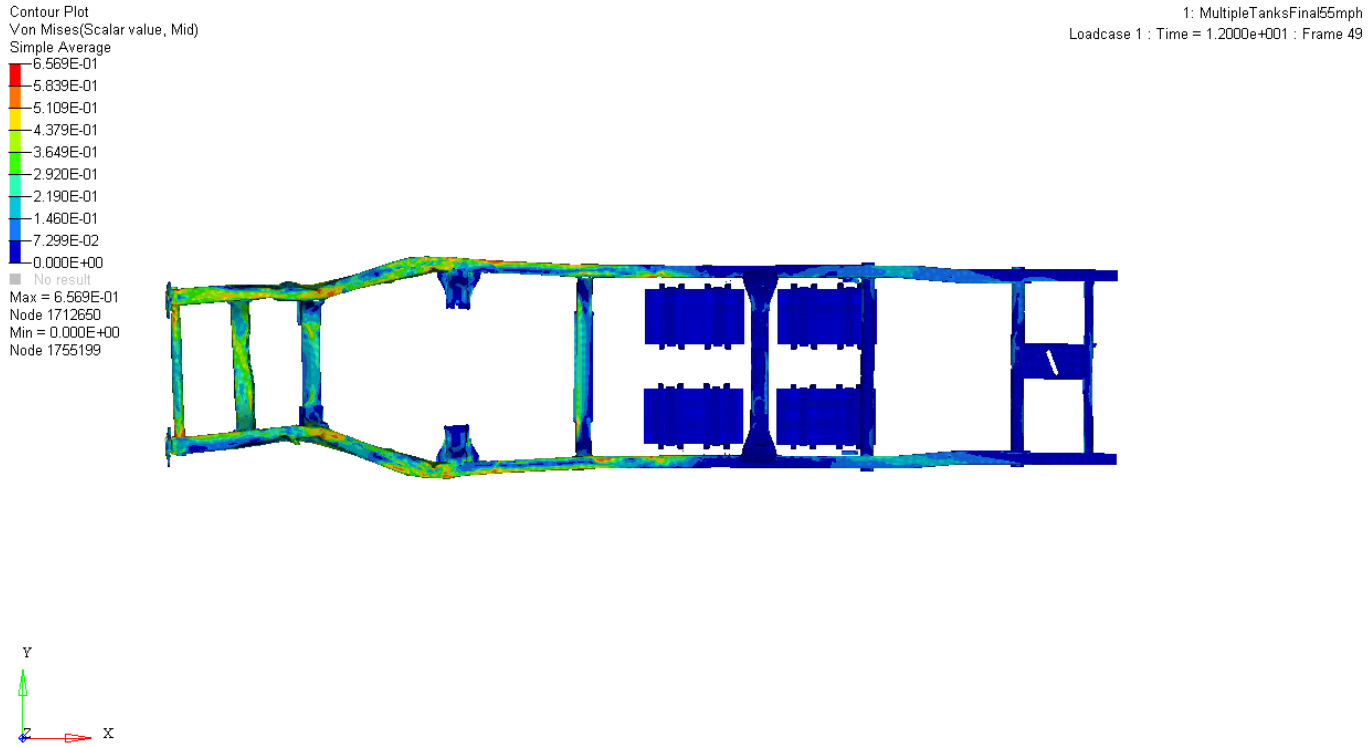

Figure 56- Screenshot of Results for 55mph (Top View)

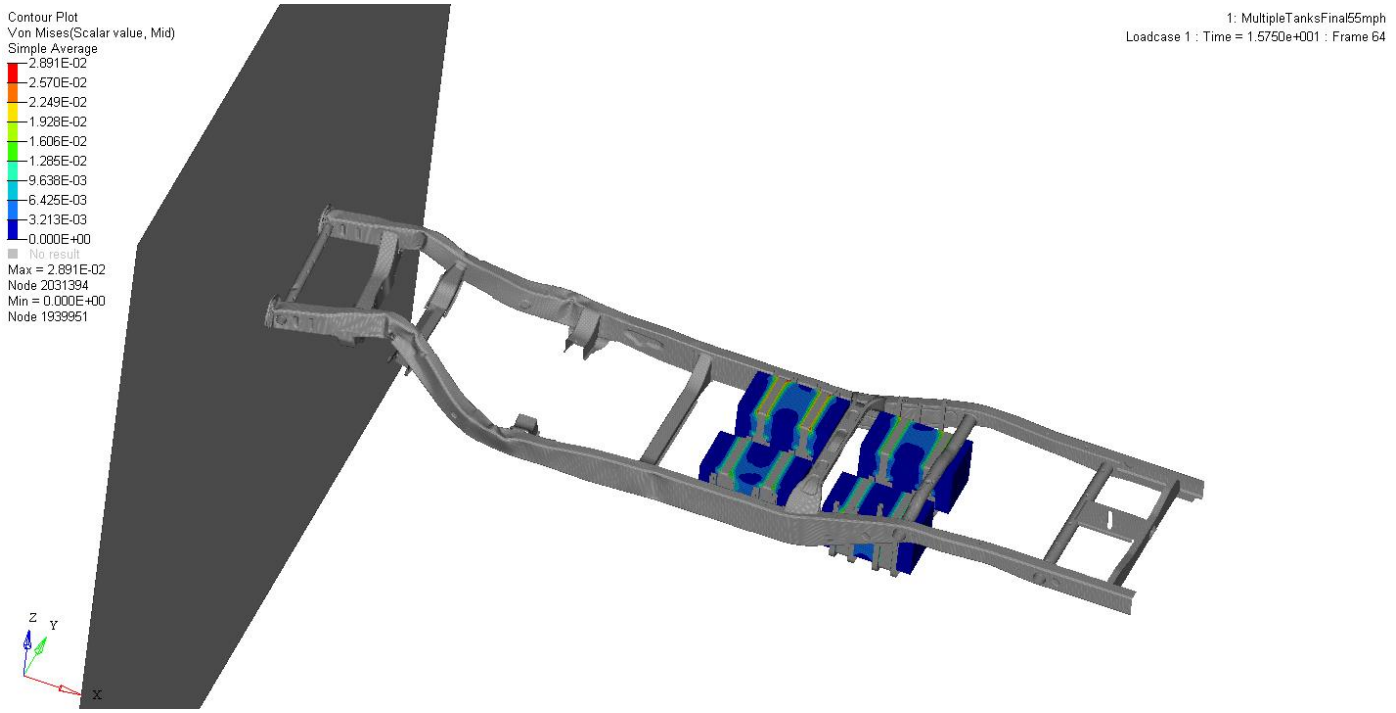

Figure 57-Von Mises stress on the tanks- 55mph

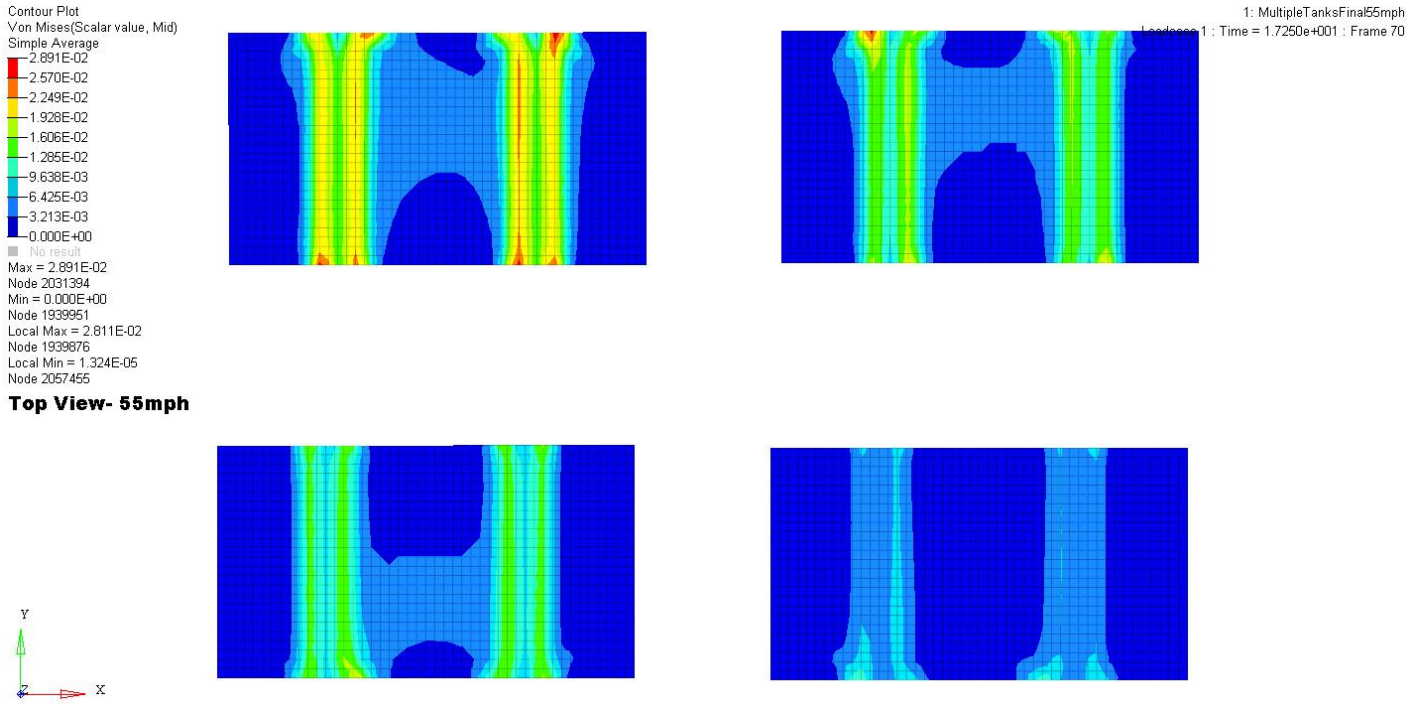

Figure 58-Von Mises stress on the tanks- 55 mph (Top View)

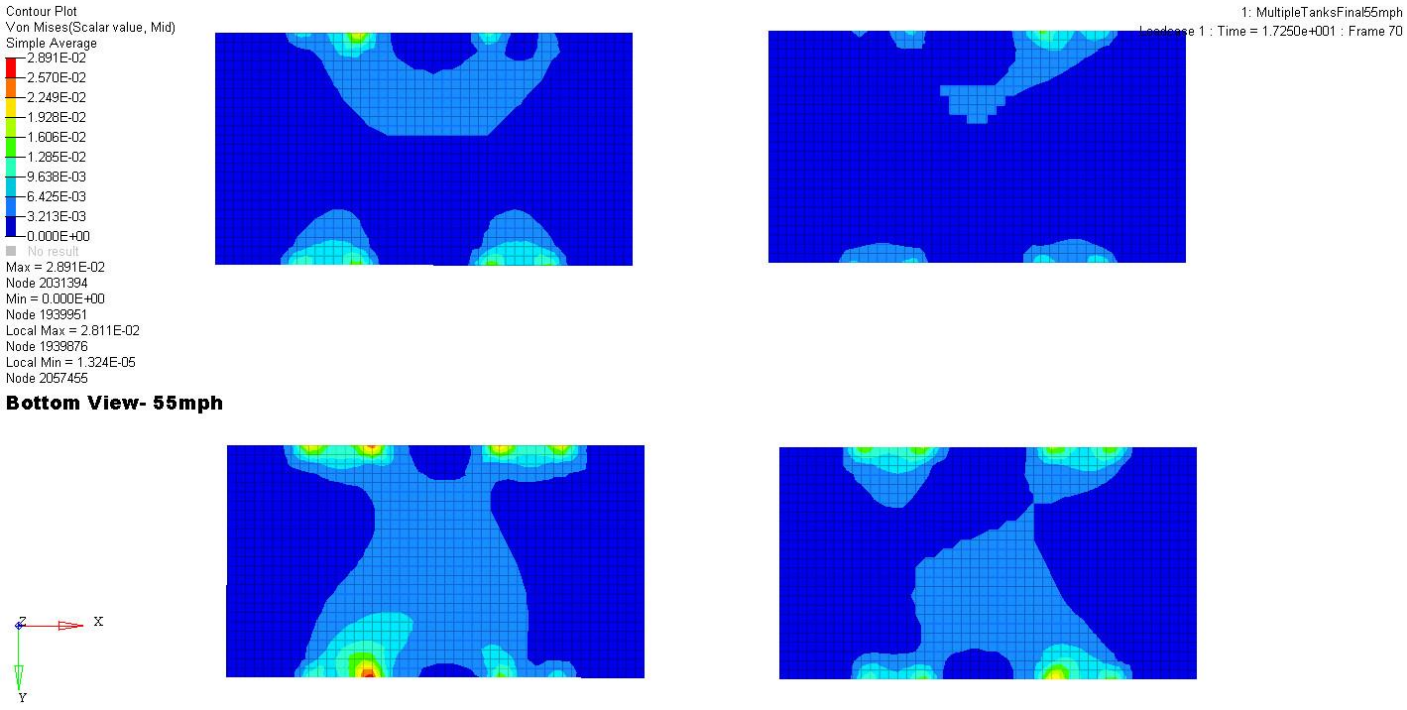

Figure 59- Von Mises stress on the tanks- 55mph (Bottom View)

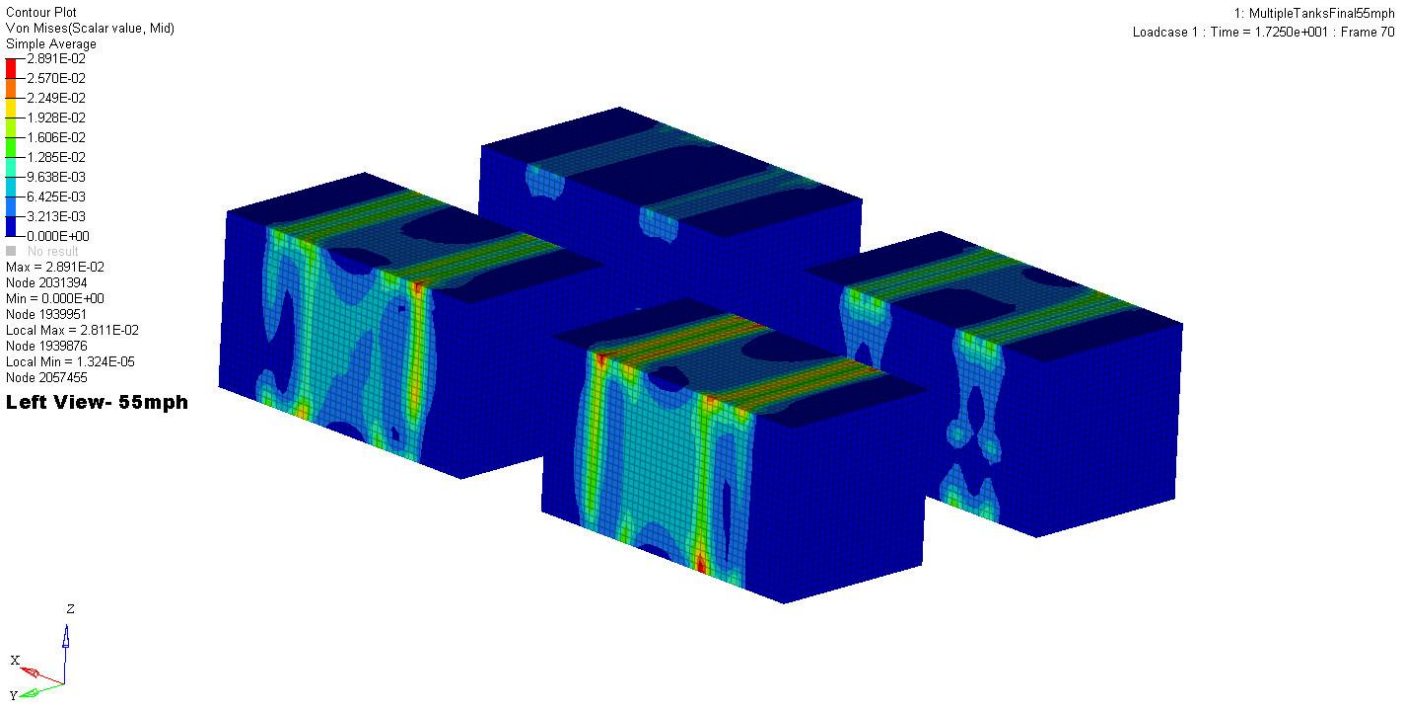

Figure 60-Von Mises stress on the tanks- 55mph (Left View)

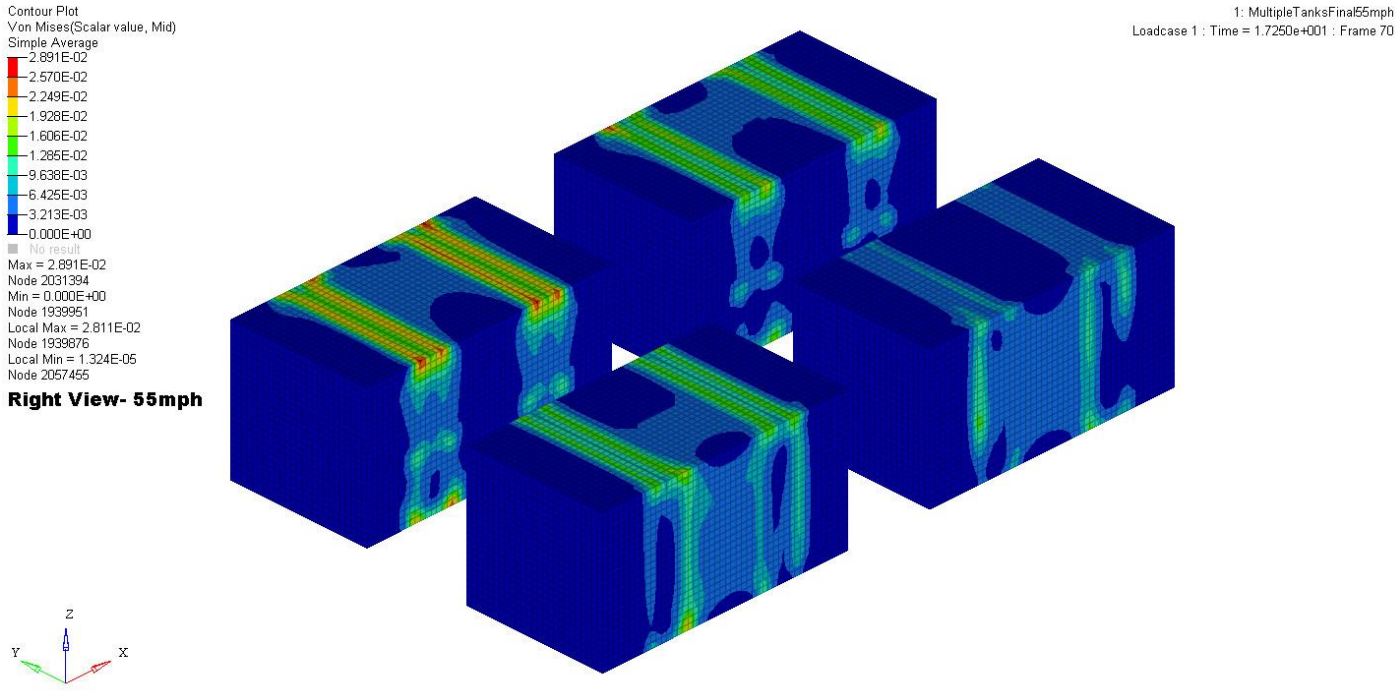

Figure 61- Von Mises stress on the tanks- 55mph (Right View)

Table 13-Max von Mises stress on the tanks for Speed of 55 mph

Speed-55 mph		
	Max von-Mises Stress (MPa)	Yield Stress (MPa)
Frontal Tank 1	28.61	164.25
Frontal Tank 2	28.91	164.25
Rear Tank 1	27.93	164.25
Rear Tank 2	25.62	164.25

Figure 58 to 61 show the von Mises stress distribution of the tanks in different views at a particular instance. From the table 13 we can see that for the frontal crash (55 mph) the maximum von Mises stress in the four tanks are in the range of 25-28 MPa. The maximum von Mises stresses in the tanks are far less than the yield stress. This is because most of stresses are absorbed in the chassis before it reaches the tank. The location of the maximum von Mises stress is on the region of the tank where the brackets are in contact.

7.2 Plastic Strain in the Brackets

The brackets play a very important role as they hold the tanks firmly and connect them to the chassis. The brackets have to design in such a way that even in the worst case condition, they should not break and the tank's should not fall down. As the design of the bracket was created by using the available dimensions, they had to be validated to check if they are similar enough to the original one and they function properly. To analyze the brackets, the maximum plastic strain is considered to check if there is any permanent deformation in the bracket. If there in any plastic strain present in the bracket, it means that at that particular location there is a permanent deformation and a possible crack formation. The depth of the permanent deformation decides whether the brackets will break or not.

To analyze the results, the brackets are named as Frontal 1A,1B,2A,2B and Rear 1A,1B,2A,2B respectively as shown in Figure 62.

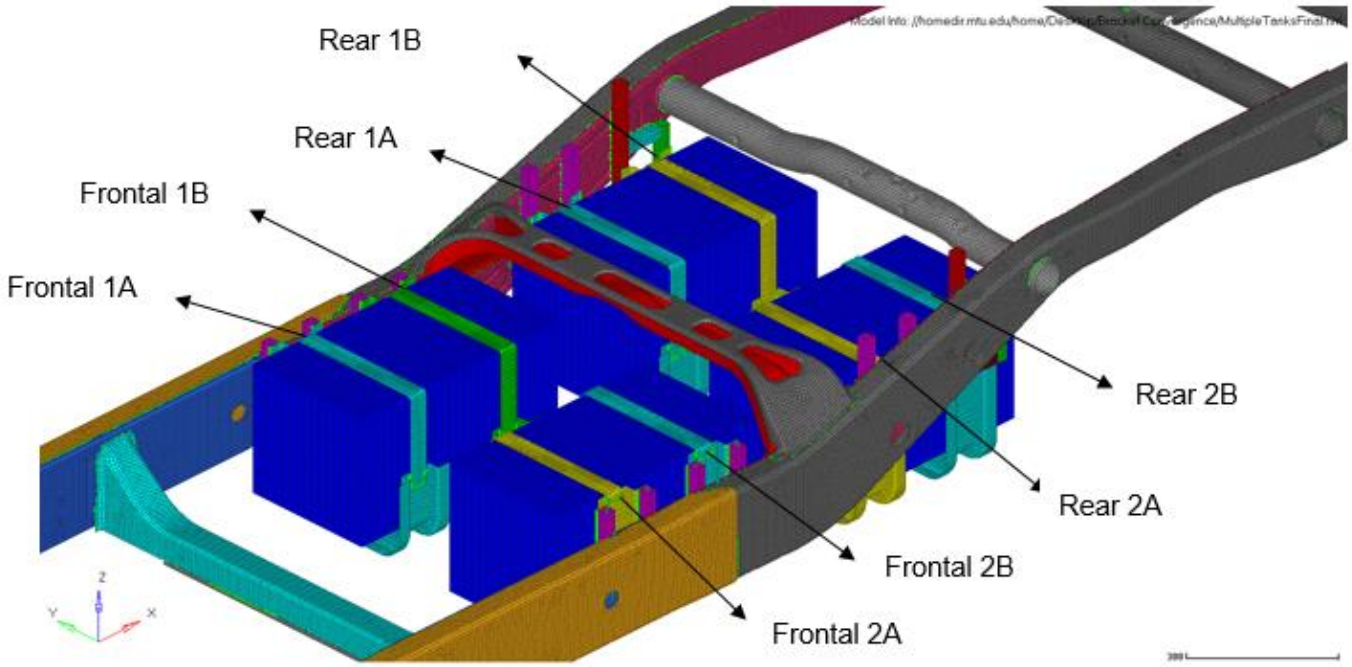

Figure 62-Nomenclature of brackets

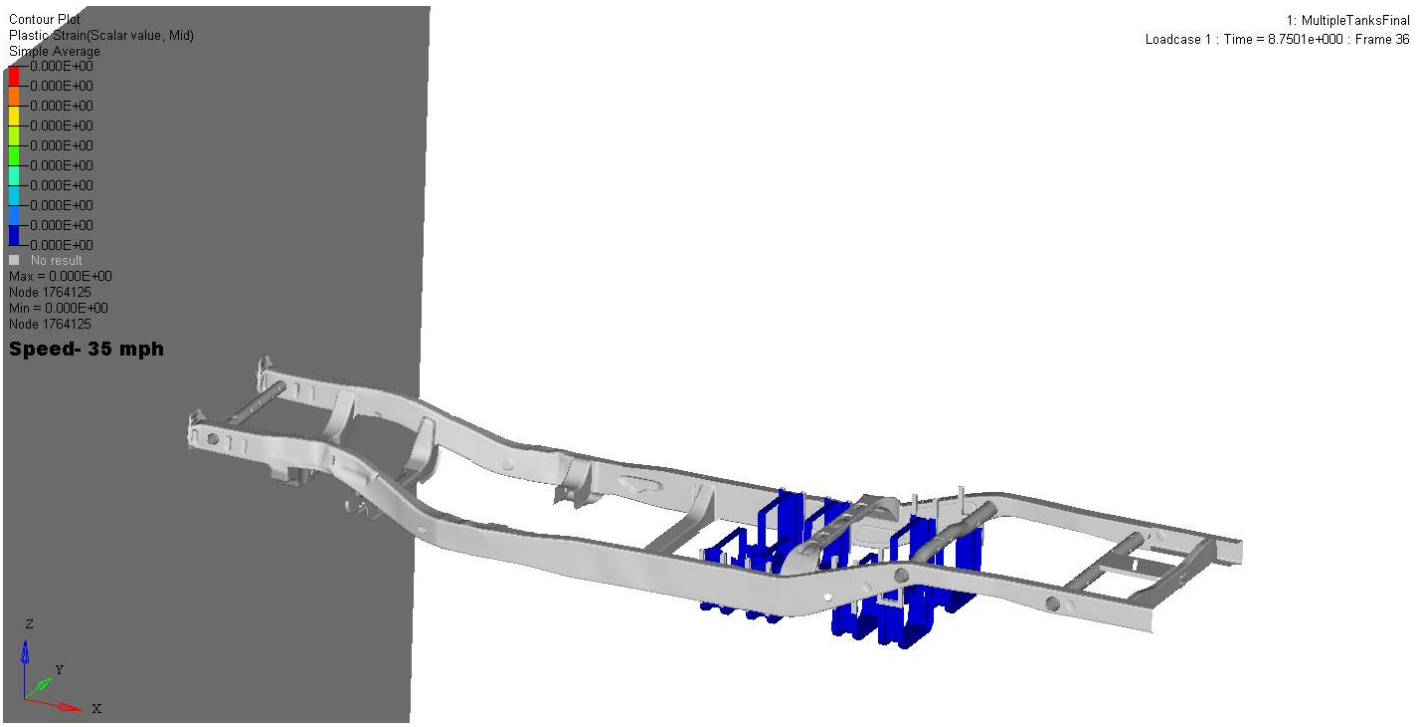

Figure 63- Plastic Strain in the Brackets (35 mph)

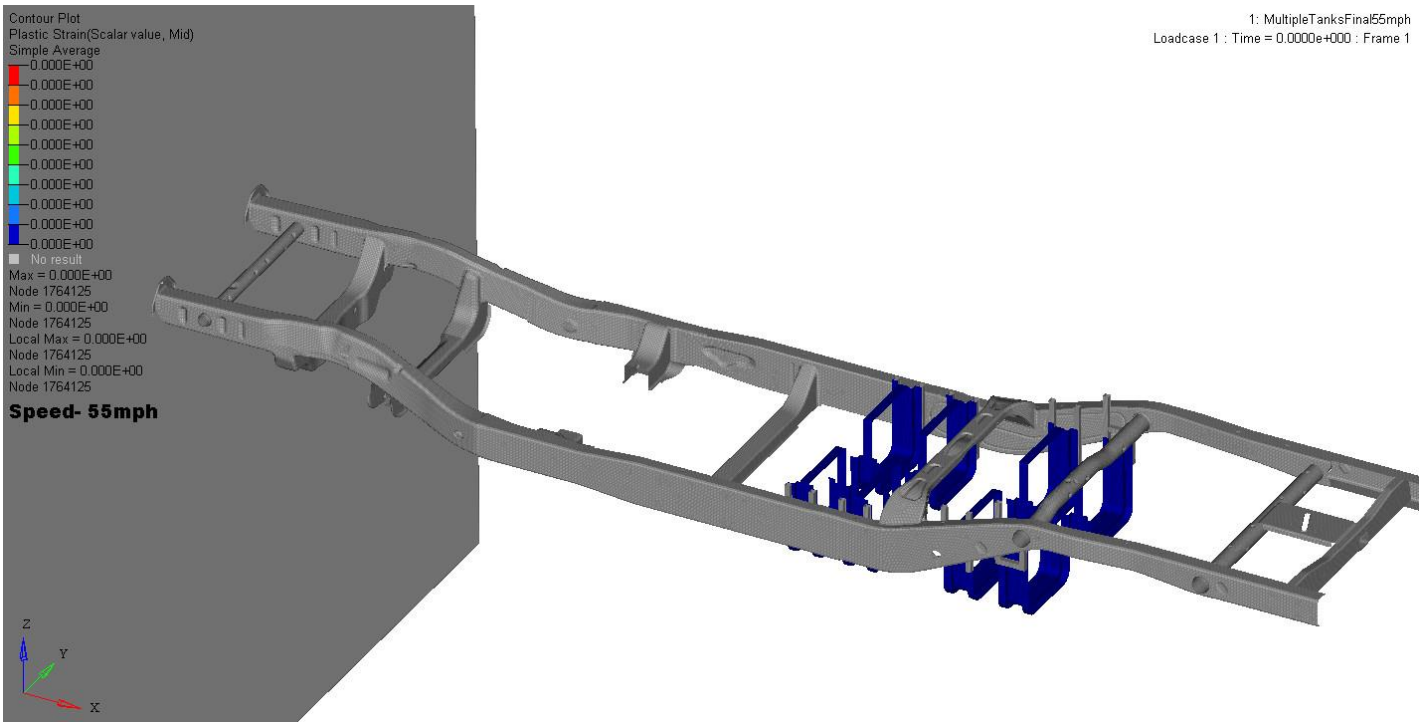

Figure 64-Plastic Strain in the Brackets (55 mph)

Figure 63 and 64 show the plastic strain distribution for the brackets. As we can see the maximum plastic strain in the frontal brackets and the rear brackets are zero for frontal crash for both 35 mph and 55 mph. We can see that brackets that are designed using the measurable dimensions can handle the tanks and do not fail in frontal crash, as the brackets have zero plastic strain. Thus we can conclude that none of the brackets fail in the frontal crash. As the model is symmetric, we can conclude that even for rear impact the brackets or the tanks would not fail.

7.3 Positioning of the Tanks

The positioning of the tanks is validated by checking the movement of the brackets and tanks. After a crash event, the tanks may be displaced and due to their movement, there can be interaction of the tanks with other components. This interaction can cause stresses in the tanks or the other part. As all other assemblies are deleted and only the chassis and tank-bracket assembly is used, the movement of the tanks can be found out to get a clear idea how much it displaces. To compute the movement of the tank, the movement of the bracket is first found out. The movement of the brackets is computed by finding the rotation of the bracket relative to the chassis. By computing the rotation of the bracket, we can find out the movement of the tank.

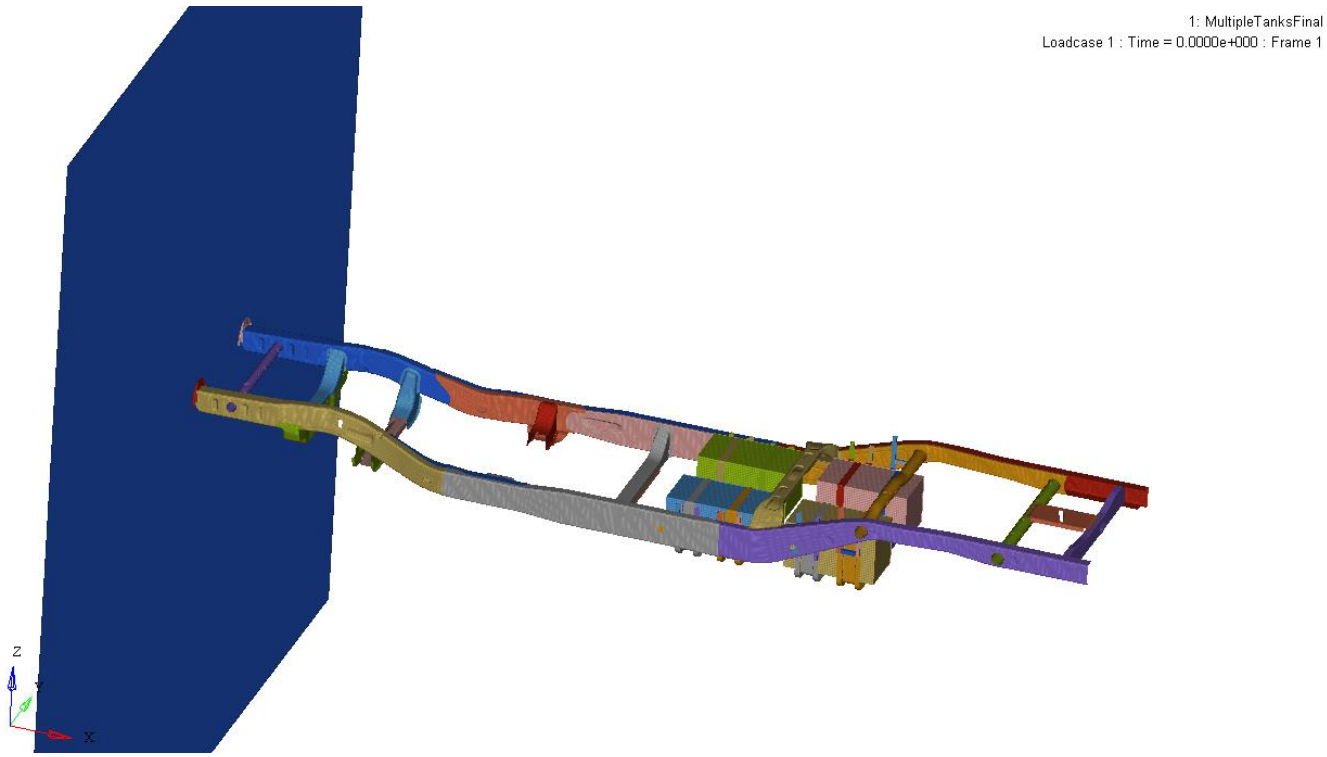

Figure 65- Full Model view

Figure 66 shows the detailed view of the frontal bracket and the chassis component relative to which the rotation has been measured. Figure 67 shows the initial angle which is measured at T=0. Figure 68 shows the rotation at a random time.

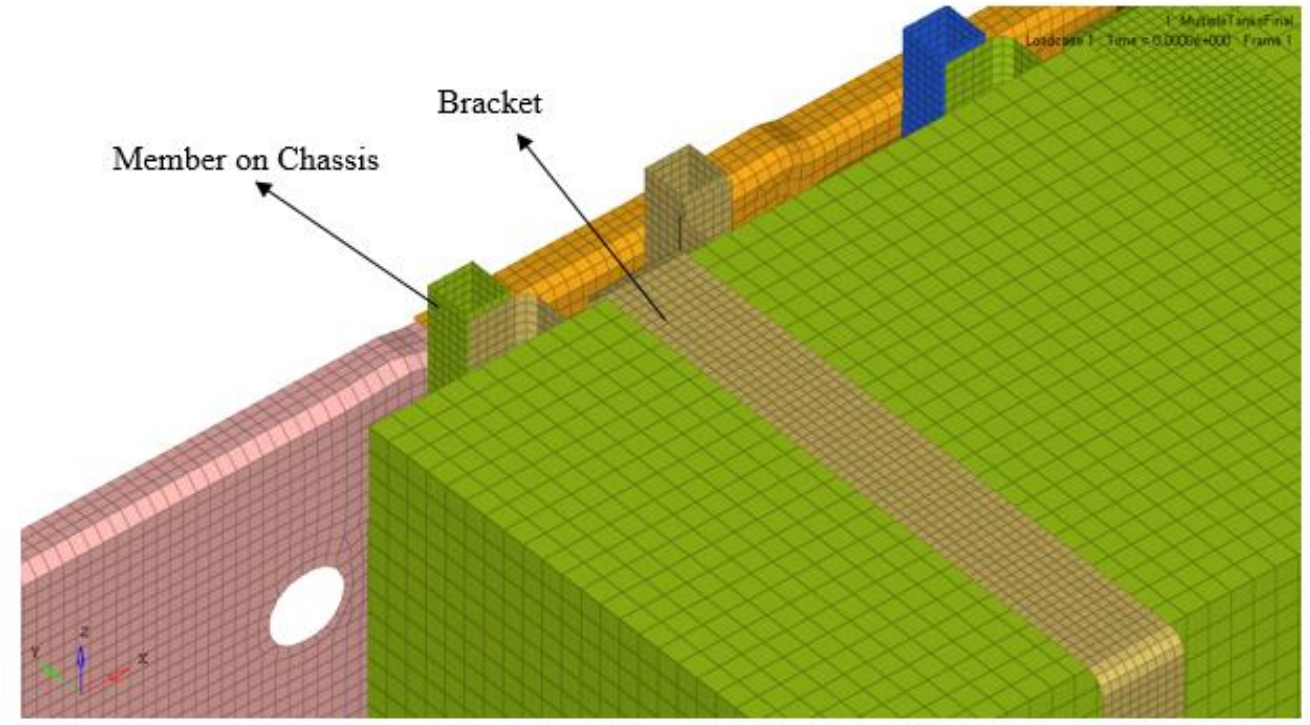

Figure 66- Detailed View for rotation of bracket

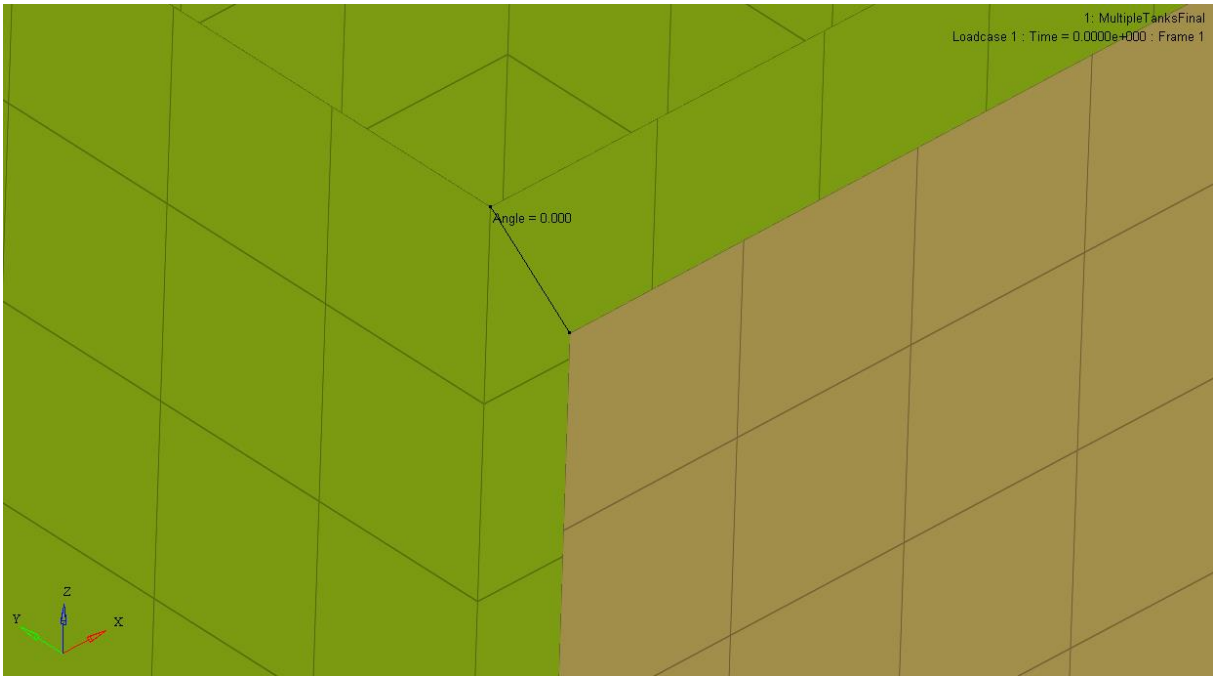

Figure 67- Initial Measurement of rotation of bracket relative to chassis

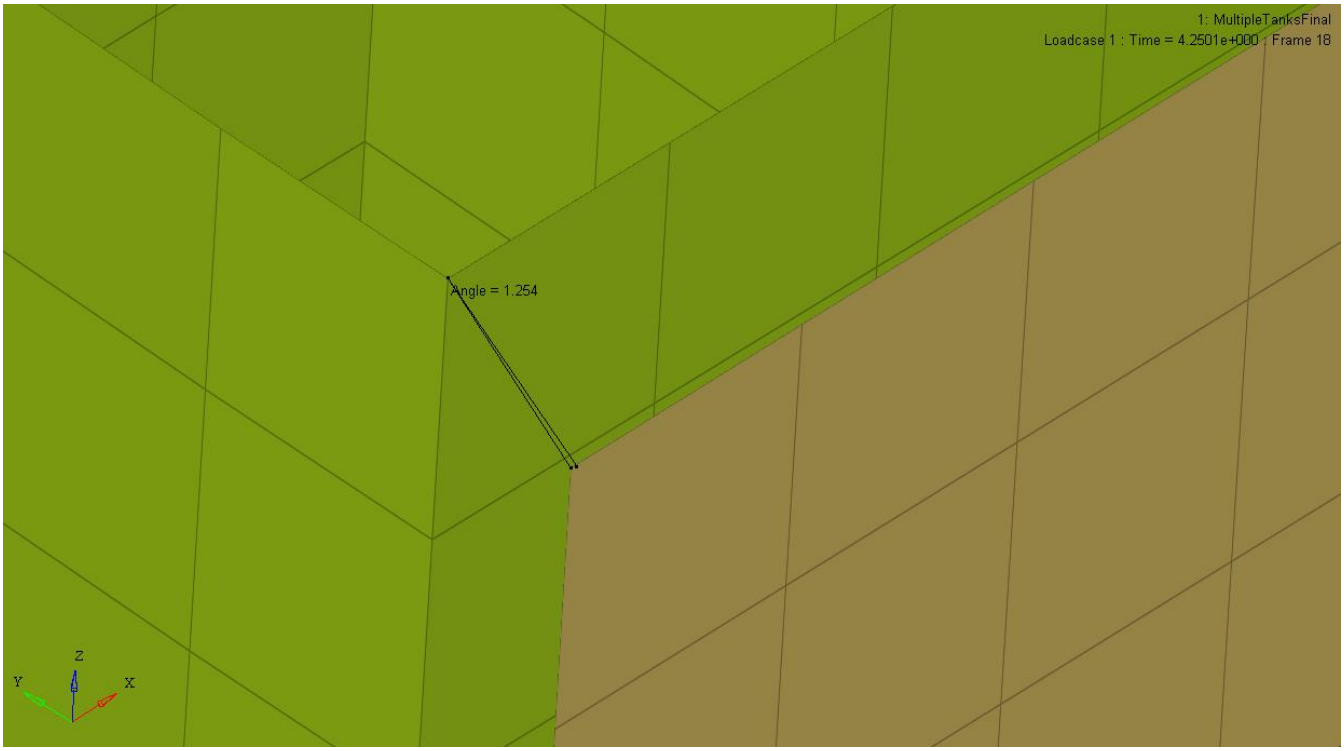

Figure 68- Rotation of bracket relative to chassis

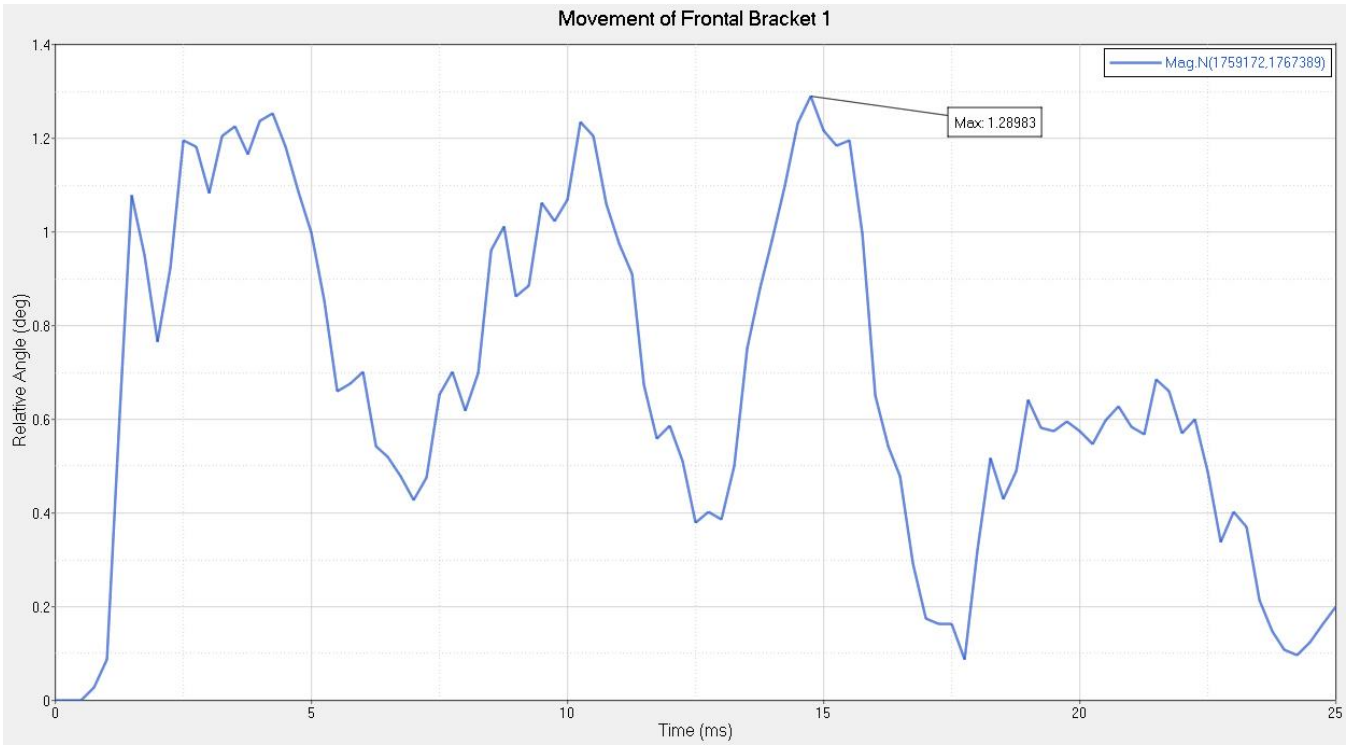

Figure 69- Movement of Frontal Bracket 1 [35 mph]

Figure 69 shows the rotation of the Frontal Bracket 1 for 35 mph. We can see that the movement of the bracket does not follow a particular trend and is very random. We also see that the maximum angle by which the Frontal 1A bracket rotates is 1.289 deg. This rotation is what we expect and close to reality as the bracket is firmly attached to the chassis.

Table 14-Rotation of Brackets – 35mph

Maximum Rotation of Brackets - 35mph	
Bracket	Angle (deg)
Frontal 1A	1.289
Frontal 2A	1.326
Rear 1A	0.887
Rear 2A	0.49

Table 15-Rotation of Brackets – 55mph

Maximum Rotation of Brackets - 55mph	
Bracket	Angle (deg)
Frontal 1A	1.383
Frontal 2A	1.456
Rear 1A	0.876
Rear 2A	0.572

Table 14 shows the rotation of the brackets for 35mph. We can see that the maximum rotation of the bracket is 1.456 deg in Frontal 2A. Table 15 shows the rotation of the brackets for 55mph. We can see that the maximum rotation of the bracket is 1.456 deg in Frontal 2A. We can see that, for both the load cases the rotation of the brackets follow a similar trend.

Figure 70 shows the displacement of the tanks due to the rotation of the bracket. The displacement of the tank was found out by measuring the movement of the tank by measuring the displacement of a single edge. Figure 71 shows the movement of Frontal Tank 1 for 35 mph.

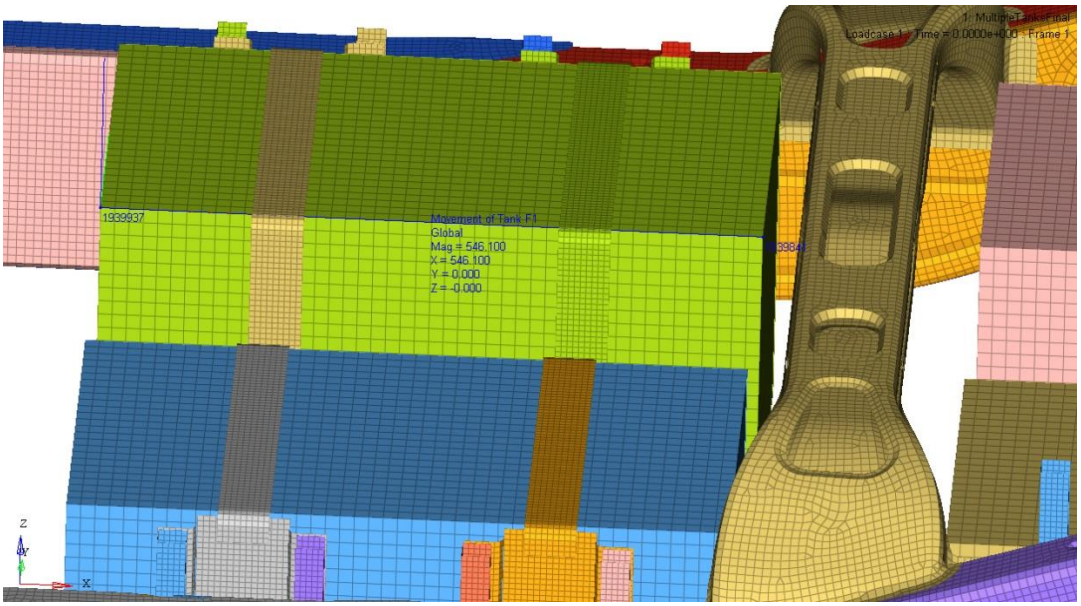

Figure 70- Movement of Tank

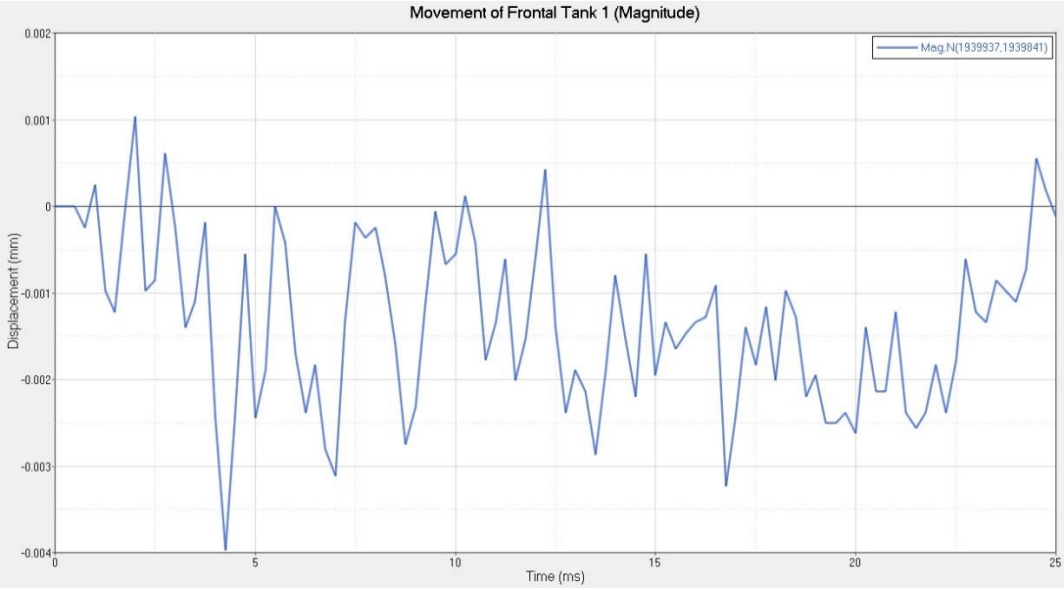

Figure 71- Movement of Frontal Tank

Table 16-Movement of the Tanks- 35mph

Maximum Deflection of the Tanks -35mph (mm)				
Tank	Magnitude	X	Y	Z
Frontal 1	0.004	0.005	0.481	1.669
Frontal 2	0.003	0.004	0.451	1.69
Rear 1	0.003	0.003	0.444	1.159
Rear 2	0.002	0.003	0.445	1.147

Table 17-Movement of the Tanks- 55mph

Maximum Deflection of the Tanks -55mph (mm)				
Tank	Magnitude	X	Y	Z
Frontal 1	0.004	0.006	0.573	1.683
Frontal 2	0.002	0.004	0.427	1.794
Rear 1	0.003	0.002	0.451	1.357
Rear 2	0.003	0.002	0.397	1.042

From table 16 and table 17 we can see that because of the inertial effect, the maximum deflection of the tanks is significant in the Z direction. The maximum deflection is 1.669 mm in the Frontal 1 for a speed of 35 mph and 1.794 mm in the Frontal 2 for speed of 55-mph. From this we can clearly observe that the tanks are placed in the right position and the movement of the tanks in an event of frontal crash does not affect any other parts.

8. Conclusion and Recommendations for future work

The frontal crash analysis of the conformable CNG tank has been performed for two velocities of 35 mph and 55 mph according to FMVSS 208 standard by Finite Element Analysis using HyperMesh/RADIOSS. An equivalent CNG tank has been modelled to replace the non-cylindrical conformable CNG tank. The effective stiffness and yield stress of this tank are computed for the equivalent tank and they are 49.925 GPa compared to 70 GPa of the conformable tank. The yield stress of the effective tank is found out to be 164.25 MPa compared to 350 MPa of the original tank.

The maximum von Mises stress in the tanks for frontal impact are 28.26 MPa (35 mph) and 28.91 Mpa (55 mph), which are way less than the yield stress of the tank (164.25 MPa). The plastic strain in the brackets is zero, which validates the design of the brackets. The maximum movement of the brackets is 1.326 deg (35 mph) and 1.456 deg (55 mph). The maximum movement of the tank is 1.669 mm (35 mph) and 1.794 mm (55 mph).

It can be observed from the maximum von Mises stress on the tanks that the tanks do not fail in frontal or rear crash. The positioning of the tanks is also validated, as the movement of the tanks are so small that they are insignificant. Due to these movements, no other parts near to the tank are affected and this validates the packaging of the tank.

Some recommendations for future work –

- Loads of the vehicle and the passengers can be applied on the Chassis and the same analysis can be done.
- Side impact to the chassis can be performed. Side impact can be a better load case to check for the failure of the tanks as in side impact the tanks are more vulnerable to fail.
- The crash analysis of the pressurized tanks can be performed.
- The FMVSS Standard 301- Fuel System Integrity, Standard 303- Fuel System Integrity of Compressed Natural Gas Vehicles and Standard 301 Compressed

Natural Gas Fuel Container Integrity can be tested using FEA. These standards are used to mainly check the safety of the fuel tanks. By simulating these standards, we can assure that the CNG tank is safe in all conditions and the injuries from fire due to any burst or leak is minimal.

9. References

1. "What is CNG?" [Online] Available: http://www.cngnow.com/what-is-cng/Pages/default.aspx [Accessed 27 February 2017]
2. Aslam, M. U., Masjuki, H. H., Kalam, M. A., Abdesselam, H., Mahlia, T. M. I., & Amalina, M. A. (2006). An experimental investigation of CNG as an alternative fuel for a retrofitted gasoline vehicle. *Fuel, 85*(5–6), 717-724. doi: http://dx.doi.org/10.1016/j.fuel.2005.09.004
3. "The Benefits of Compressed Natural Gas (CNG) Vehicles" [Online] Available: http://www.cng-one.com/info/benefits.asp [Accessed 27 February 2017]
4. Deshpande, Prathamesh Prashant, "STRUCTURAL ANALYSIS OF INTEGRATION OF A NON-CYLINDRICAL CNG FUEL TANK", Master's report, Michigan Technological University, 2015.
5. "Conformable Compressed Natural Gas Tank," [Online] Available: http://www.relinc.net/advanced-materials/conformable-natural-gas-tank/ [Accessed 27 February 2017]
6. Famuyiwa, Abayomi, "INTEGRATION AND TESTING OF AN ADVANCED CONFORMABLE CNG TANK IN A FULL-SIZED LIGHT-DUTY PICKUP", Open Access Master's Thesis, Michigan Technological University, 2016.
7. "1986 Chevy C10 Truck Rear Side Mounted Fuel Tank Hanger With Strap" [Online] Available:https://www.1aauto.com/fuel-tank-hanger-with-strap/i/1afts00167?f=891963&y=1986&utm_campaign=gb_csv_br&utm_content=FTS&gclid=CImQ57GundICFQMxaQodaBoNjw
8. "Practical Aspects of Finite Element Simulation". Retrieved from http://www.altairuniversity.com/free-ebooks-2/free-ebook-practical-aspects-of-finite-element-simulation-a-study-guide/ on 29 February 2016.
9. "Crash Analysis with Radioss". Retrieved from https://connect.altair.com/CP/downloads.html on December 4 2015.

10. Kulkarni, Amruta V., "FINITE ELEMENT ANALYSIS OF CONFORMABLE CNG TANK – TOPOLOGY OPTIMIZATION AND DROP TEST SIMULATION", Campus Access Master's Report, Michigan Technological University, 2016.
11. Rashid, M. (1977). GM 980X - Potential Applications and Review. SAE Technical Paper 770211, 1977, doi: 10.4271/770211.
12. "SAE 980X HSLA Steel" [Online] Available: http://www.matweb.com/search/datasheet.aspx?matguid=486b2a0df1354c6da10830e1da621aa9&ckck=1 [Accessed 20 July 2016]
13. "Aluminum A206.0-T7 Casting Alloy" [Online] Available: http://www.matweb.com/search/datasheet.aspx?matguid=28da9c9490bc4bfebf987d14afe02f61 [Accessed 25 October 2016]
14. "RADIOSS_13.0_USER_GUIDE" Retrieved from https://connect.altair.com/CP/downloads.html on June 4 2016.
15. "RADIOSS for Impact Analysis" Retrieved from https://connect.altair.com/CP/downloads.html on June 4 2016.
16. "Introduction to Mechanics of Materials". Retrieved from http://madhuvable.org/books-2/introduction/ on February 27 2017.
17. "Densities of Solids" [Online] Available: http://www.engineeringtoolbox.com/density-solids-d_1265.html
18. "Modulus of Elasticity or Young's Modulus - and Tensile Modulus for common Materials" [Online] Available: http://www.engineeringtoolbox.com/young-modulus-d_417.html
19. "Poisson's Ratio" [Online] Available: http://www.engineeringtoolbox.com/poissons-ratio-d_1224.html
20. Odegard, G. "Equivalent-continuum Modeling of Nano-structured Materials." *Composites Science and Technology* 62.14 (2002): 1869-880. Web.

10. Appendix

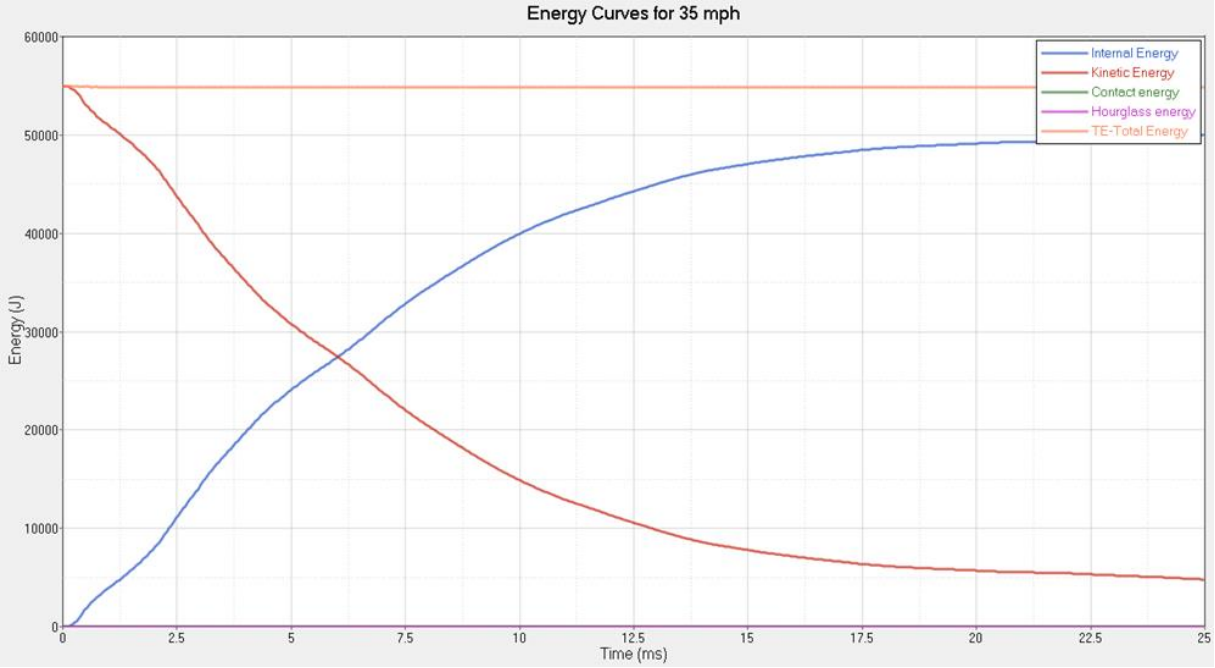

Figure 72- Energy Curves for 35mph

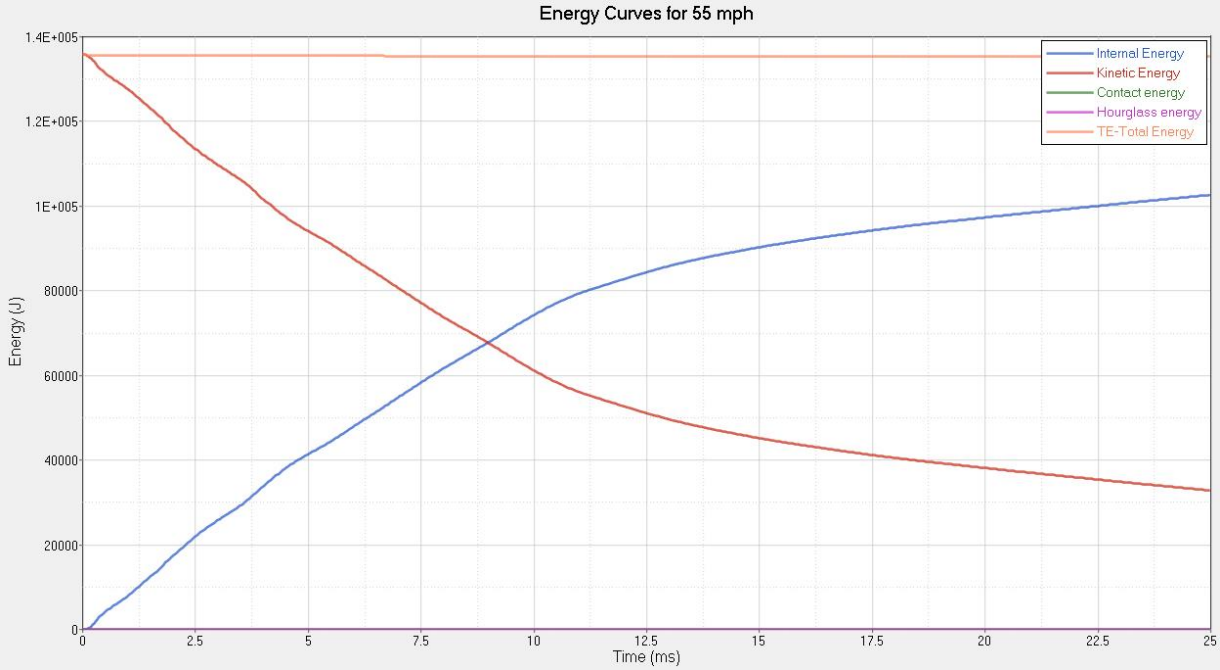

Figure 73- Energy curves for 55 mph

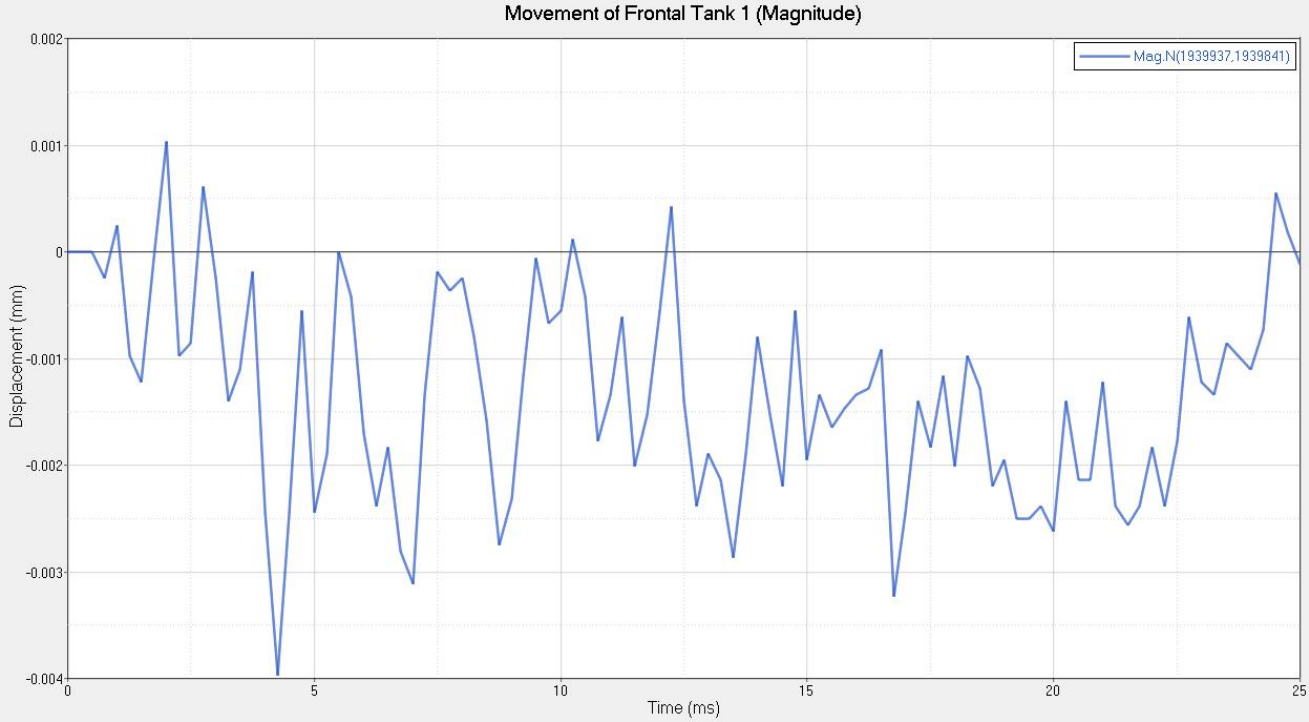

Figure 74- Movement of Frontal Tank1- Mag [35mph]

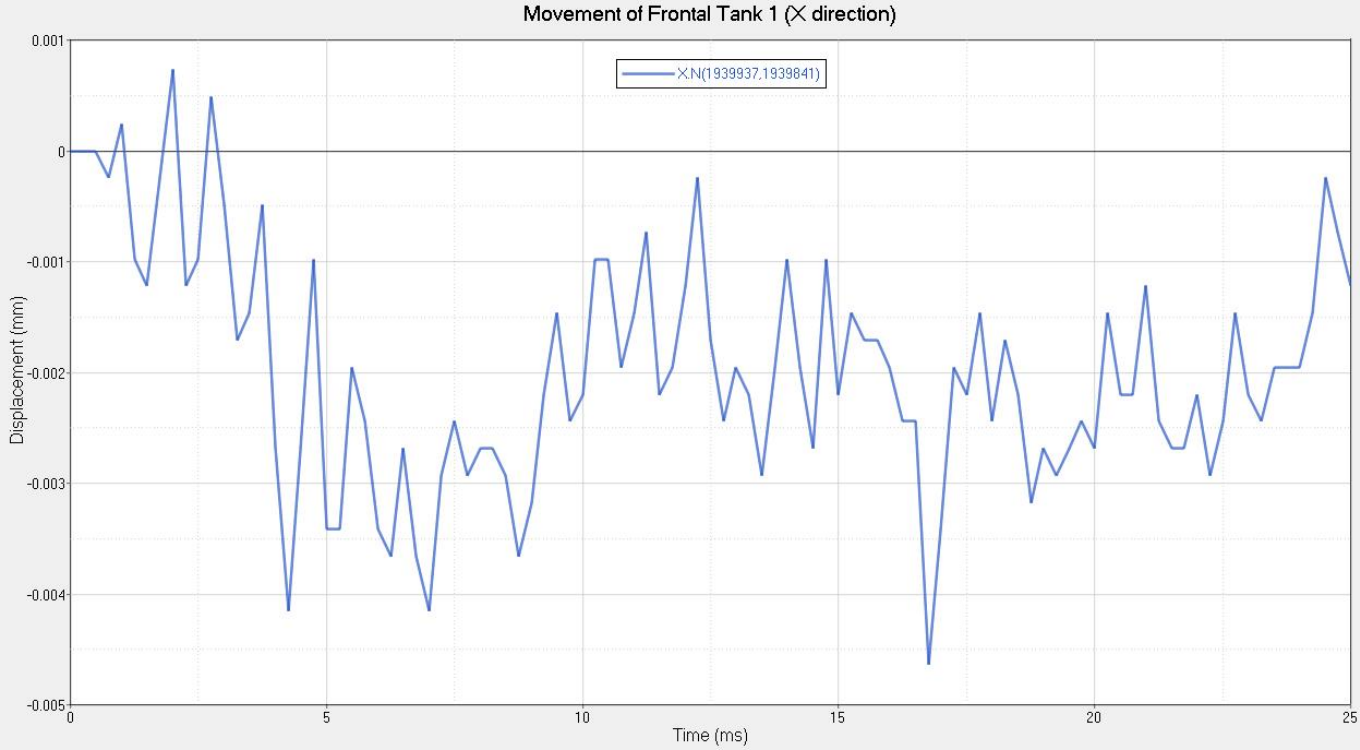

Figure 75-Movement of Frontal Tank1- X direction [35mph]

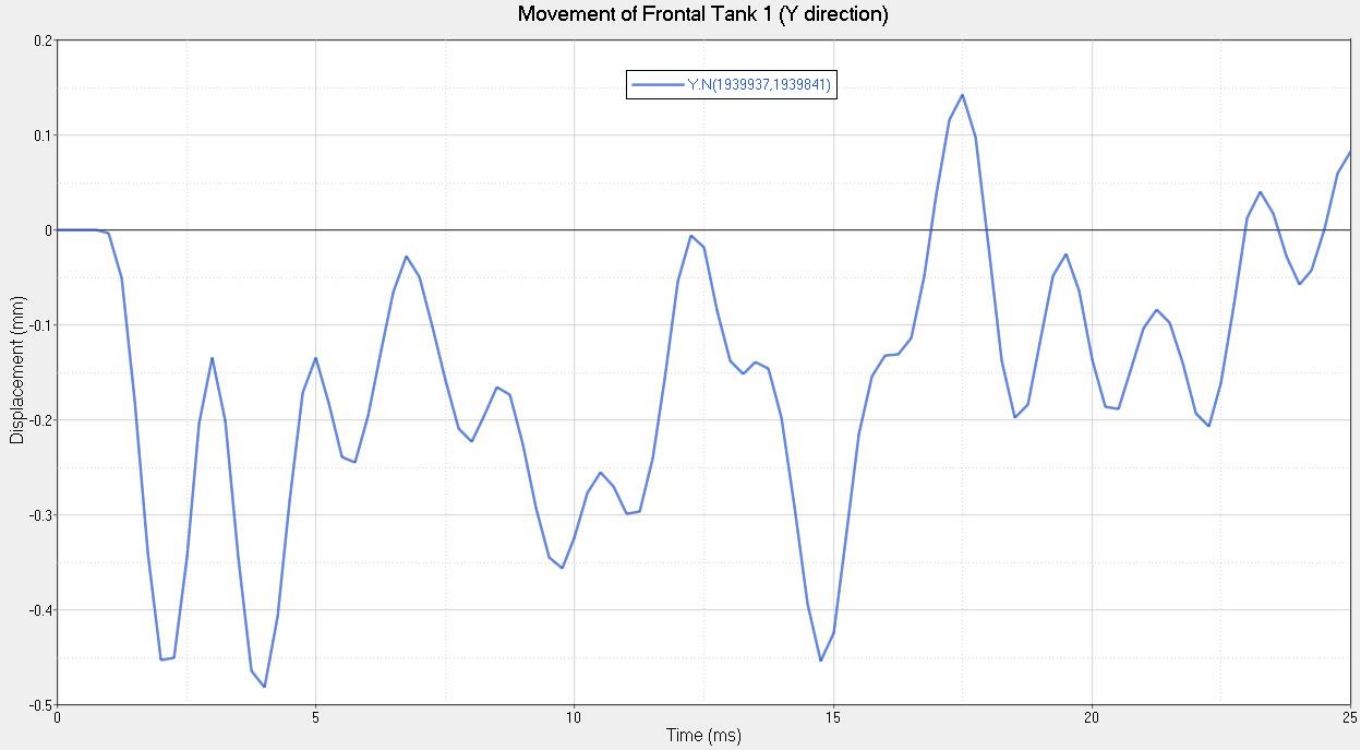

Figure 76-Movement of Frontal Tank1- Y direction [35mph]

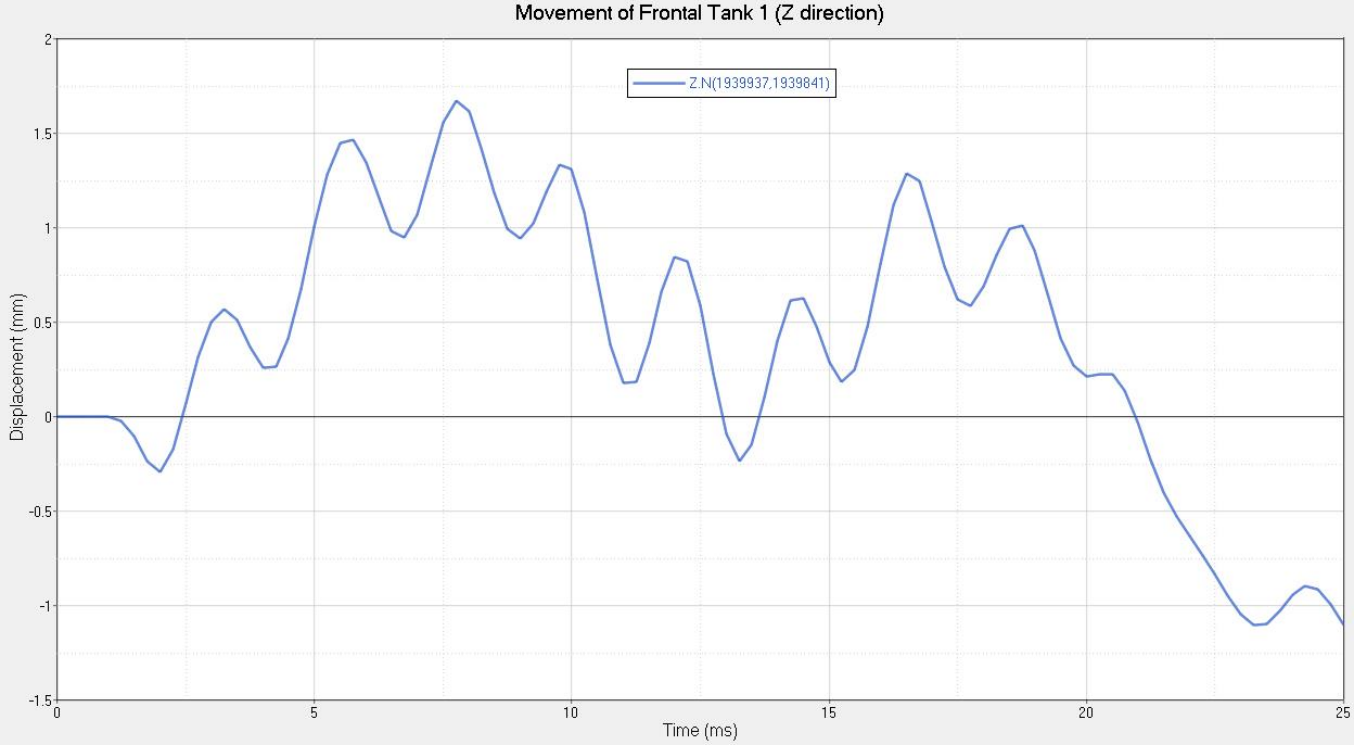

Figure 77-Movement of Frontal Tank1- Z direction [35mph]

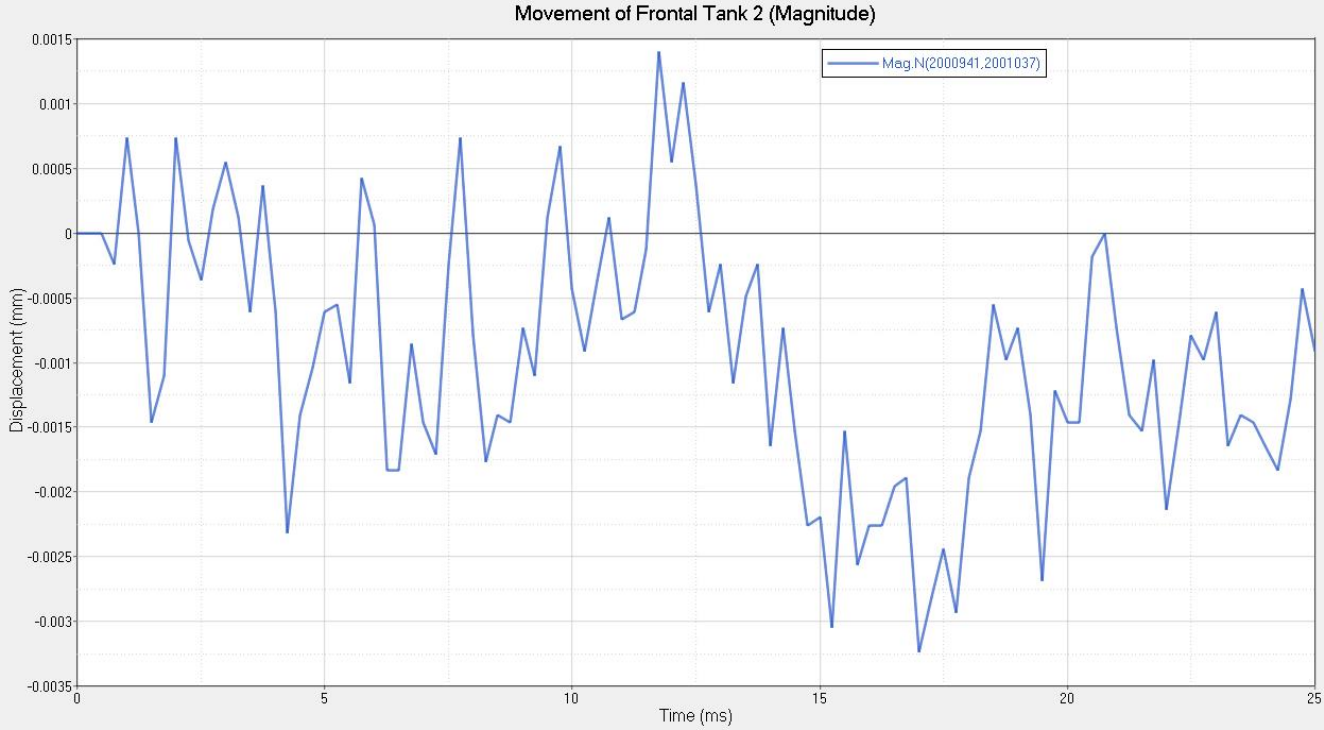

Figure 78-Movement of Frontal Tank 2- Mag [35mph]

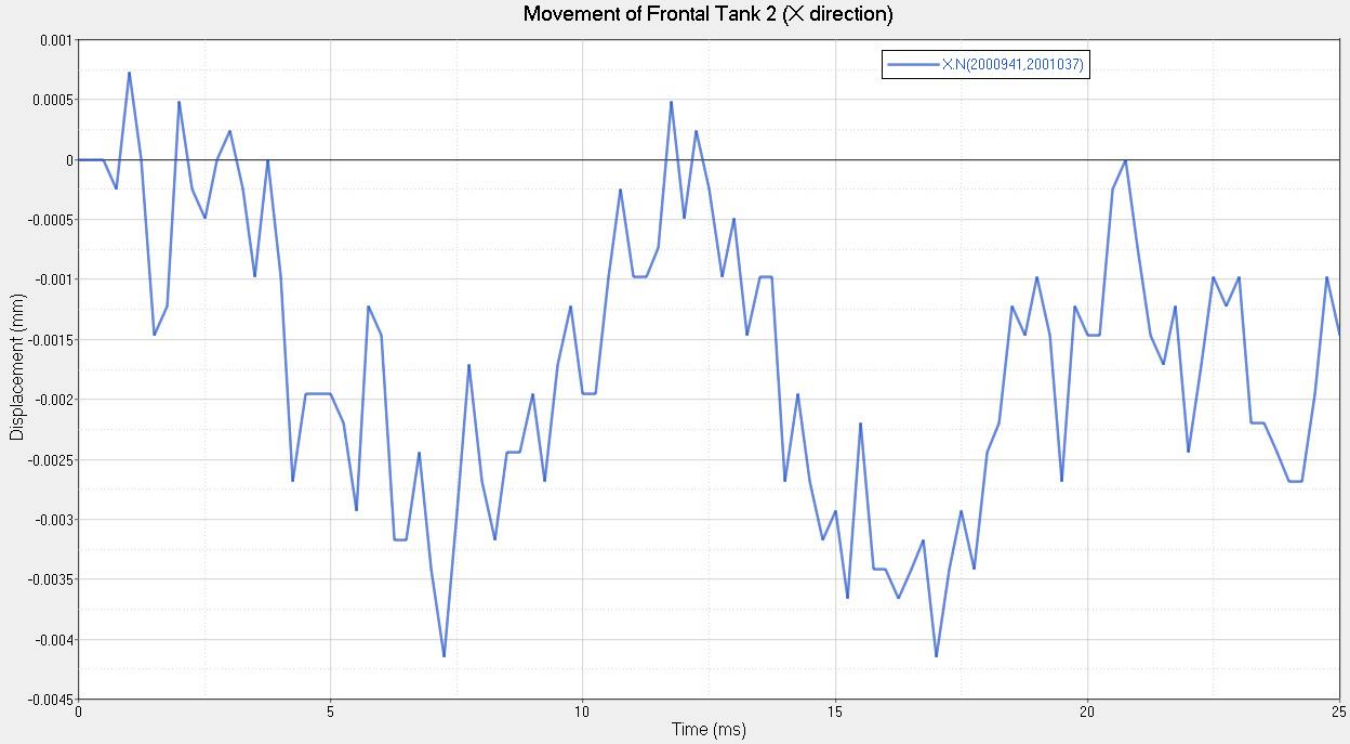

Figure 79-Movement of Frontal Tank 2- X direction [35mph]

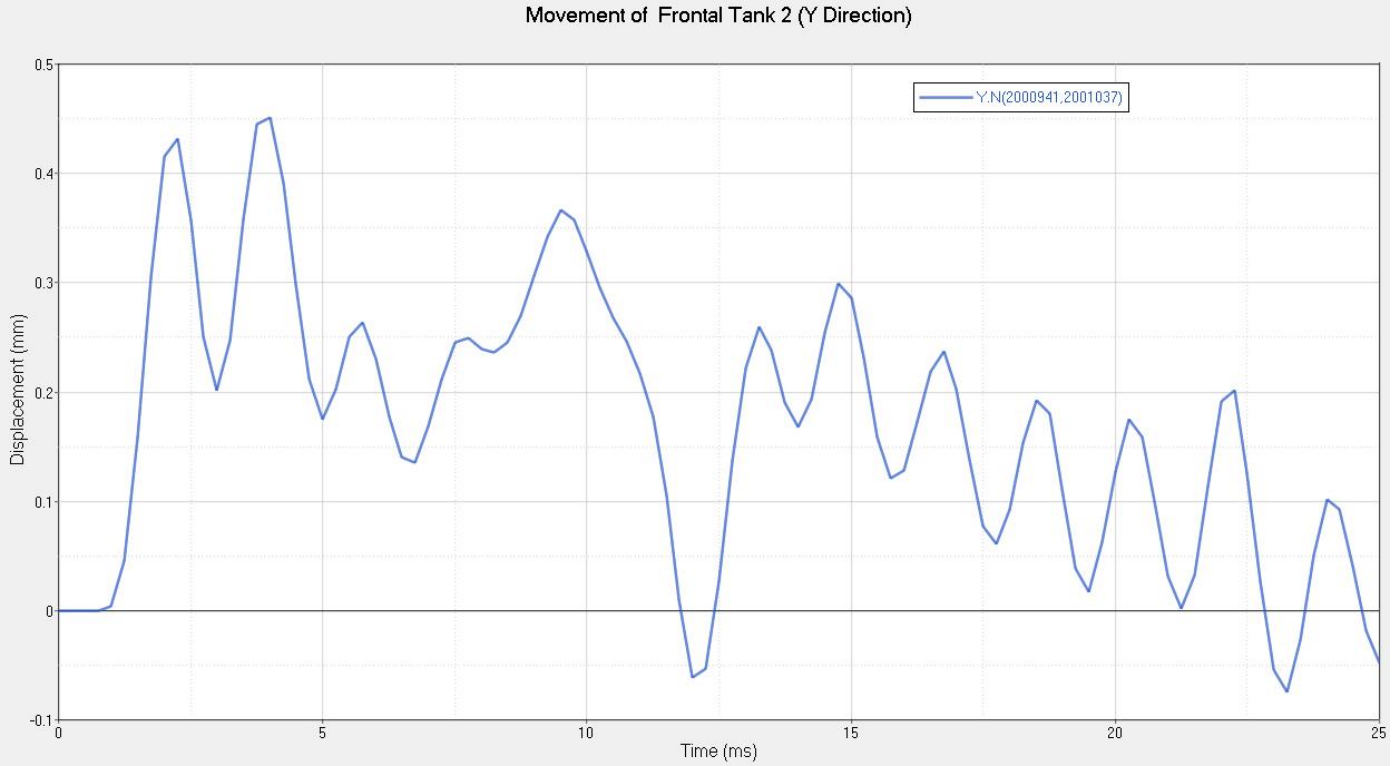

Figure 80-Movement of Frontal Tank 2- Y direction [35mph]

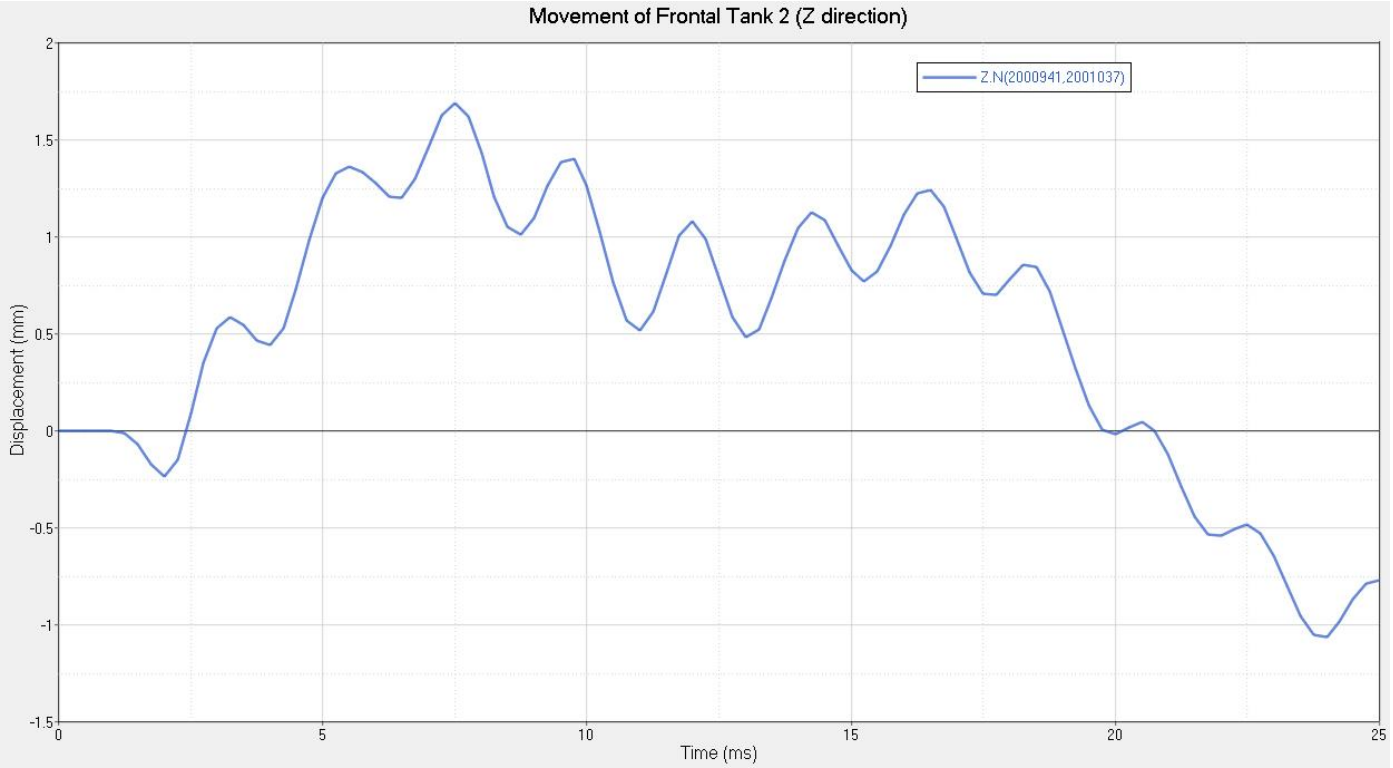

Figure 81-Movement of Frontal Tank 2- Z direction [35mph]

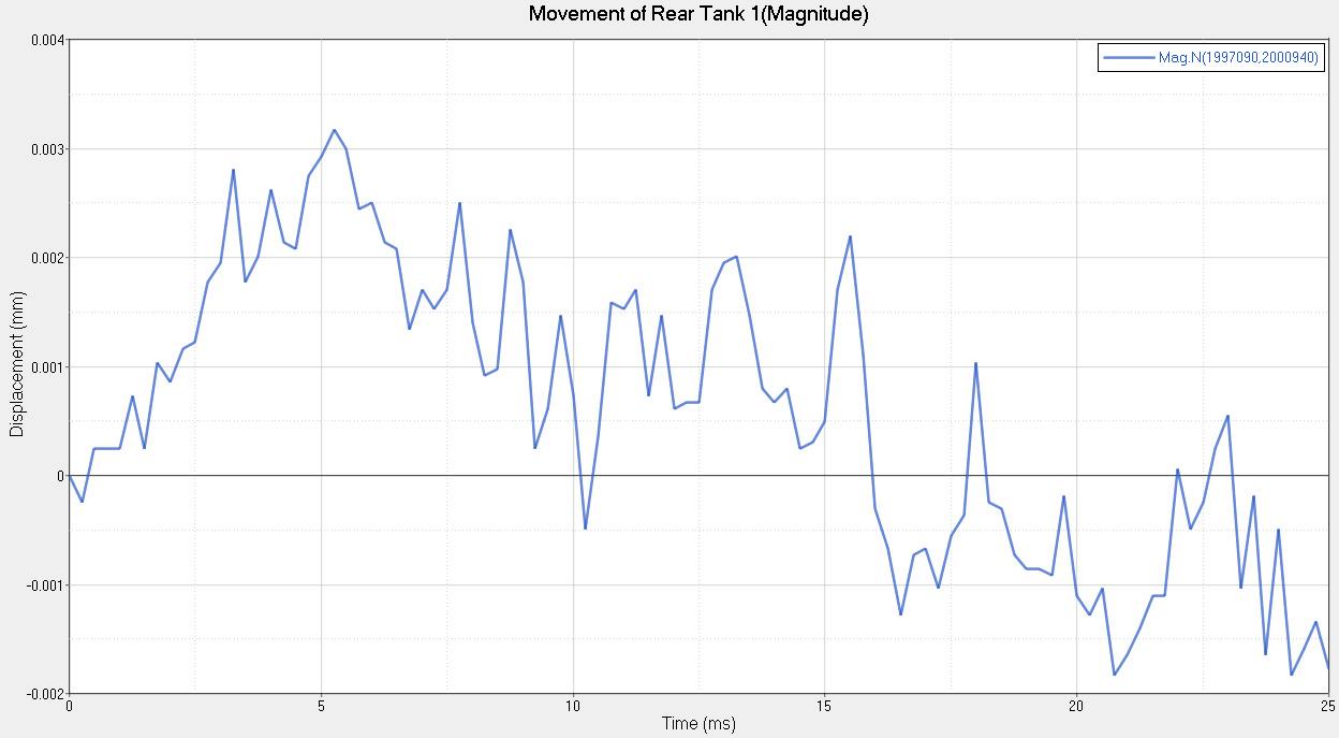

Figure 82-Movement of Rear Tank 1- Mag [35mph]

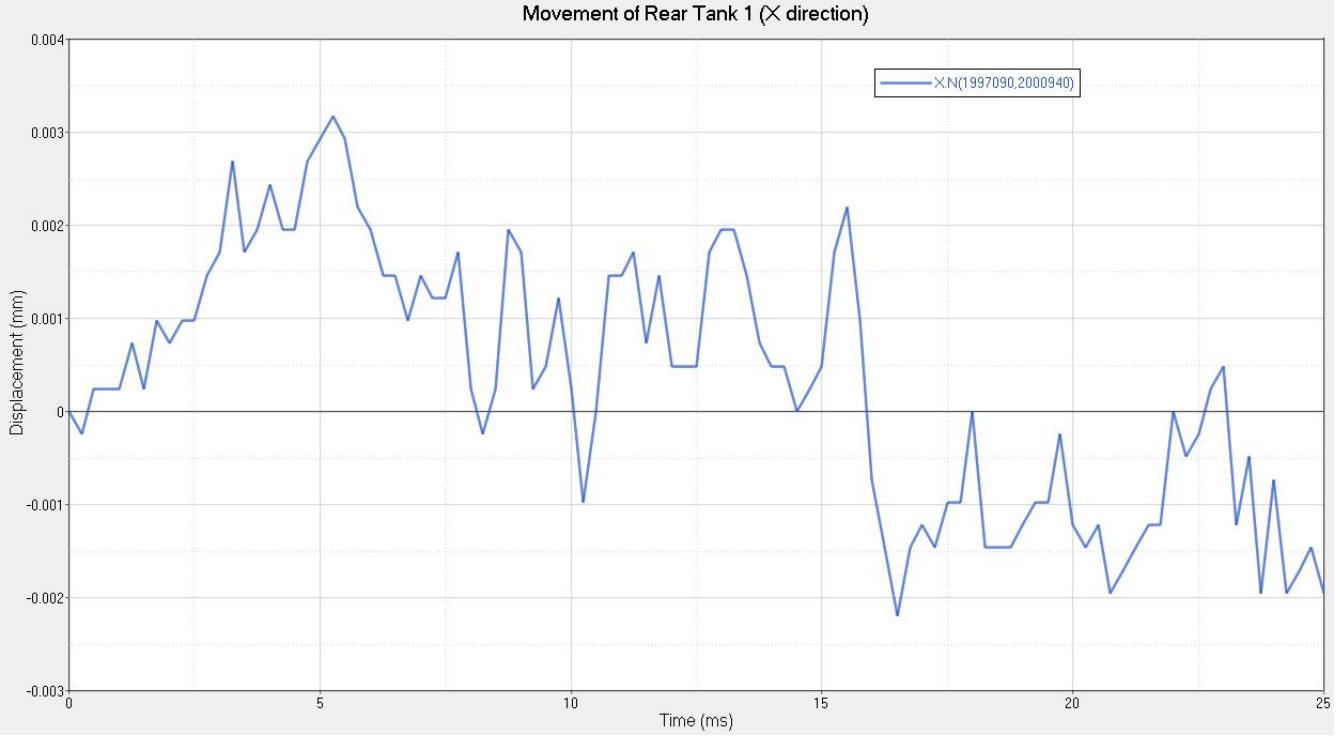

Figure 83-Movement of Rear Tank 1- X direction [35mph]

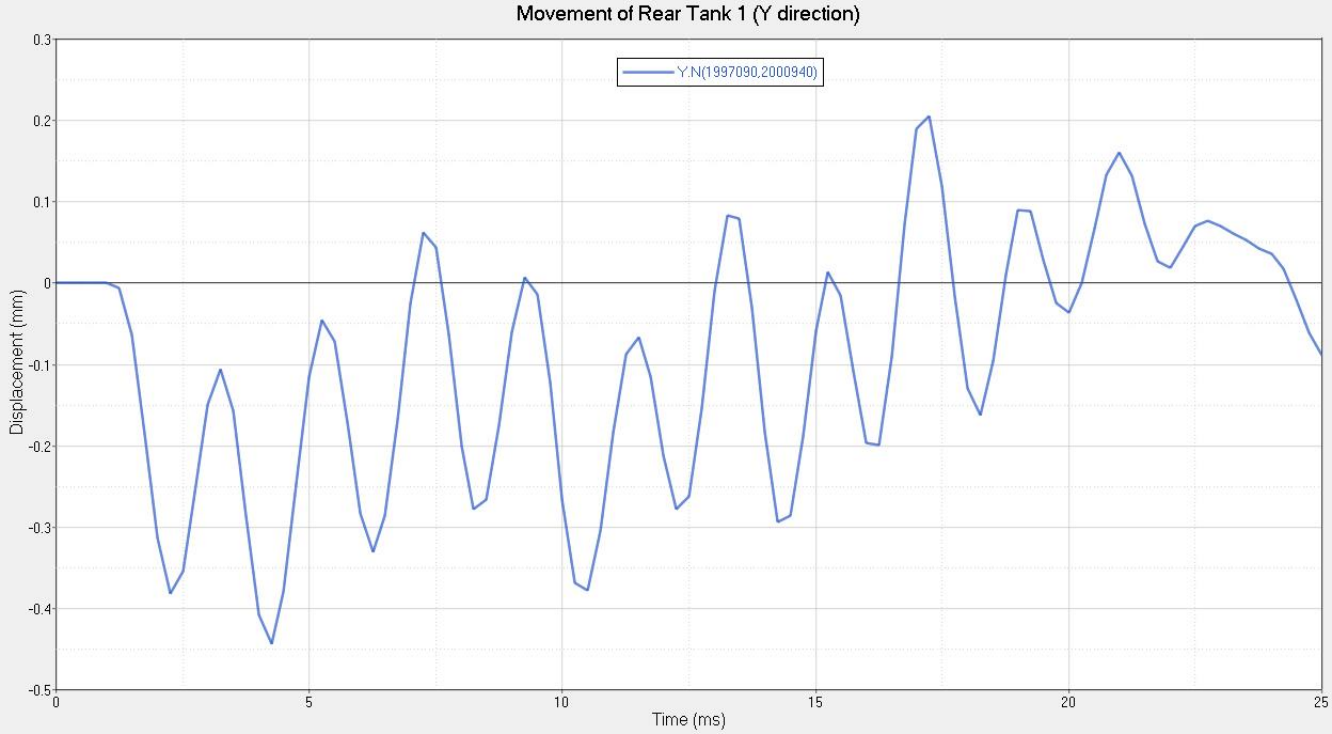

Figure 84-Movement of Rear Tank 1- Y direction [35mph]

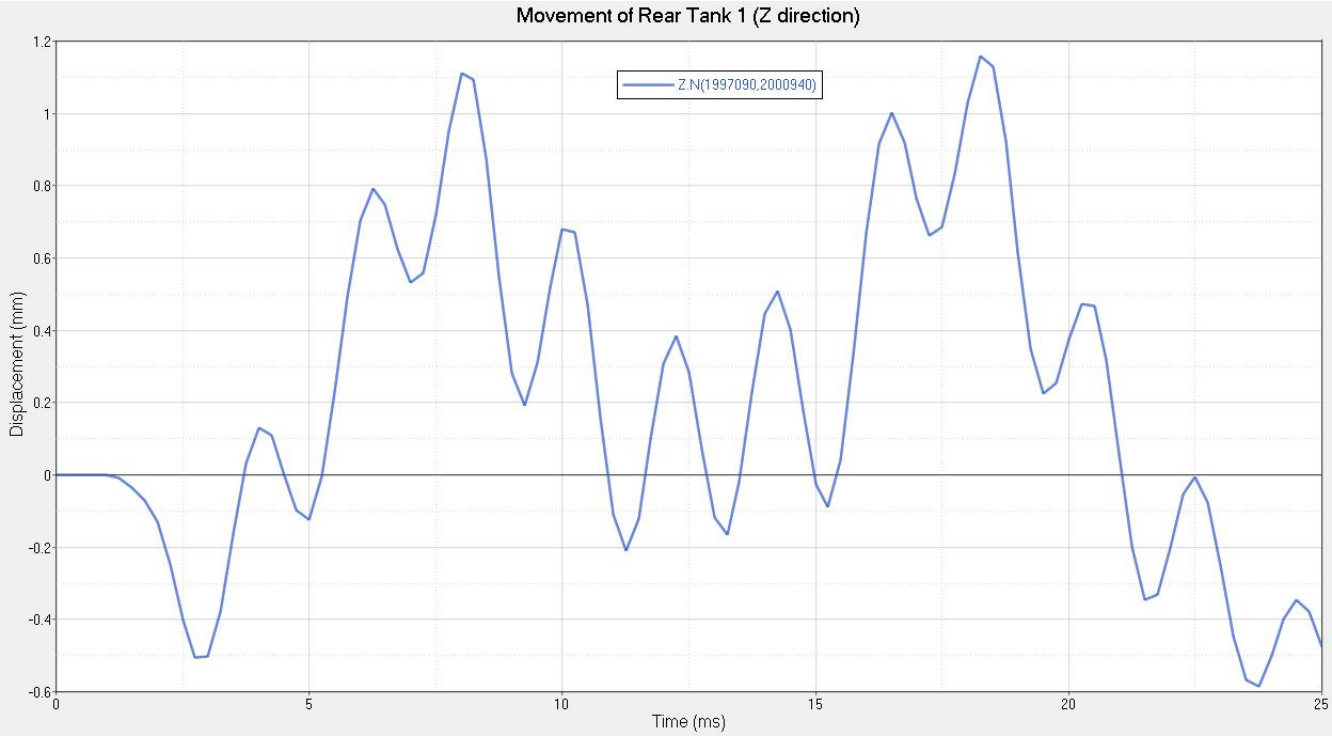

Figure 85-Movement of Rear Tank 1- Z direction [35mph]

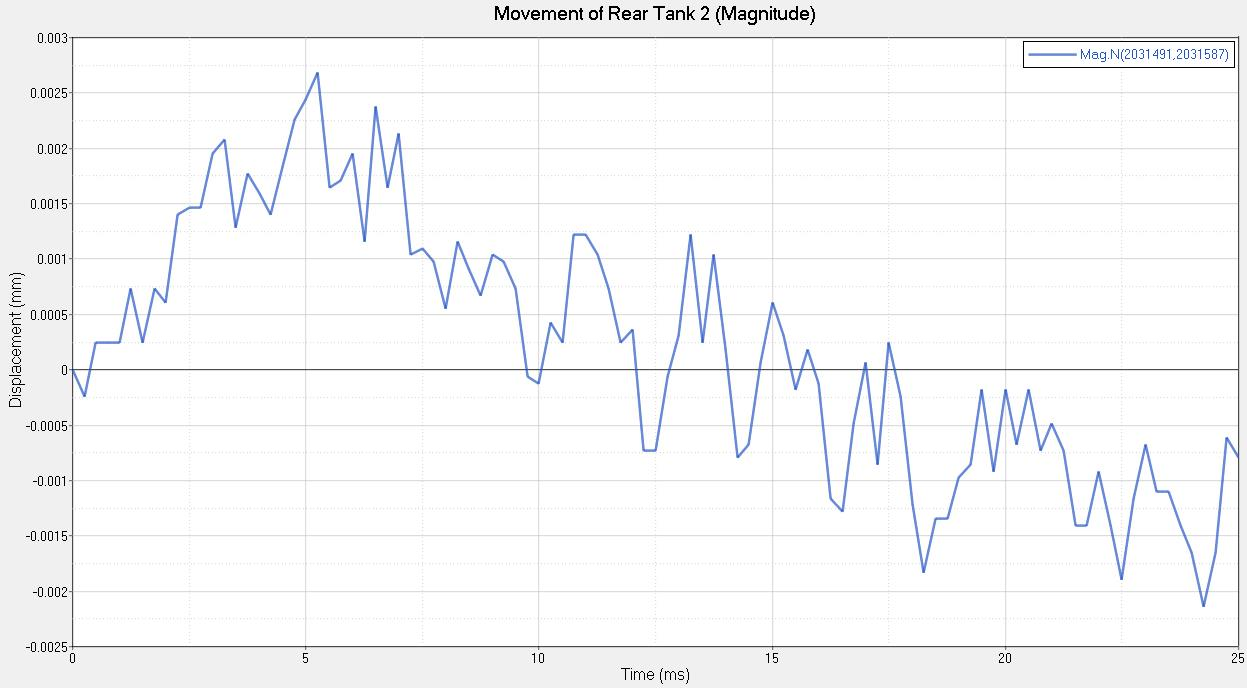

Figure 86-Movement of Rear Tank 2- Mag [35mph]

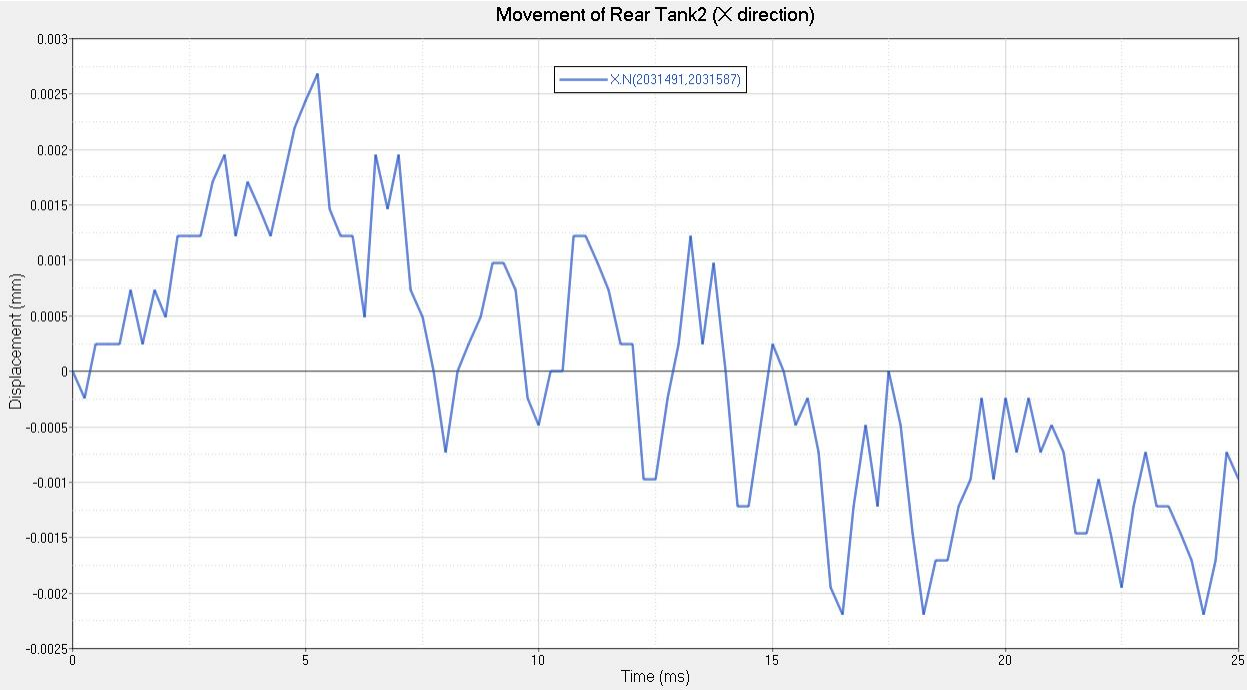

Figure 87-Movement of Rear Tank 2- X direction [35mph]

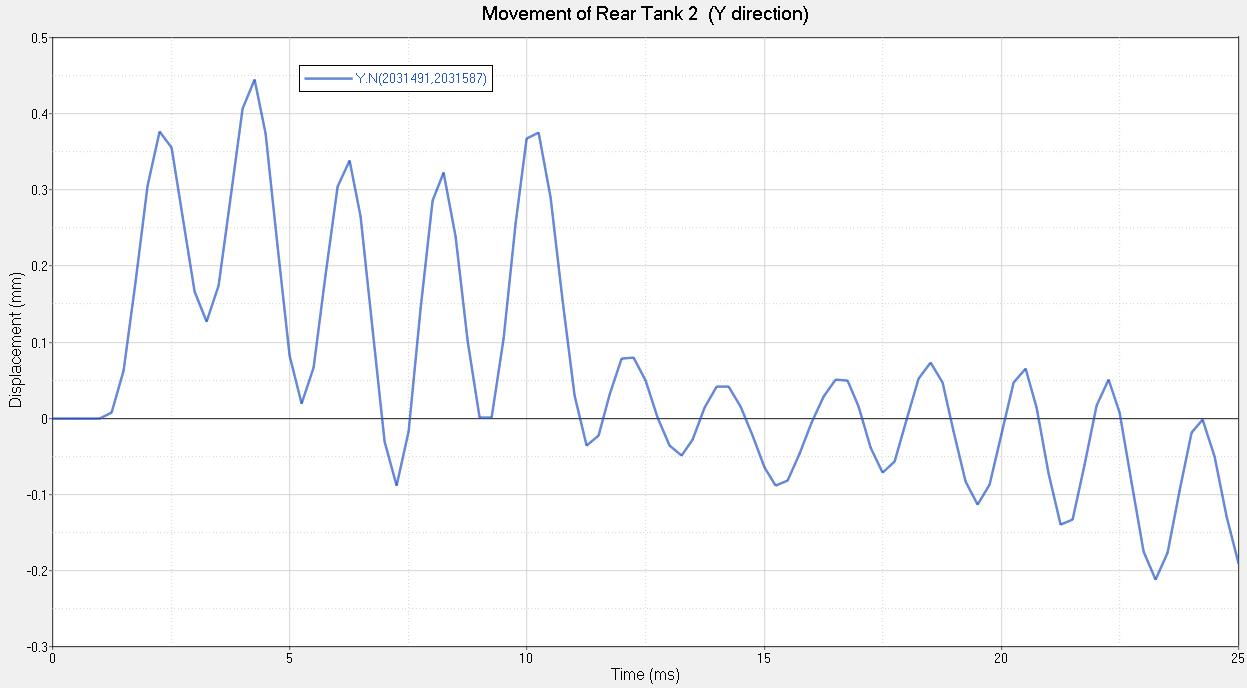

Figure 88-Movement of Rear Tank 2- Y direction [35mph]

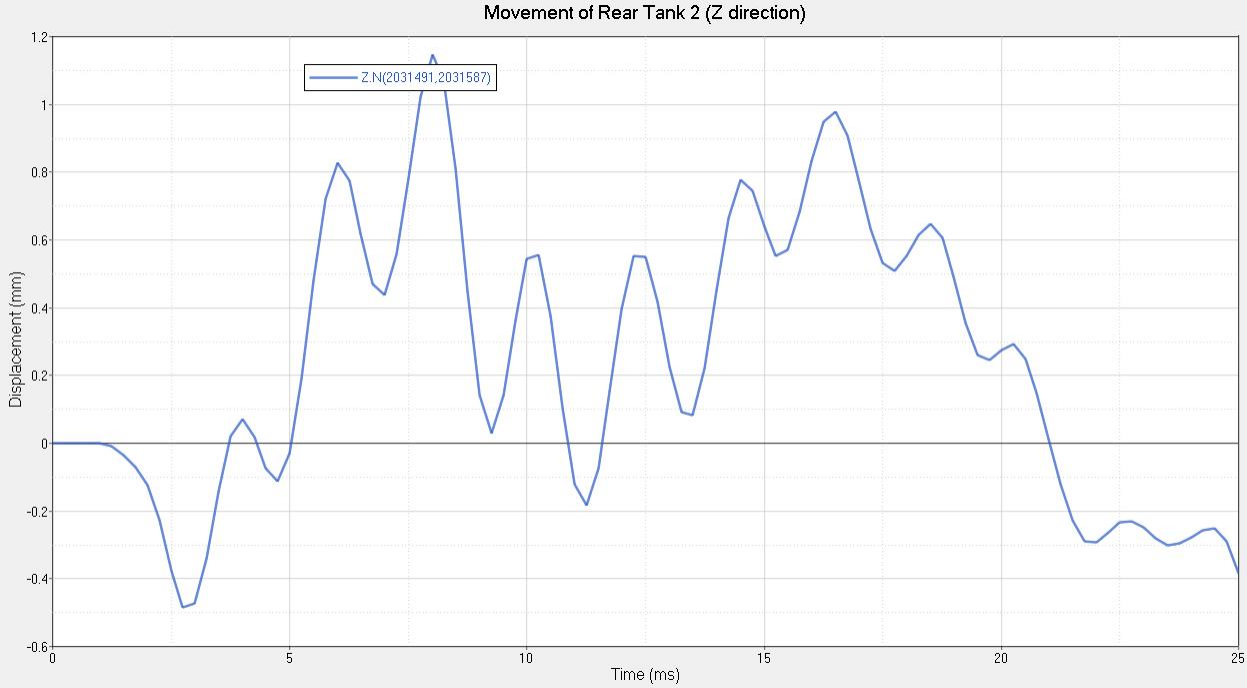

Figure 89-Movement of Rear Tank 2- Z direction [35mph]

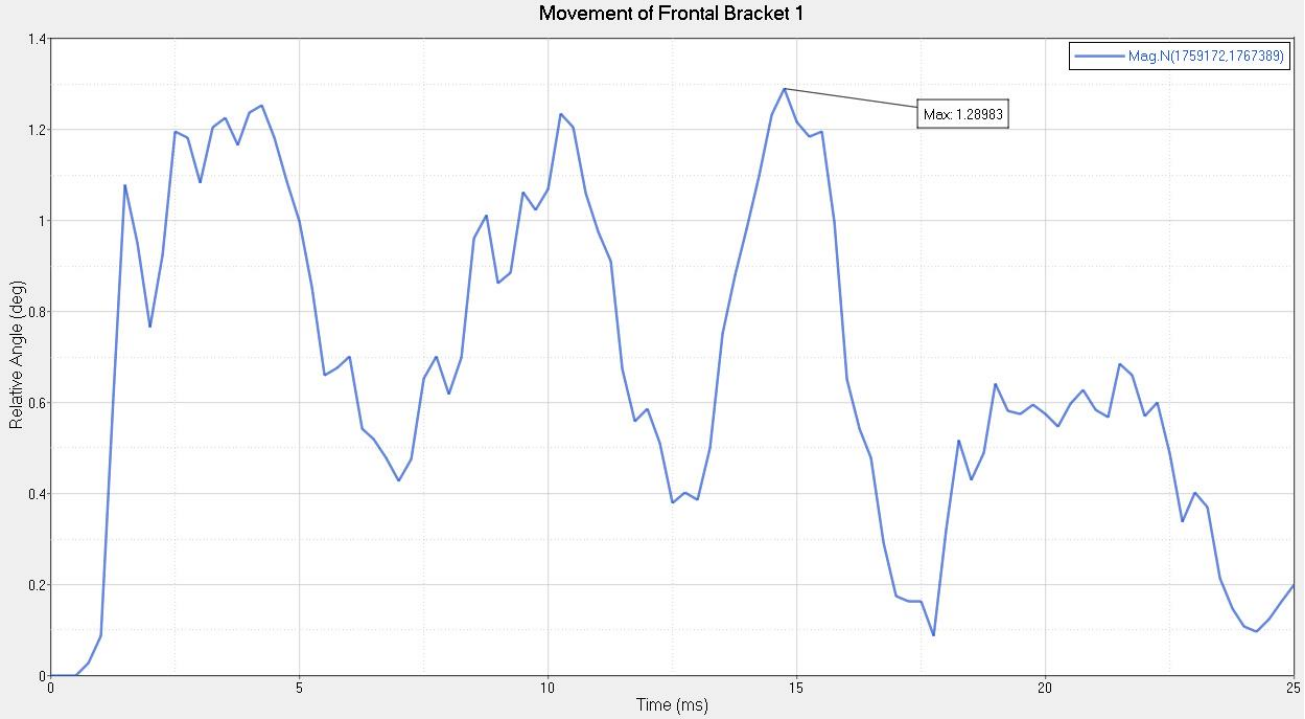

Figure 90-Movement of Frontal Bracket 1A [35mph]

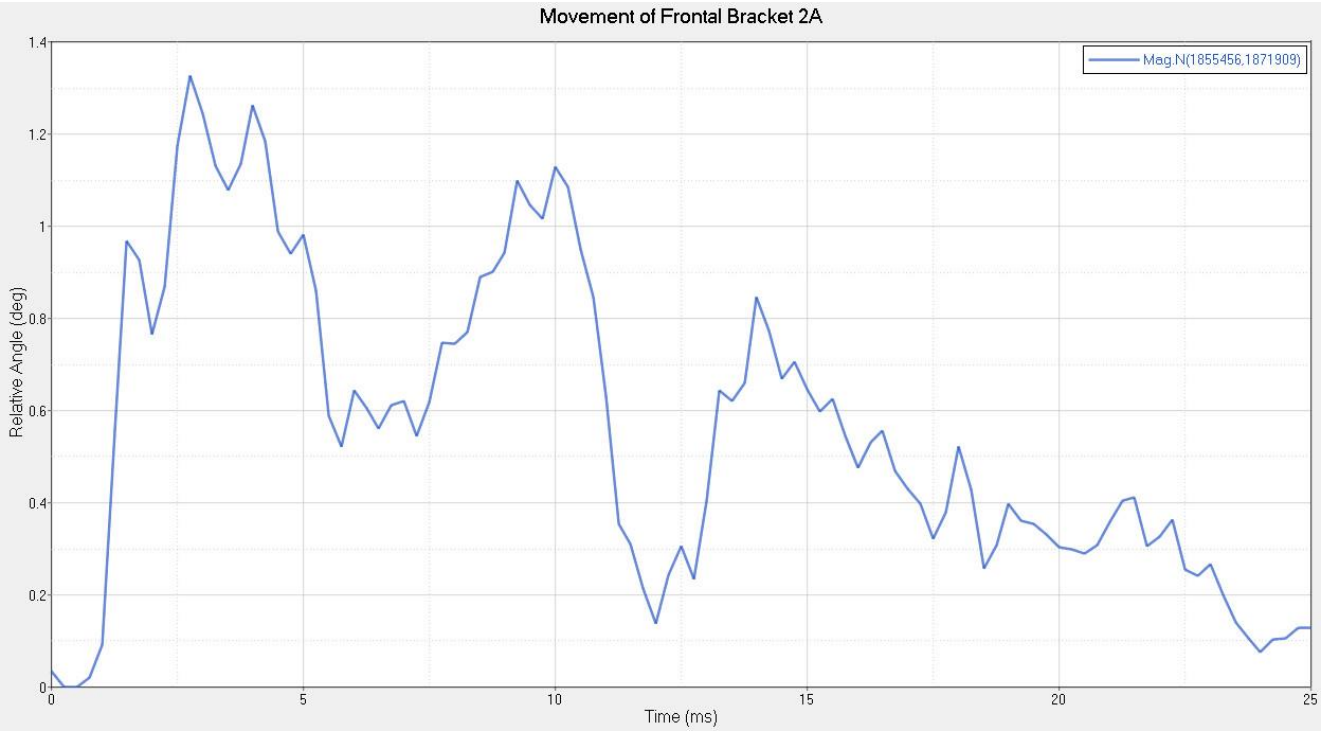

Figure 91-Movement of Frontal Bracket 2A [35mph]

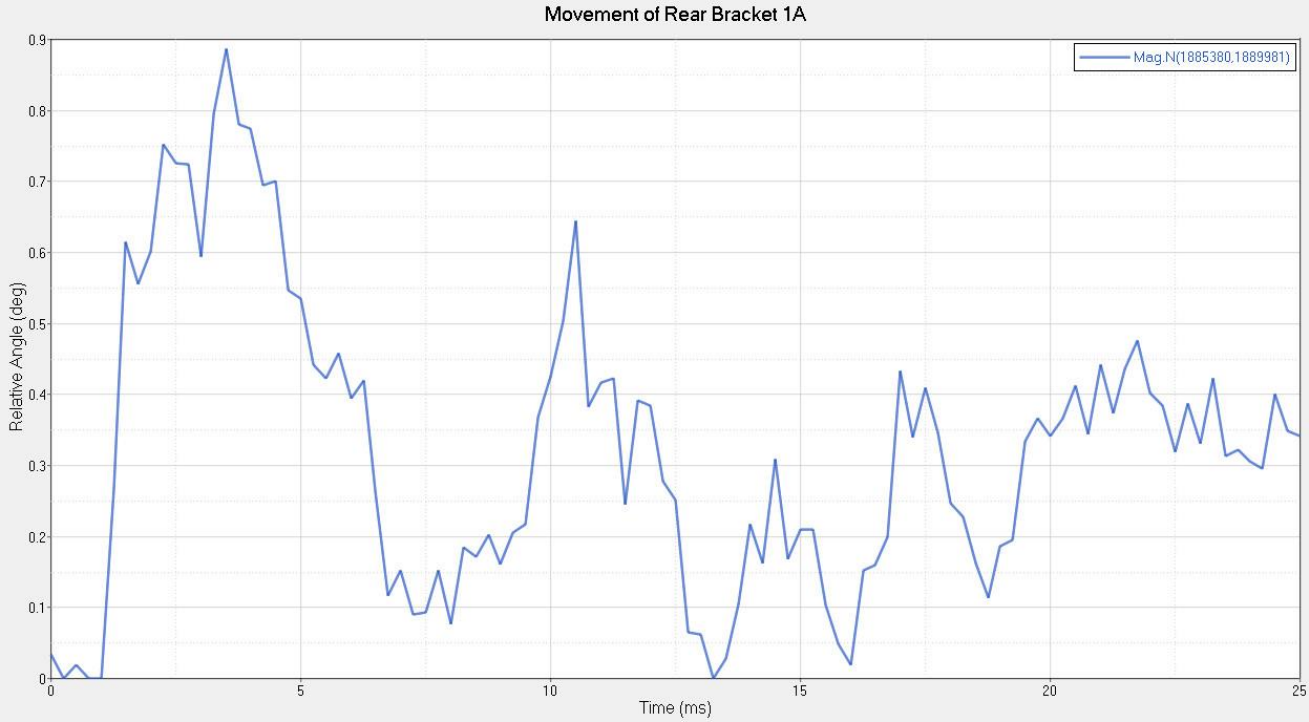

Figure 92-Movement of Rear Bracket 1A [35mph]

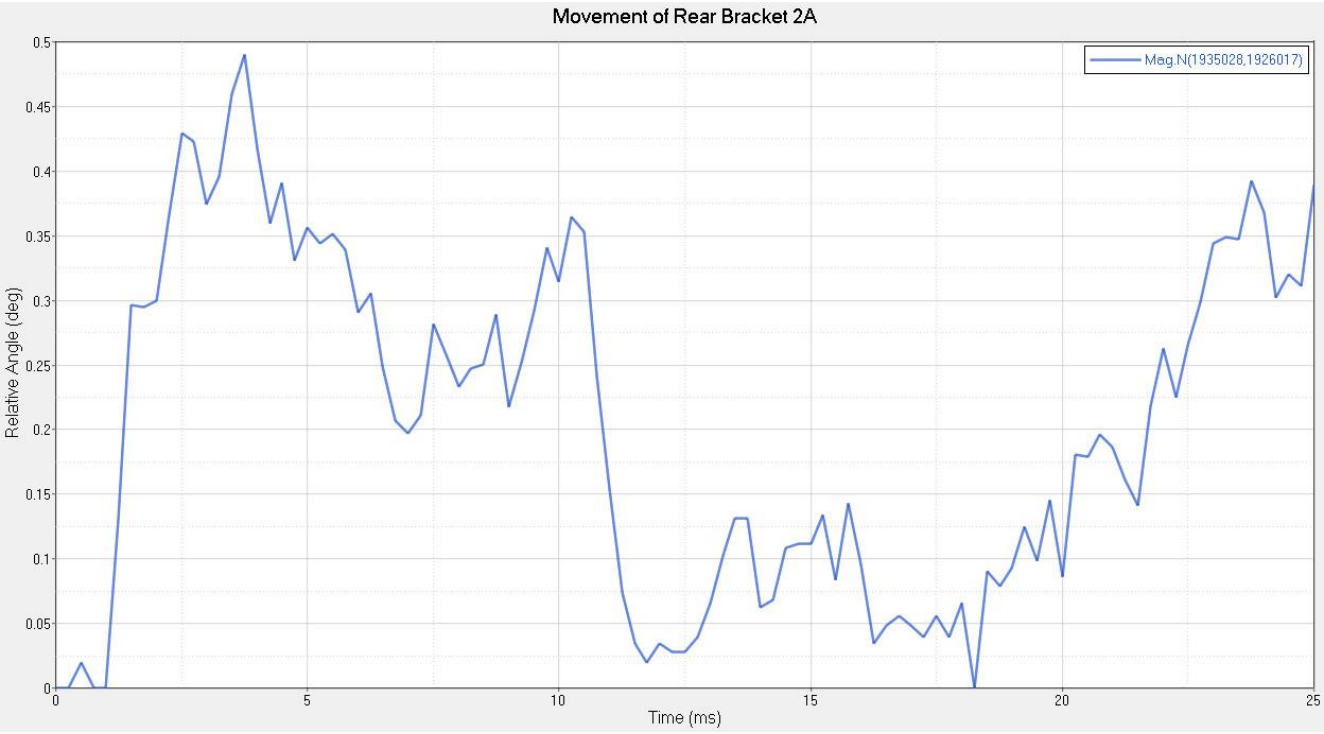

Figure 93-Movement of Rear Bracket 2A [35mph]

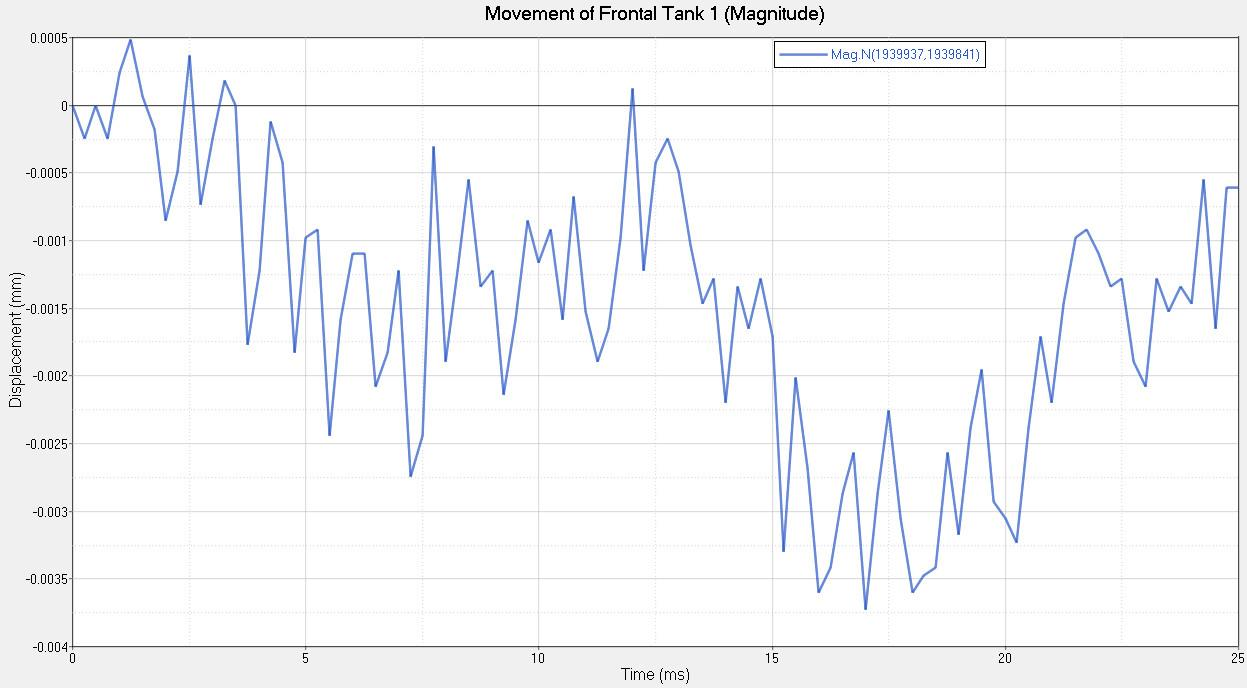

Figure 94-Movement of Frontal Tank 1- Mag [55mph]

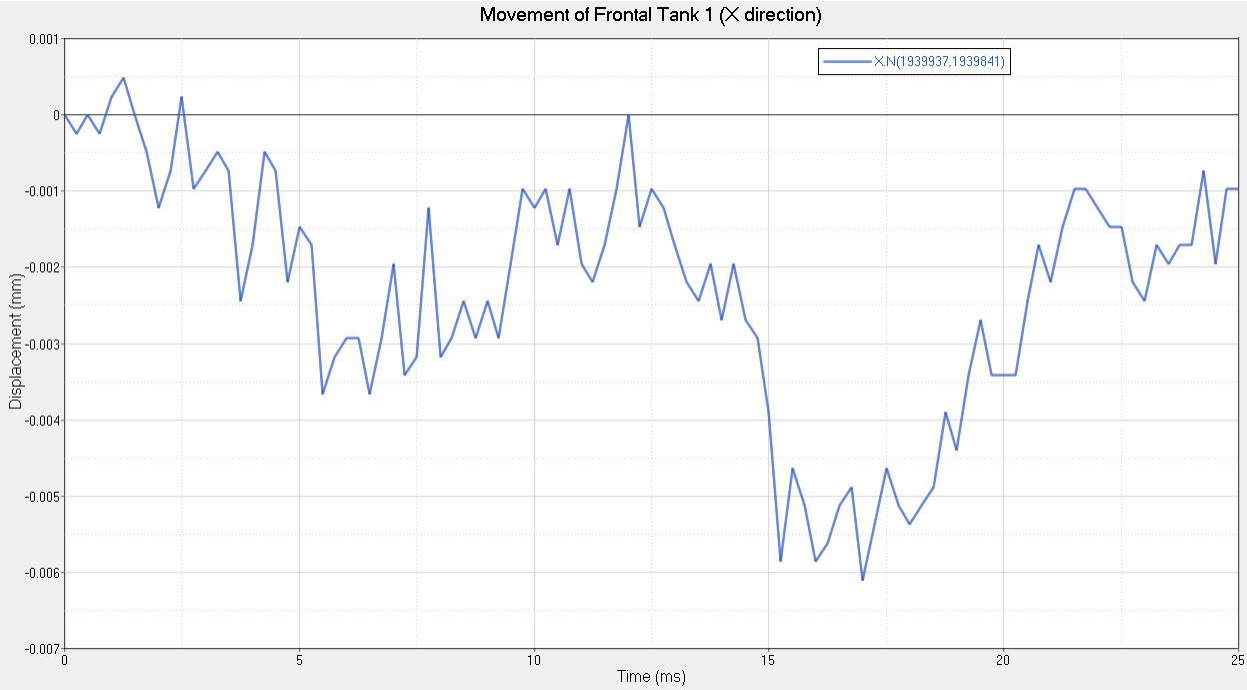

Figure 95- Movement of Frontal Tank 1- X direction [55mph]

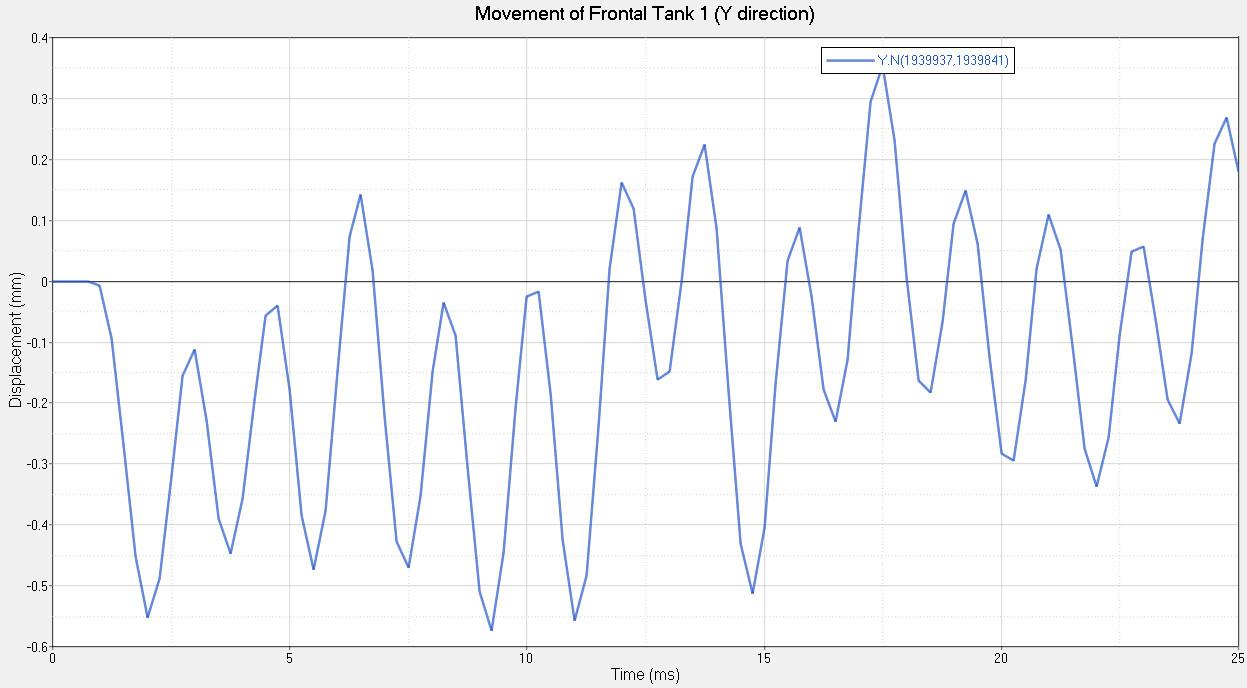

Figure 96-Movement of Frontal Tank 1- Y direction [55mph]

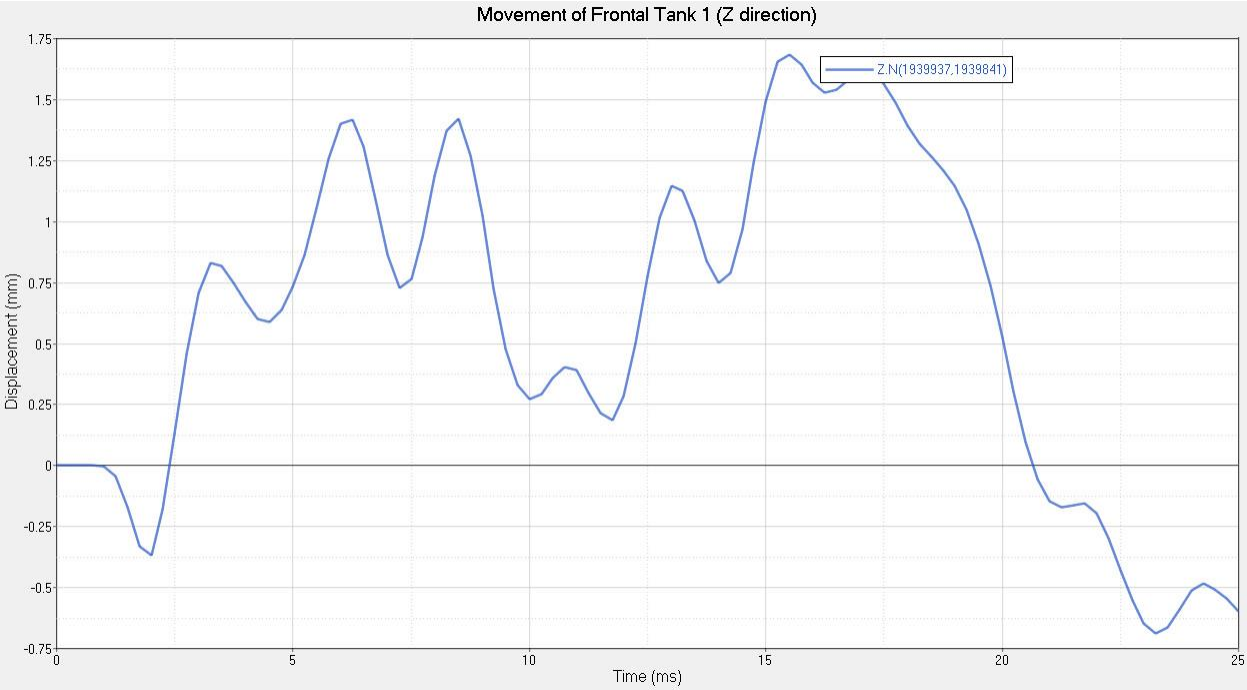

Figure 97-Movement of Frontal Tank 1- Z direction [55mph]

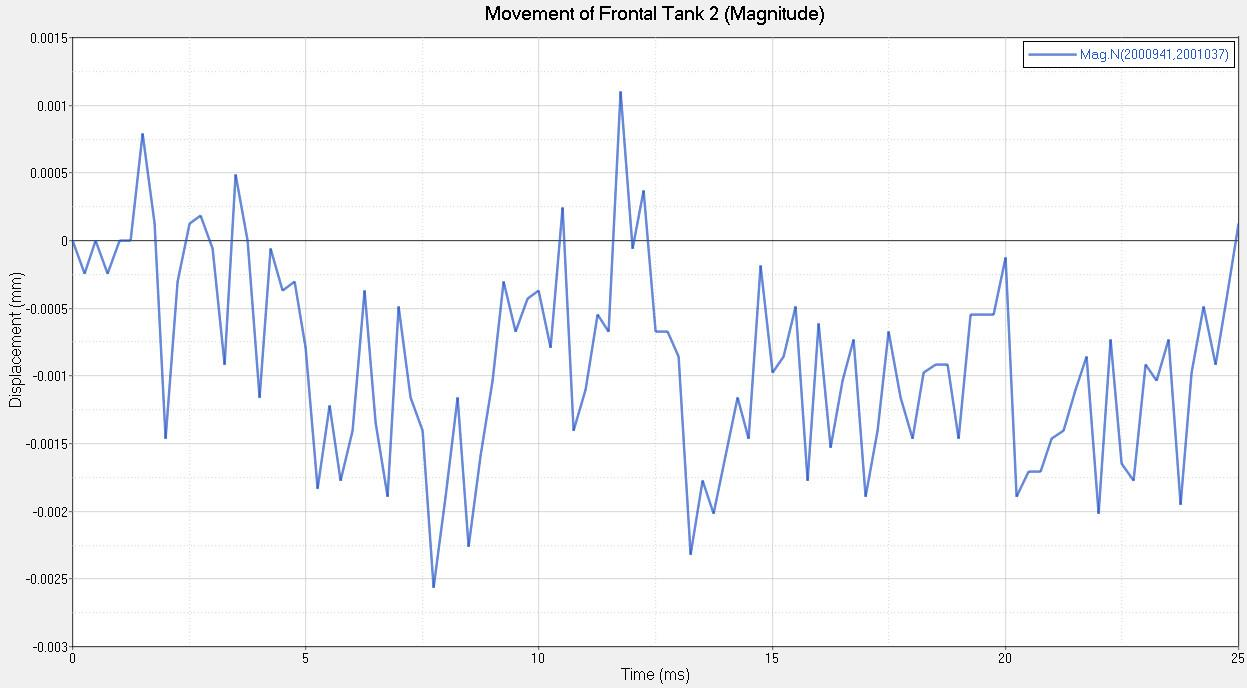

Figure 98-Movement of Frontal Tank 2- Mag [55mph]

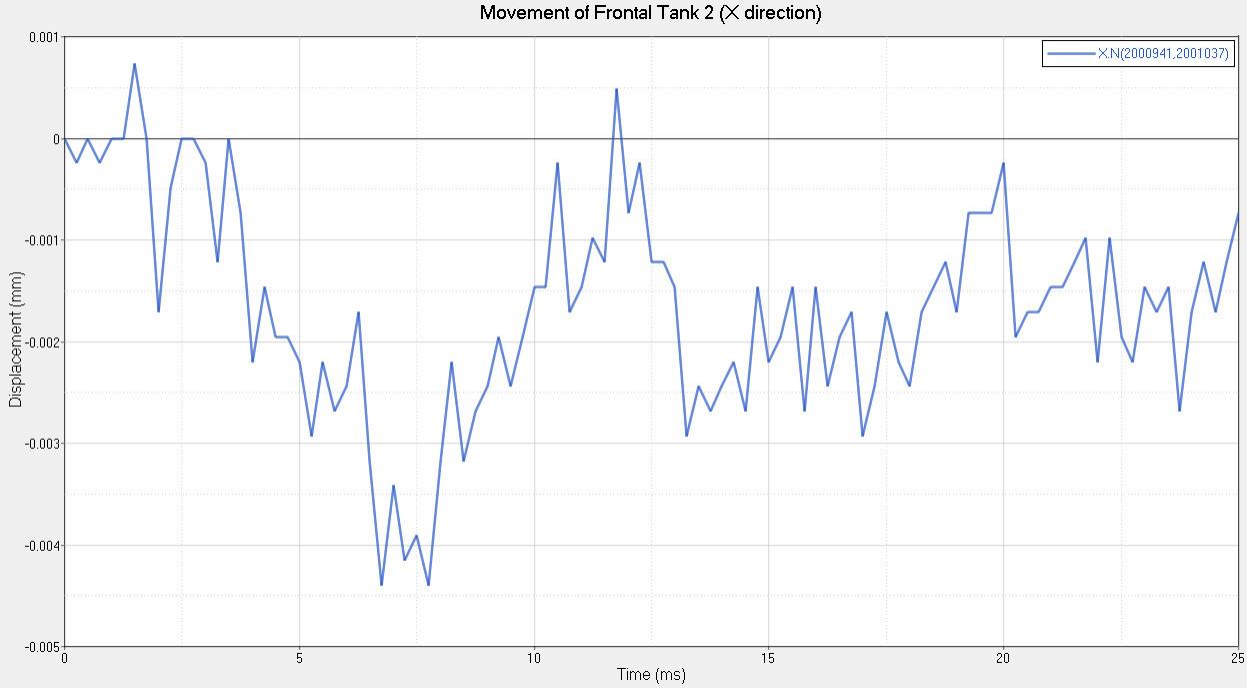

Figure 99-Movement of Frontal Tank 2- X direction [55mph]

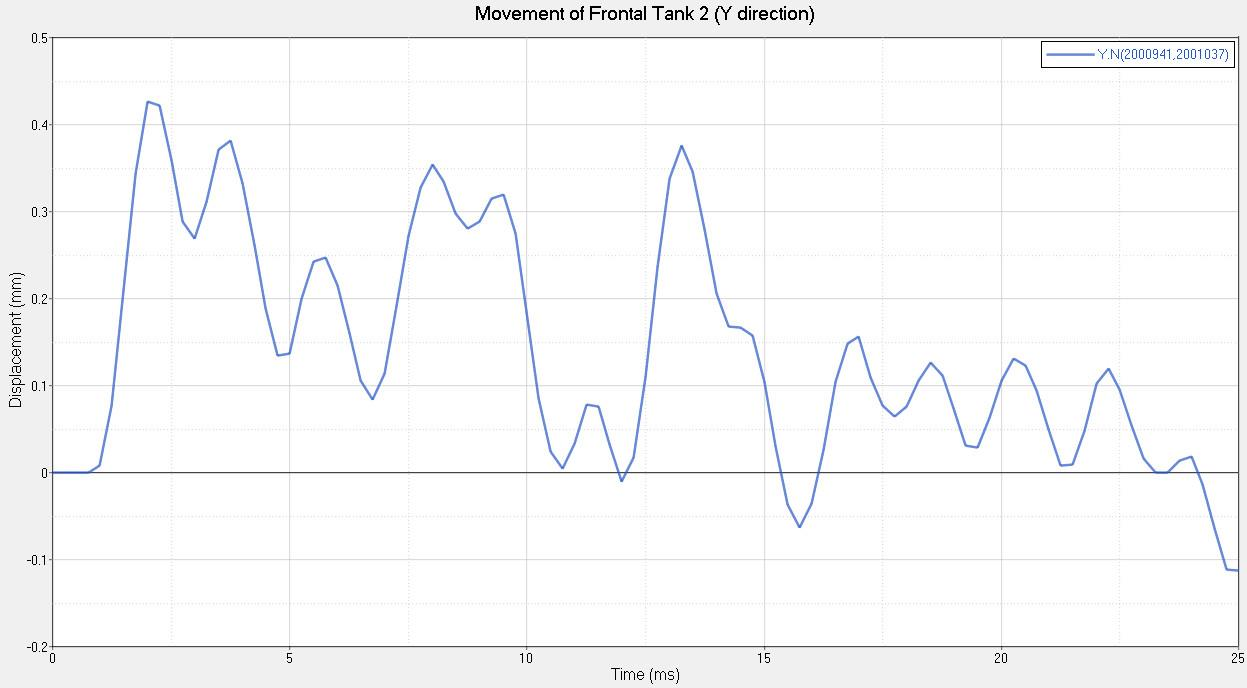

Figure 100-Movement of Frontal Tank 2- Y direction [55mph]

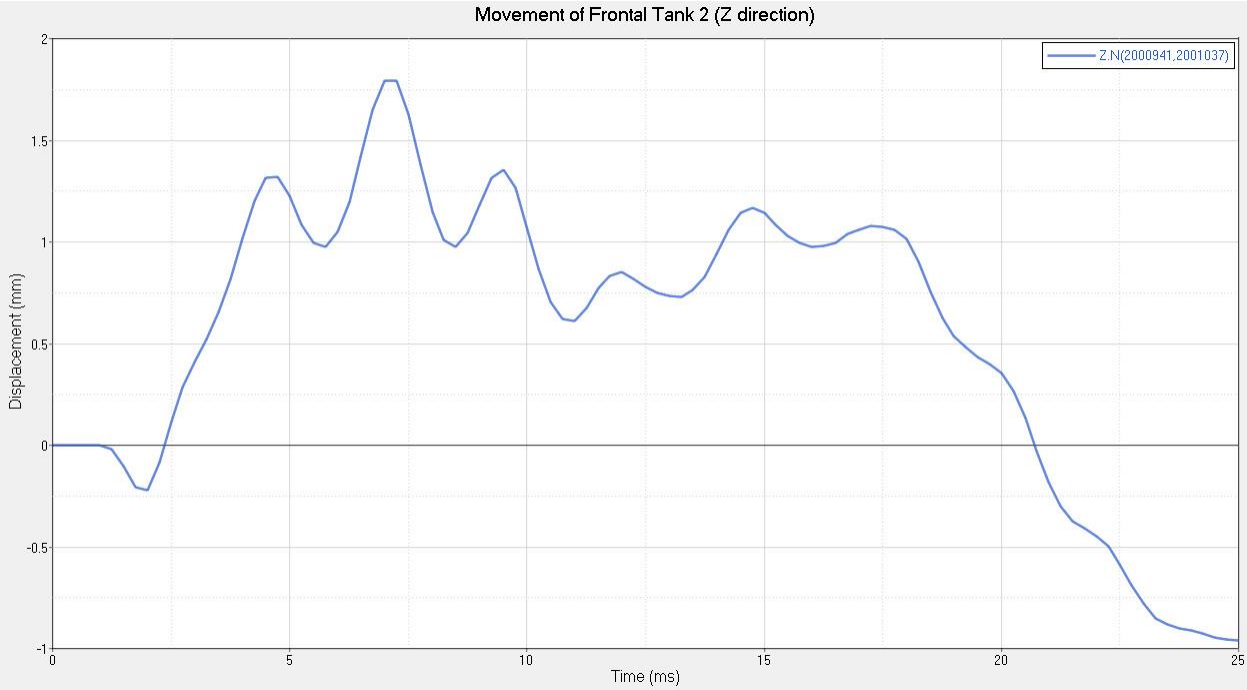

Figure 101-Movement of Frontal Tank 2- Z direction [55mph]

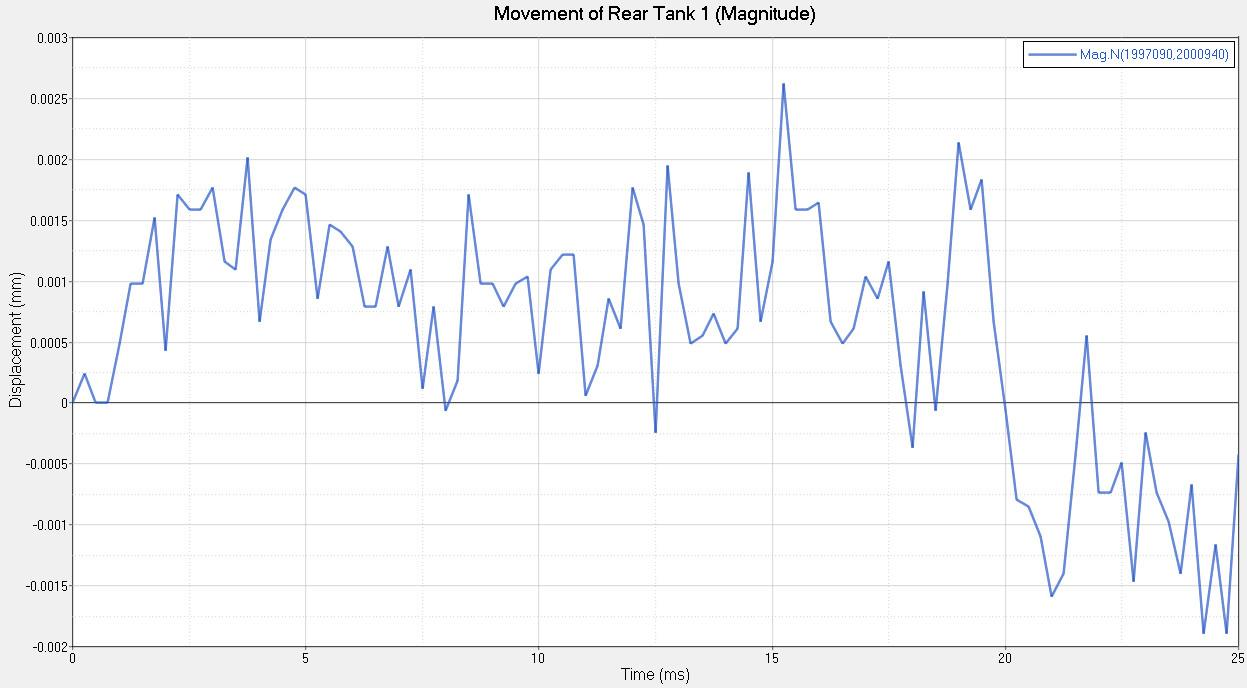

Figure 102-Movement of Rear Tank 1- Mag [55mph]

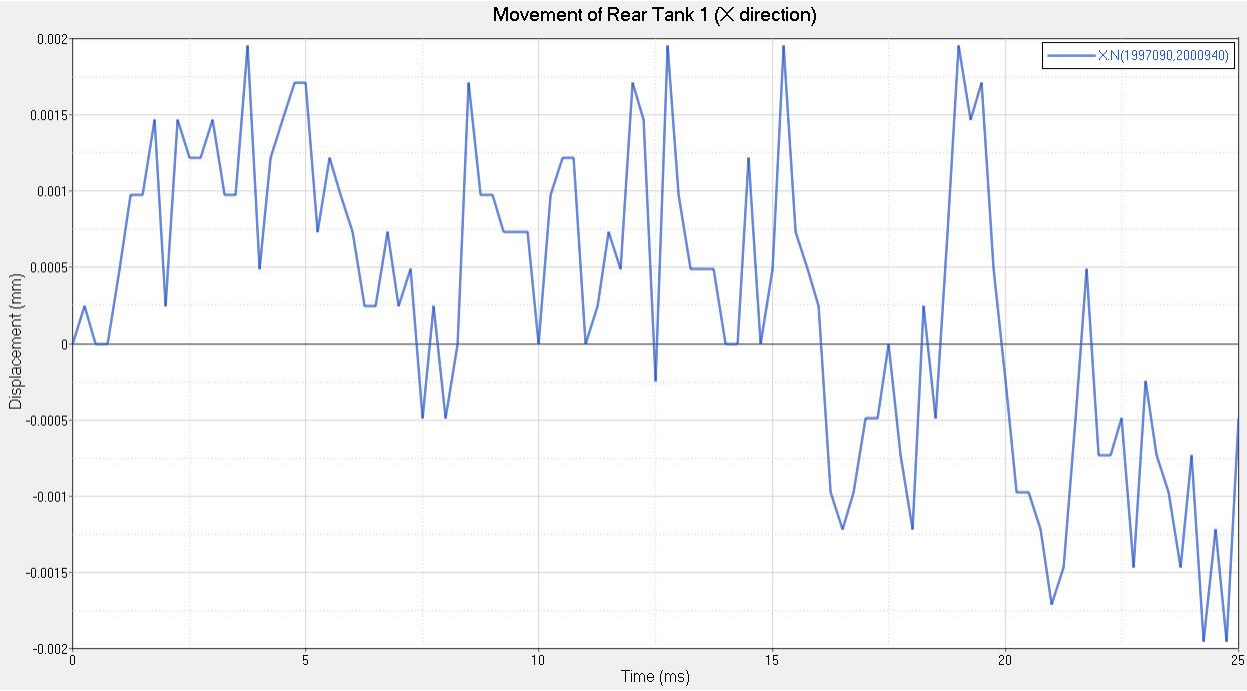

Figure 103-Movement of Rear Tank 1- X direction [55mph]

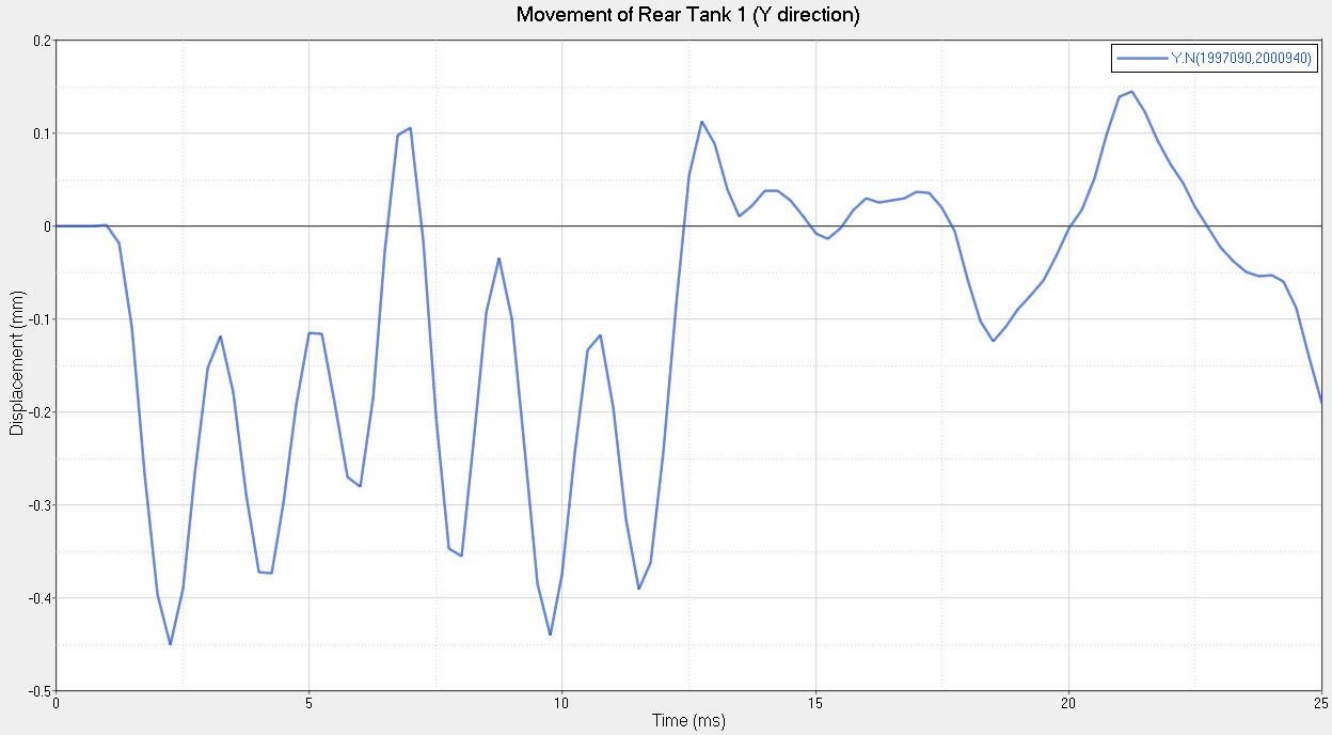

Figure 104-Movement of Rear Tank 1- Y direction [55mph]

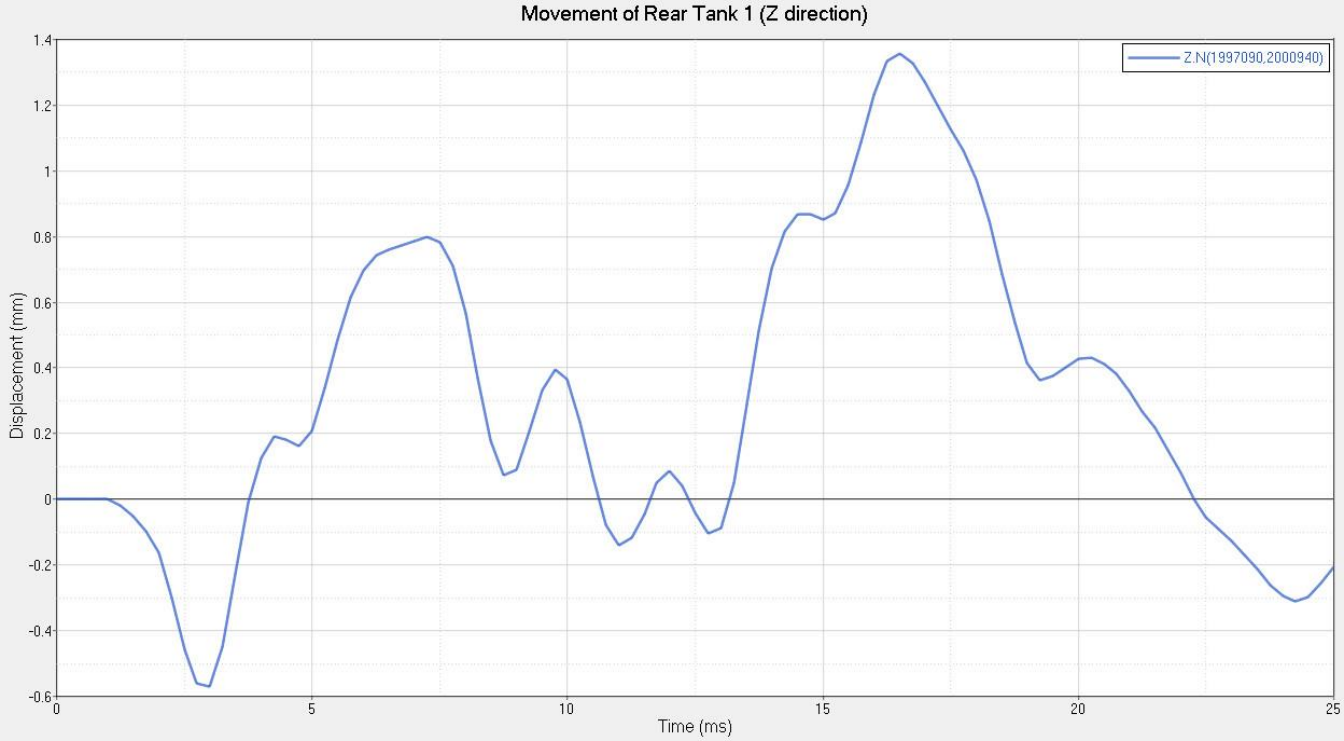

Figure 105-Movement of Rear Tank 1- Z direction [55mph]

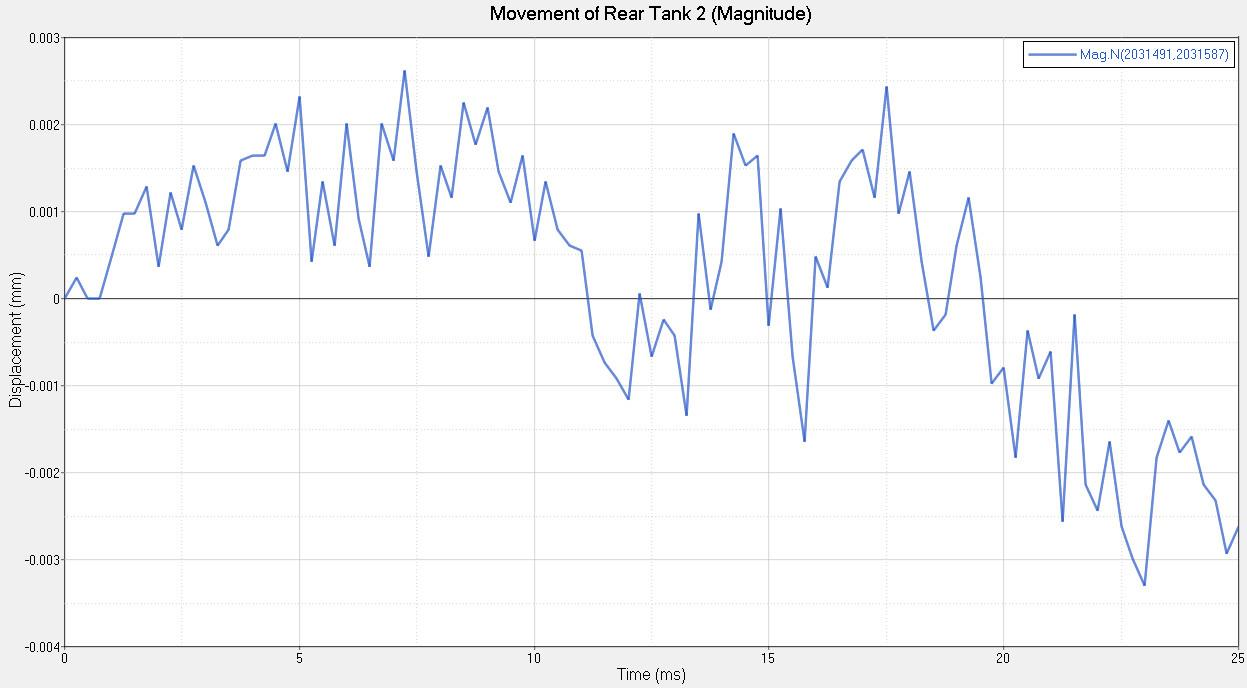

Figure 106-Movement of Rear Tank 2- Mag [55mph]

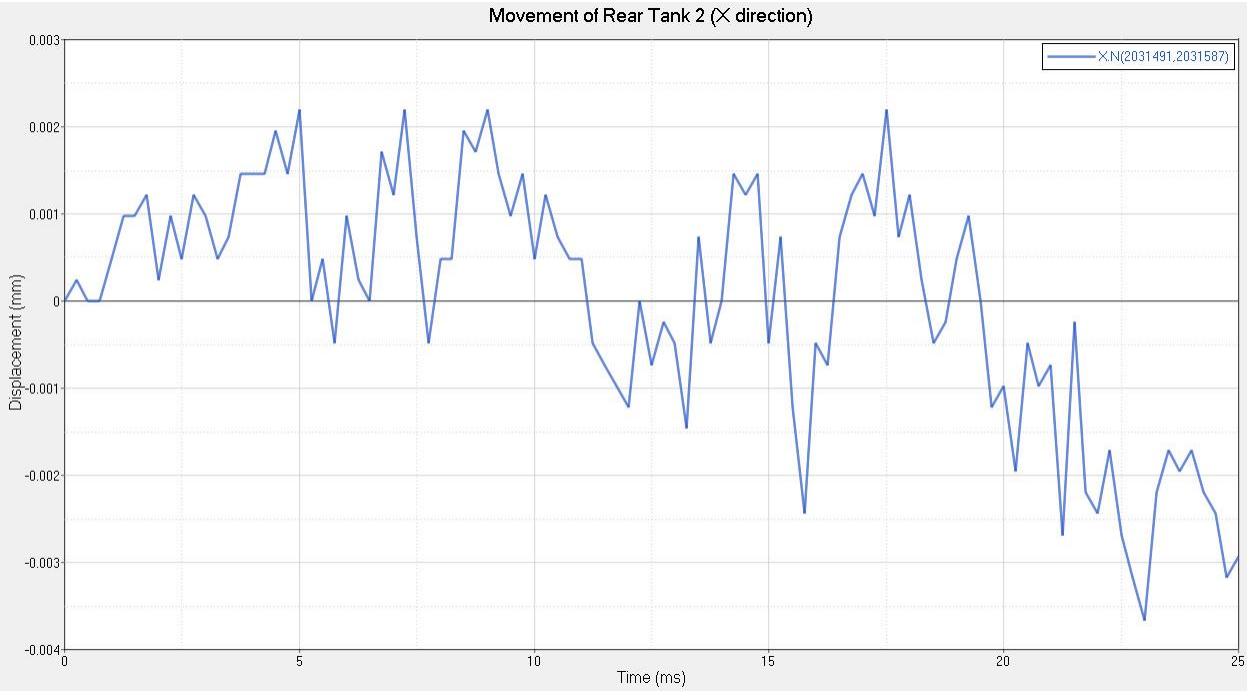

Figure 107-Movement of Rear Tank 2- X direction [55mph]

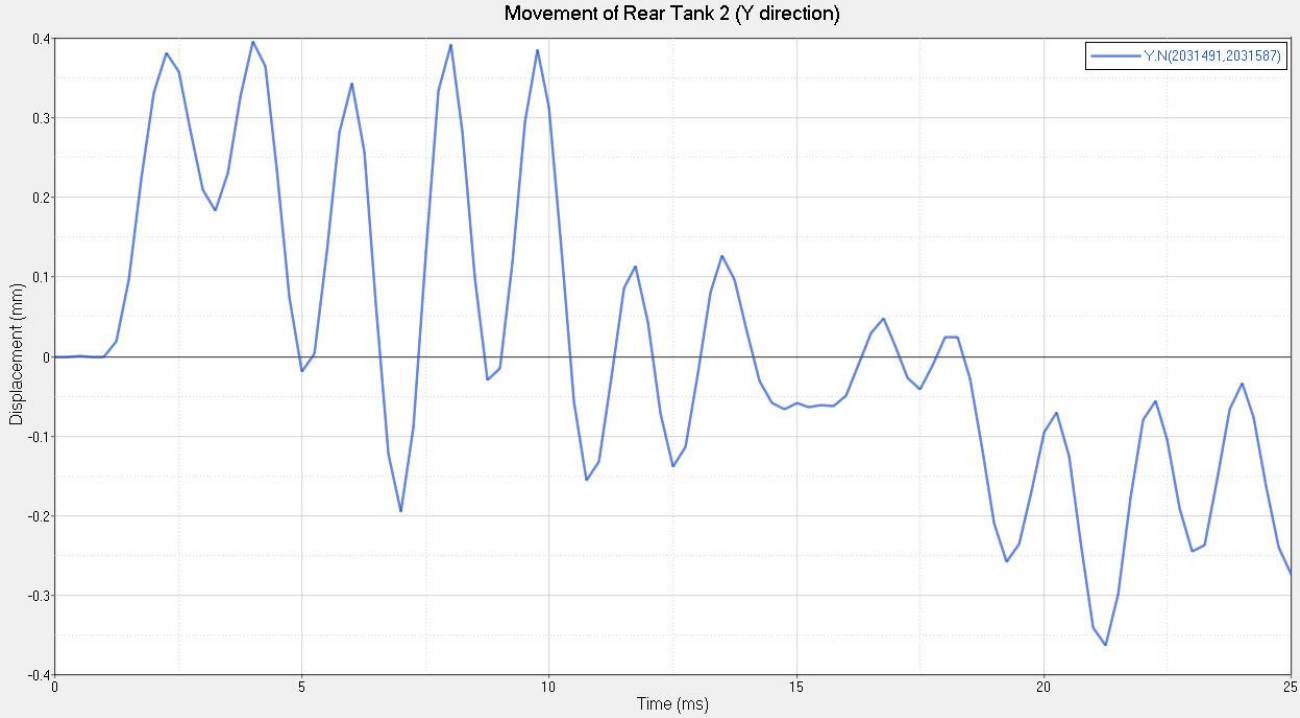

Figure 108-Movement of Rear Tank 2- Y direction [55mph]

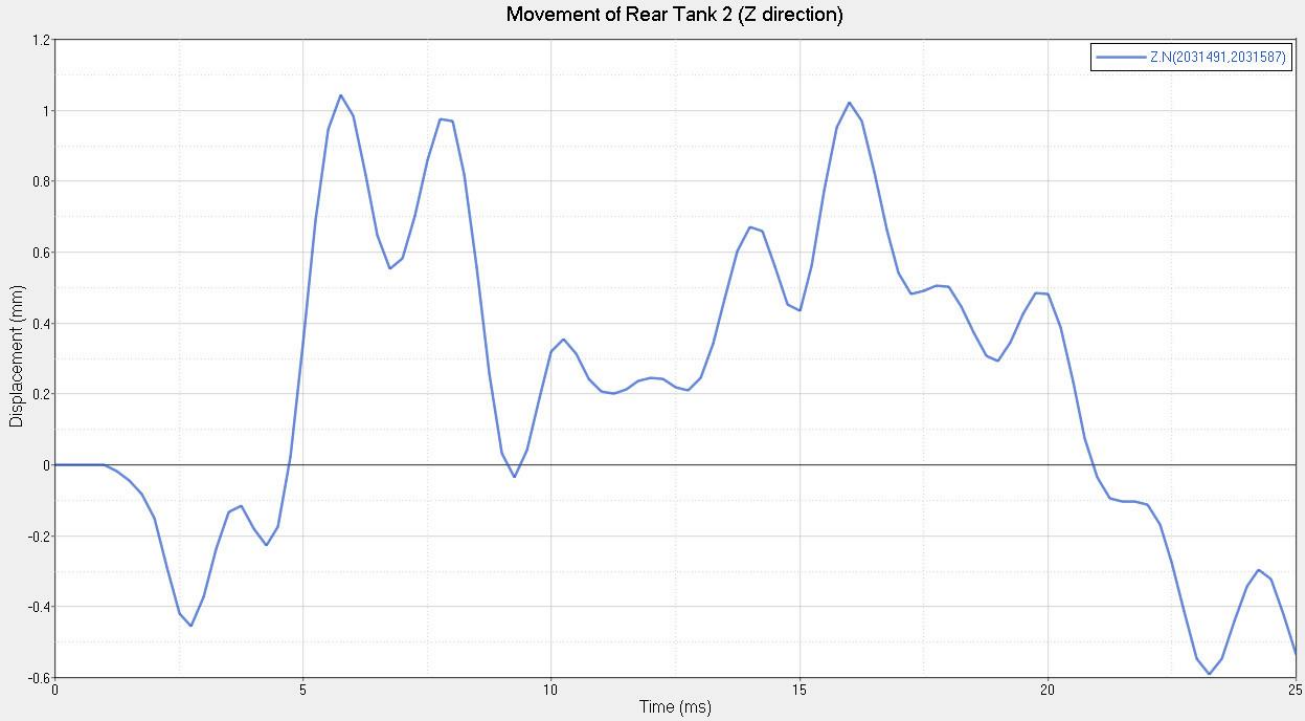

Figure 109-Movement of Rear Tank 2- Z direction [55mph]

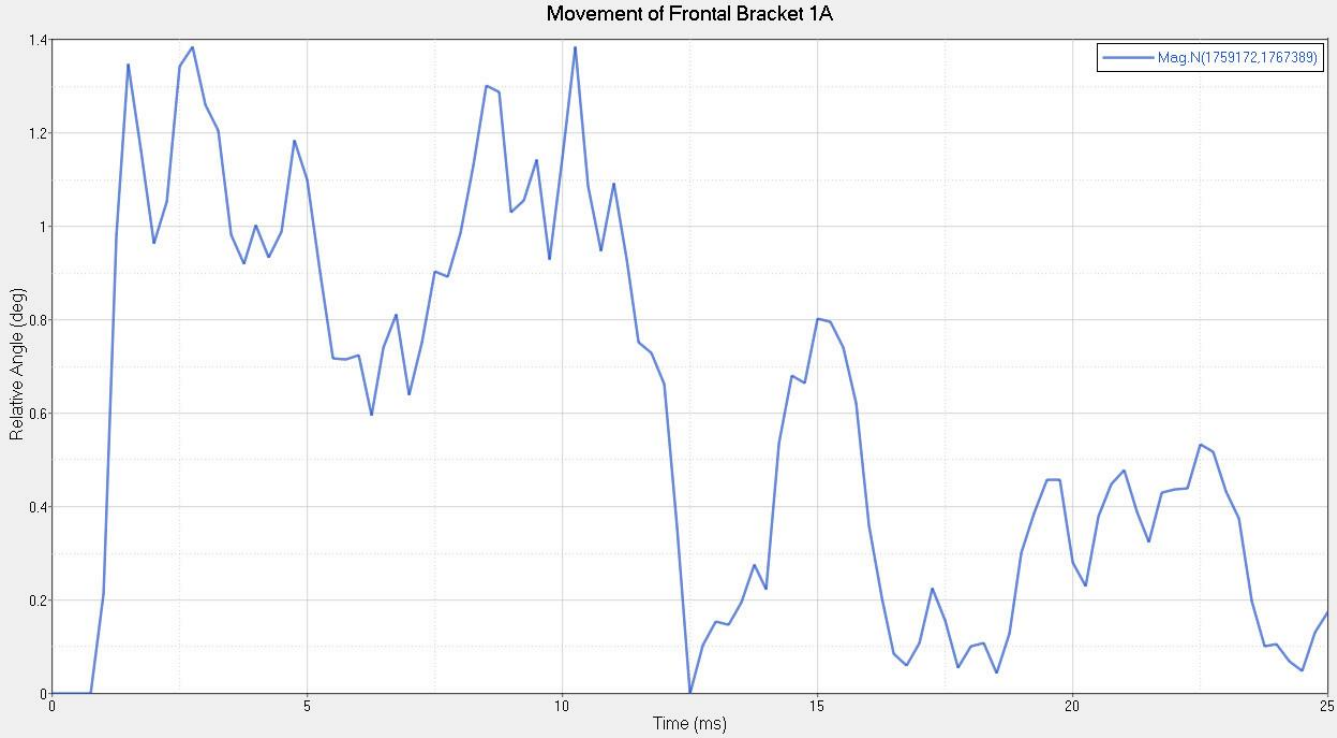

Figure 110-Movement of Frontal Bracket 1A [55mph]

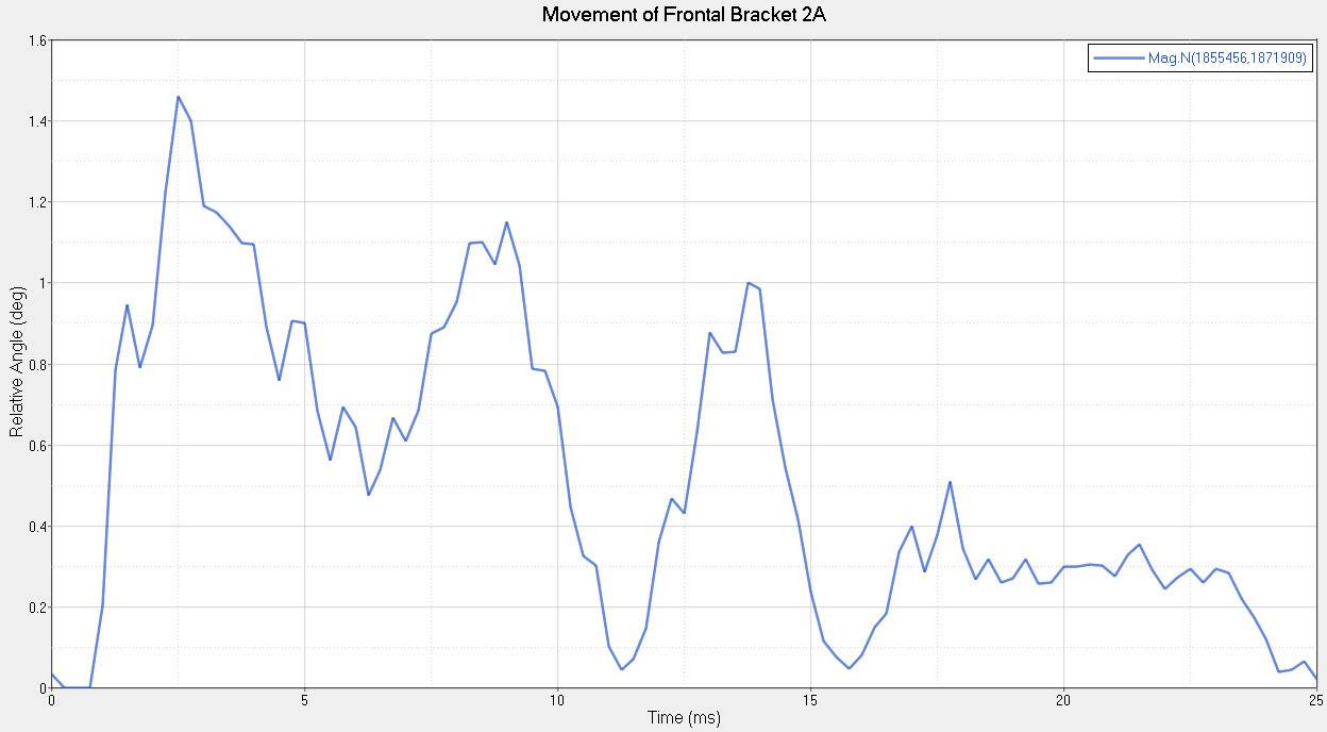

Figure 111-Movement of Frontal Bracket 2A [55mph]

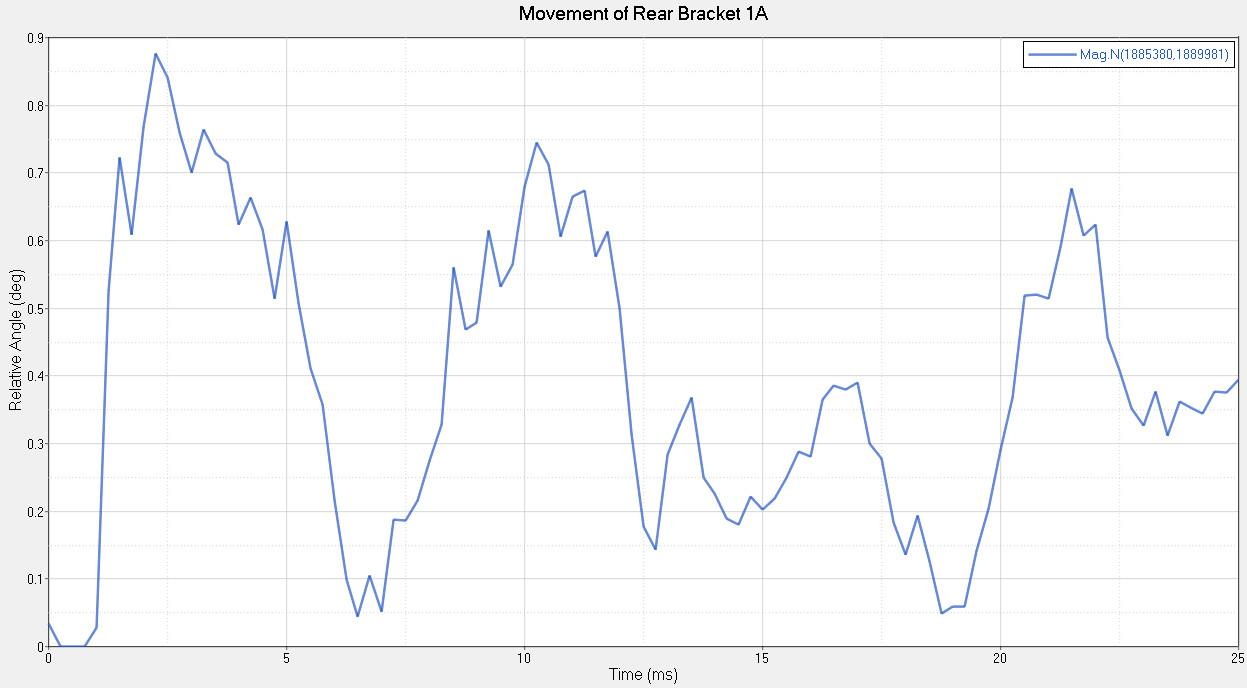

Figure 112-Movement of Rear Bracket 1A [55mph]

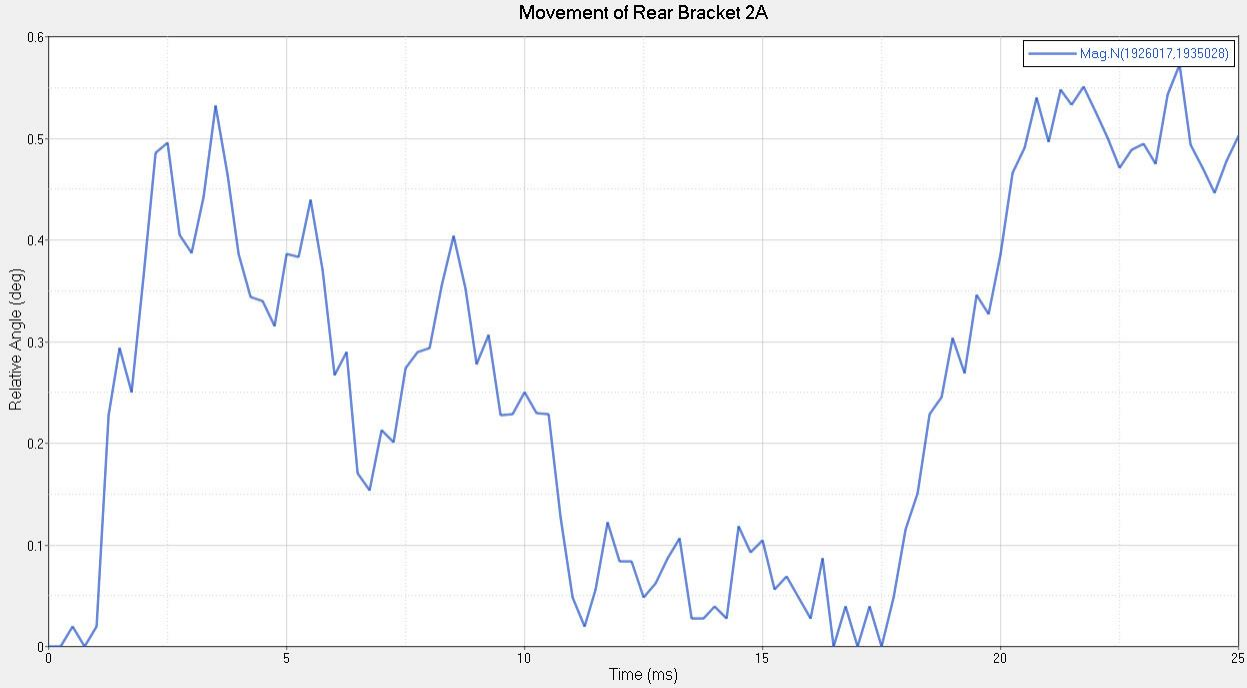

Figure 113-Movement of Rear Bracket 2A [55mph]